Habitat Suitability Modeling for the Houston Toad

Final Report March 2024

Texas A&M NRI Natural Resources Institute

Texas Parks & Wildlife

Habitat Suitability Modeling for the Houston Toad

FINAL REPORT MARCH 2024

Prepared by:

Texas A&M Natural Resources Institute

1001 Holleman Drive East
College Station, TX 77840

Suggested citation: Bowers, B.C., D.K. Walkup, T.J. Hibbitts, P.S. Crump, A.M. Lawing, W.A. Ryberg*. 2024. Habitat Suitability Modeling for the Houston Toad. Texas A&M Natural Resources Institute, College Station, Texas. [URL when added to NRI website]

*Corresponding author: Wade Ryberg, waryberg@tamu.edu

Front page photo credit: Andrew A. Austin

Habitat Suitability Modeling for the Houston Toad

1. Grant Details:

1. Grant Number:	F21AP03555 Contract Number: CA-0002648
2. Grant Title:	Habitat Suitability Modeling for the Houston Toad
3. Period of Performance:	1 January 2022 – 31 March 2024
4. Pass-thru Recipient:	
5. Principal Investigator:	Drs. Wade Ryberg, Danielle Walkup, Toby Hibbitts, and Roel Lopez, Texas A&M Natural Resources Institute, 578 John Kimbrough Blvd., 2260 TAMU, College Station, TX 77843. Point of Contact: Wade Ryberg, (979) 595-3211, waryberg@tamu.edu Dr. A. Michelle Lawing, Department of Ecology and Conservation Biology, Texas A&M University, Wildlife Fisheries and Ecological Sciences Building, 2238 TAMU, College Station, TX 77843.
6. TPWD Project Coordinator:	Dr. Paul Crump, Nongame and Rare Species Program, Wildlife Division Texas Parks and Wildlife Department, 4200 Smith School Road, Austin, TX 78744.

1. What type of report is this? (Select one):

☐ Interim Performance Report ☒ Final Performance Report

2. Report Narrative

Abstract
Our objectives were to update the Buzo (2008) habitat suitability model for the Houston Toad (*Anaxyrus houstonensis*) with current spatial data and habitat variables, quantify suitable habitat amount, develop a Species Distribution Model (SDM) to better understand environmental variable importance, and conduct connectivity modeling to prioritize areas for conservation and recovery actions. For the updated Buzo habitat suitability model, we constructed scripts to generate models that incorporate tree canopy cover, soils, and geology at varying weights and initially evaluated it with models for Bastrop County. We used four different model setups designed to estimate occurrence, in order of most restrictive to least restrictive: (1) Occurrence-informed Presence Prediction Models, (2) Evenly Weighted Presence Prediction Models, (3) Integrated Substrate Presence Prediction Models, and (4) Restoration and Reintroduction Potential Prediction Models. We then ran the four models for each of the remaining 12 counties and mapped the resulting outputs and quantified the suitable habitat amounts (Appendix 1).

We also constructed five ensemble species distribution models using different subsets of the Houston Toad occurrence data. We found that all five ensemble models generally identified consistent core areas for the Houston Toad, with variation among models occurring outside of those core areas. We found the proportion of deep sand (60-100 cm) in soil samples to be the most important variable in every model, generally having at least 6x the variable importance of the next most important variable. While the core areas contain generally acknowledged Houston Toad presence areas, there were some additional sites that stood out as having a higher predicted probability of presence (> 0.5) despite having no known occurrences in these areas. These areas include southern Bastrop County (south of the Colorado River) and areas north of known occurrences in Robertson and Leon counties. One important conclusion from our species distribution modeling results is that the variables included in the Buzo model (i.e., soil and forest cover) were also the most important variables in the species distribution models (in addition total March precipitation), despite the inclusion of other climate, vegetation, and elevation variables. This suggests the Buzo model is truly capturing the key elements of the Houston Toad's habitat.

Finally, connectivity analysis showed little habitat connectivity among several or two core areas for threshold probability of presence values greater than 0.5 or 0.75, respectively. The isolation of these core areas suggests that population connectivity among them will have to be achieved through the captive breeding process for this species.

Introduction

The Houston Toad (*Anaxyrus* [*Bufo*] *houstonensis*) is an amphibian endemic to Texas, where its populations are currently limited to Bastrop, Burleson, Colorado, Freestone, Lavaca, Lee, Leon, Milam, and Robertson Counties. Historically, populations of the species were also known from Austin, Fort Bend, Harris, and Liberty Counties (USFWS 2011, Dixon 2013). Population declines motivated a listing of the species as federally endangered in 1970 (USFWS 2011). Since then, overall trends for Houston toad abundance have continued declining across its range (McHenry and Forstner 2009). A recovery plan (USFWS 1984), species action plan (USFWS 2009), species listing review (USFWS 2011), and habitat management plan (USFWS 2017) have helped guide range-wide conservation actions to recover the species by protecting, enhancing, and restoring occupied, breeding, and dispersal habitat, and increasing population sizes through reintroduction and supplementation. As habitat suitability for the Houston Toad can change slowly (e.g., habitat management prescriptions) or quickly over time (e.g., catastrophic fire), an updated model of habitat suitability is required to support these conservation efforts throughout the species' current range. Here, we report on preliminary results from a study that updates habitat suitability models for the Houston Toad and builds from methods and habitat variables used in Buzo (2008).

The Houston Toad has a complex life-cycle with different life stages, and like many other amphibians, the habitat requirements vary for each of those life stages (Forstner and Dixon 2011). Reproductive and larval life stages require aquatic habitat in the form of small pools, ephemeral ponds, and permanent water bodies (Kennedy 1962, Brown 1971). Typically, heavy rains with warm temperatures (minimum air temperature above 14 C) from mid-February through early June trigger calling and spawning behaviors in adults (Kennedy 1962). The resulting eggs and larvae develop in shallow water, which must persist for at least 60 days to accommodate 4-7 days for hatching plus 3-9 weeks for metamorphosis, depending on water temperature (Hillis et al. 1984, Quinn and Mengden 1984, Greuter 2004).

After metamorphosis, juveniles and adults are supported by adjacent upland habitat, which provides food (e.g., small terrestrial arthropods) and refuges (e.g., burrows, litter, coarse woody debris) for individual toads (Forstner 2003, Forstner and Dixon 2011), but in a population context, it provides corridors for movement and dispersal among breeding habitats (Seal 1994, Hatfield et al. 2004). Following metamorphosis, juvenile dispersion from breeding habitat appears to be gradual with individuals remaining within 3-5 m for up to 3 weeks and 50 m for at least 13 weeks (Greuter 2004). As such, juvenile habitat requirements are thought to transition from breeding habitat with shaded edges to a forest habitat with pine or mixed deciduous plant composition, dense canopy (ideally 80%), and open herbaceous understory (McHenry and Forstner 2009). Adults are thought to have similar habitat requirements as juveniles, although adults are likely to move between several breeding habitats (Forstner and Dixon 2011). When inactive during hot, dry seasons, the coldest months, and daily sheltering, adults and juveniles are thought to seek refuge under objects or underground in deep sandy soils, the only habitat characteristic common to all current (e.g., Bastrop County) and historical localities (e.g., Harris County; Forstner and Dixon 2011).

The Houston Toad distribution appears to be naturally patchy, most likely due to the narrow habitat requirements described above. With specialized habitat requirements and a restricted distribution, the Houston Toad, like many similar species, is sensitive to habitat changes and vulnerable to anthropogenic disturbances that result in habitat loss, degradation, and fragmentation (Hillis et al. 1984, Welsh 1990). Anthropogenic disturbances thought to have negative effects on Houston Toad populations through loss, degradation, and fragmentation of suitable habitat include urban expansion with road development, forest conversion to agricultural, natural resource extraction (e.g., logging, mining), fire suppression, alteration of watershed drainages, and wetland degradation, destruction, or addition (e.g., permanent livestock tanks; Brown 1971, Seal 1994, Forstner and Dixon 2011). Several of these disturbances can also increase mortality of individual toads directly (e.g., traffic mortality) and indirectly (e.g., urbanization increases toad predators like Red-imported fire ants (*Solenopsis invicta*); Forstner and Dixon 2011). Drought and shifts in rainfall from climate change can also threaten Houston Toad populations by increasing the frequency of drying breeding habitats (Forstner and Dixon 2011). Disease (e.g., “chytrid fungus” *Batrachochytrium dendrobatidis*) and overutilization for commercial, recreational, scientific, or educational purposes do not appear to be threats to Houston Toad populations, which puts the primary focus of conservation and recovery efforts on halting and reversing the loss, degradation, and fragmentation of suitable habitat.

Despite strong conservation and recovery efforts, suitable Houston Toad habitat continues to be lost and degraded (Forstner and Dixon 2011). To prevent extinction of the species, a population viability analysis concluded that at least three large, interconnected but self-sustaining populations should be maintained so that dispersal among them enhances species survival (Seal 1994, Hatfield et al. 2004). Unfortunately, Houston Toad populations continue to become less interconnected (Buzo 2008; McHenry and Forstner 2009; Forstner and Dixon 2011), placing the pressure of species survival on the reproductive success of each individual population. In response, captive propagation and headstarting efforts to reintroduce and supplement populations in priority areas have had some limited, but extremely important success increasing population sizes to prevent localized extirpation and extinction of the species (USFWS 2009, Duarte et al. 2014). Clearly range-wide efforts to protect and restore suitable habitats that interconnect these reintroduced and supplemented populations must continue to maximize return on captive propagation and headstarting investments in the species.

To accomplish this task, landowner cooperation throughout the Houston toad's range is critical. The U.S. Fish and Wildlife Service, Texas Parks and Wildlife Department, and other partnering state and federal agencies, local governments and non-governmental organizations have engaged with private landowners and offered information on habitat restoration and management goals and financial incentives for species conservation in priority areas (USFWS 2011). Often specific habitat restoration and management prescriptions (e.g., planting native trees or selectively thinning), as well as conservation tools and incentives (e.g., Safe Harbor Agreements, conservation easements), are decided on a case-by-case basis (USFWS 2017). Habitat suitability models have helped support this decision-making process for the Houston Toad throughout its range. For example, Buzo (2008) used soil layers and aerial imagery to model Houston Toad habitat suitability within a GIS framework (see Approach for detailed description). Over time, habitat suitability for the Houston Toad has been shown to change slowly with habitat management prescriptions or quickly with habitat conversion and catastrophic wildfire (Buzo 2008, Duarte et al. 2014). As such, models of habitat suitability for the Houston Toad must be updated to ensure that species management and restoration efforts can be applied consistently through time at landscape scales. Here, we report on an effort to develop habitat suitability models for the Houston Toad that build on methods and habitat variables used in Buzo (2008). The models will help characterize how recovery goals and priorities might have shifted in time and space given changes to the amount, configuration, and fragmentation of suitable habitats. The objectives of this study are to:

1) Update the Buzo (2008) habitat suitability model for the Houston Toad with current spatial data and habitat variables and quantify suitable habitat amount.

2) Develop a Species Distribution Model (SDM) for the Houston Toad using the same occurrence data and similar spatial habitat variables and compare the results of this statistical analysis with the results from objective 1, which was guided by subject matter expert input.

3) Conduct connectivity modeling to prioritize areas for conservation and recovery actions (e.g., habitat dispersal corridors, Safe Harbor Agreements, conservation easements, land acquisition, and community engagement).

Updated Buzo Model Methods

Geographic Space

Because future management efforts for the species will include restoration and reintroduction efforts, we quantified habitat in most counties with documented *A. houstonensis* presence and neighboring counties that have similar geological formations and soils. We constructed models using geographic space that included Austin, Bastrop, Brazos, Burleson, Colorado, Freestone, Harris, Lavaca, Lee, Leon, Milam, Robertson, and Waller counties. We did not include Liberty or Fort Bend Counties because the only occurrence records in those counties are very old and have some spatial uncertainty.

Filtering Occurrence Records

To inform categorization of environmental variables, we gathered *A. houstonensis* occurrence data from TPWD, USFWS, and from historical museum records accessed via the spocc package in R (R Core Team 2021; Owens et al. 2022). The resulting combined dataset included 6,141 observations of *A. houstonensis*, many of which were duplicate observations because we gathered data from multiple sources. Some records were of questionable validity because of spatial uncertainty, temporal uncertainty, or both spatial and temporal uncertainty. We found 60 records to be geolocated incorrectly because of confusion over street names or typos in the latitude or longitude fields but were able to relocate them with certainty because of specificity in the verbatim observer notes. We removed 181 records with spatial or both spatial and temporal uncertainty because spatial uncertainty can obscure results in these models. We removed 744 records from the dataset because they occurred in Bastrop State Park, Attwater Prairie Chicken National Wildlife Refuge, or Griffith League Ranch after reintroduction and headstarting efforts began at those sites in 2009, 1978, and 2013, respectively, because observing the temporary presence of individuals at release sites does not necessarily indicate genuine suitability. Among records without spatial certainty issues, we identified 58 records as having temporal uncertainty because the year of observation was unknown. However, because soils and geology were not likely to have changed during the period of interest, we included positions with temporal uncertainty in analyses of soil and geology. Some records were from captures or audio recordings during breeding events and were geolocated within ponds. Because some ponds have a different soil type than their banks or surrounding uplands and some ponds are merely listed as “water” in soil databases, we moved observations recorded within such ponds to the nearest bank to adequately represent the conditions of the surrounding uplands. Naturally, when combining datasets from multiple sources and when applying data from repeated surveys at the same sites, many records had identical coordinates. Additionally, having too many positions geolocated in close proximity to one another can spatially bias environmental variable results. We addressed these problems by using spatial filtering that allows for inclusion of one randomly selected sample per grid cell at 30 m and 200 m resolutions using the function thin.algorithm in the spThin package in R (Aiello-Lammens et al. 2015). When spatially filtering data, 416 grid cells had documented *A. houstonensis* presence at the 30-m resolution and 285 grid cells had documented presence at the 200-m resolution (Figure 1; Figure 2). For datasets without positions of temporal uncertainty, 368 grid cells had documented *A. houstonensis* presence at the 30-m resolution and 248 grid cells had documented presence at the 200-m resolution (Figure 3; Figure 4).

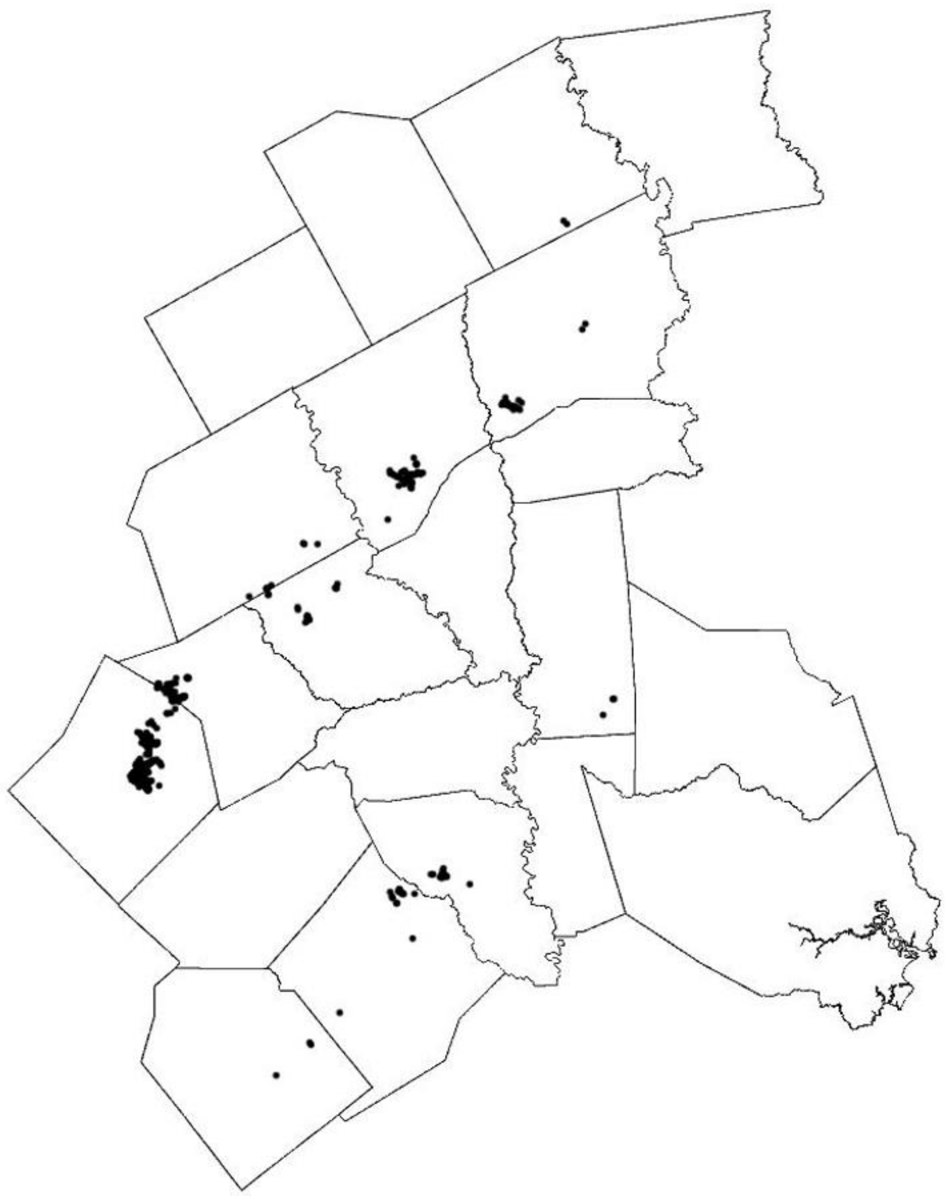

Figure 1. Map of all *A. houstonensis* occurrence records included in the study filtered at a 30-m resolution.

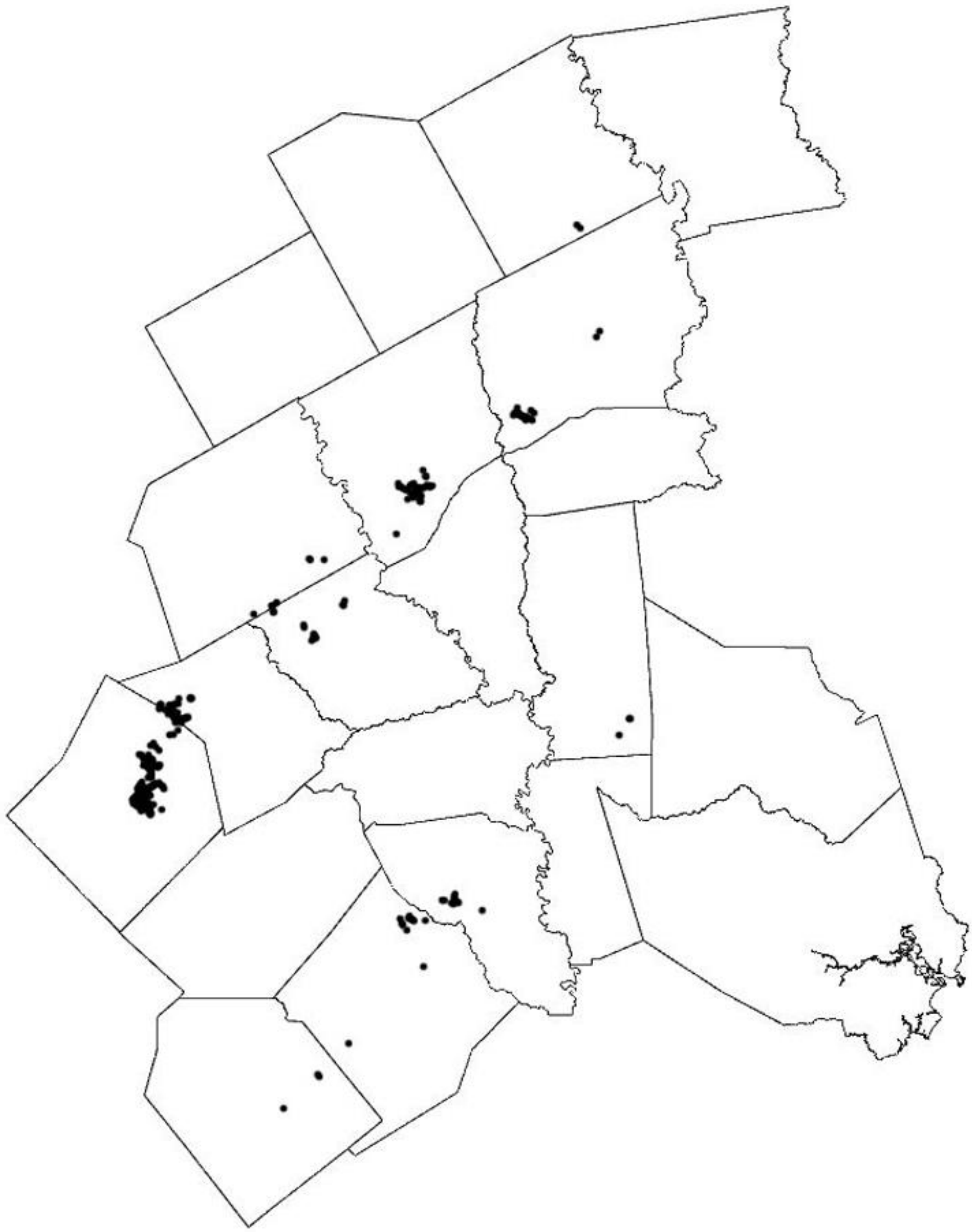

Figure 2. Map of all *A. houstonensis* occurrence records included in the study filtered at a 200-m resolution.

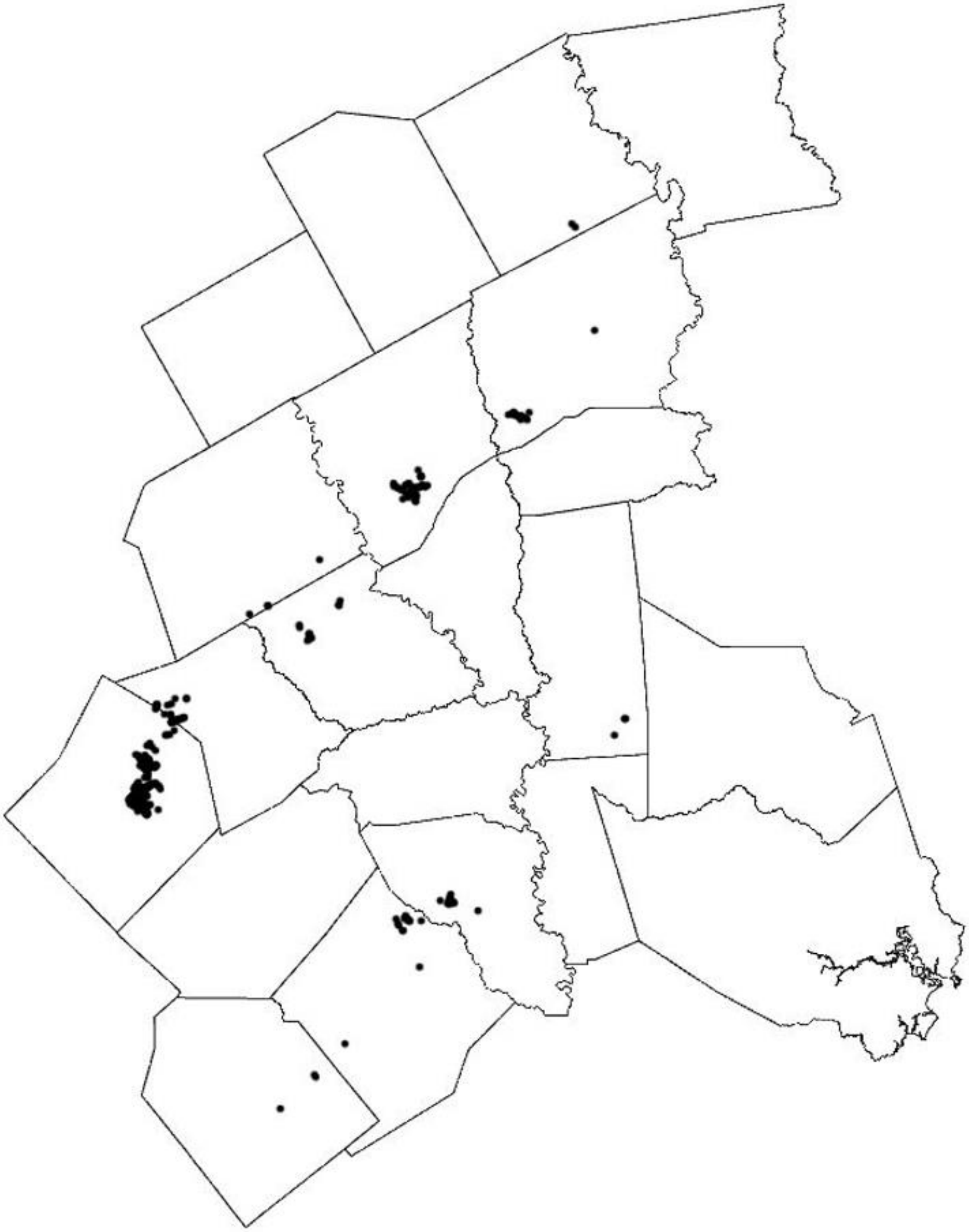

Figure 3. Map of all *A. houstonensis* occurrence records without temporal uncertainty included in the study filtered at a 200-m resolution.

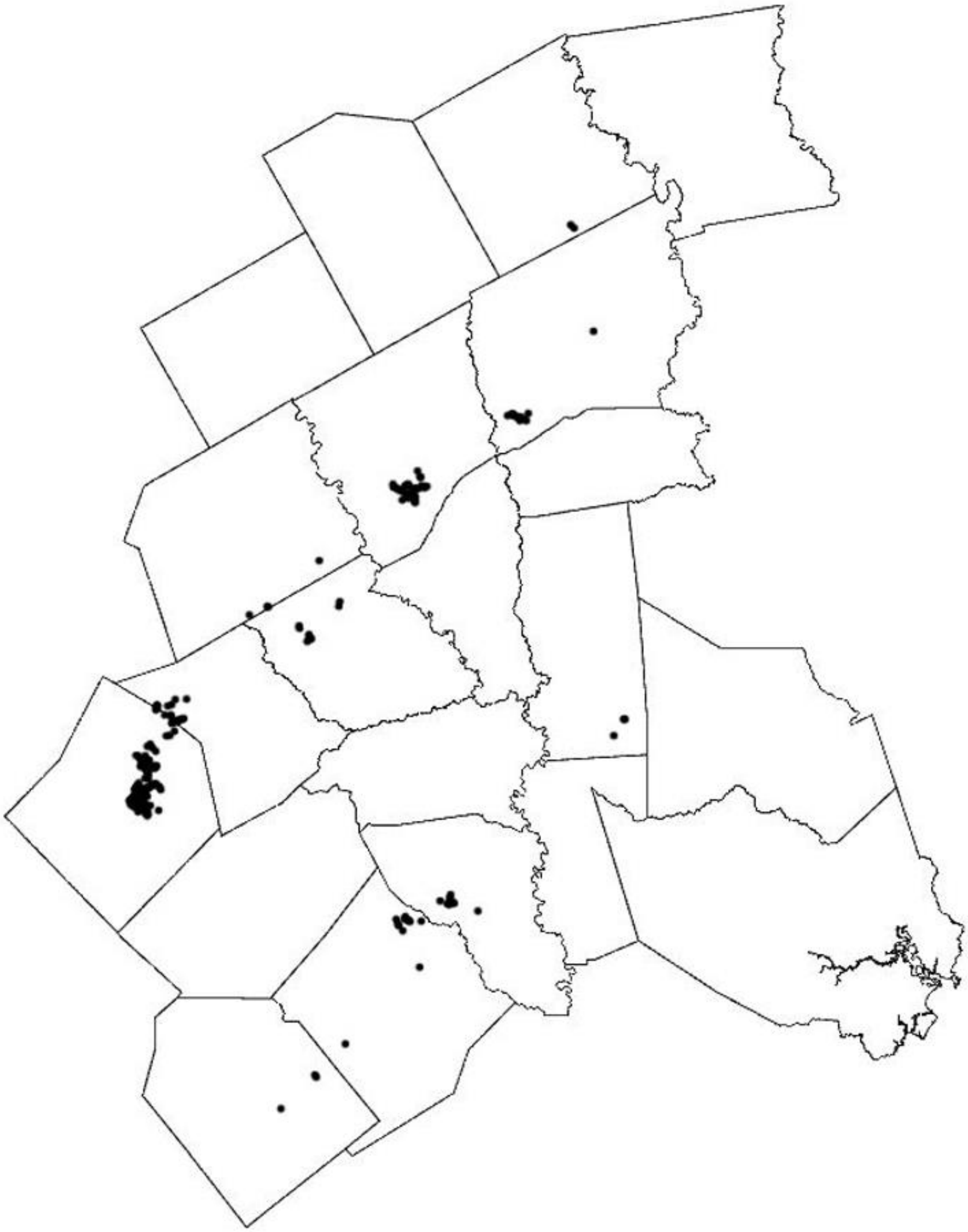

Figure 4. Map of all *A. houstonensis* occurrence records without temporal uncertainty included in the study filtered at a 30-m resolution.

Basic Model Structure

We constructed models with a 30-m grid resolution to generate an updated model comparable to the soil and canopy cover models presented in Buzo 2008 (hereafter "Buzo" models). For each environmental variable, we assigned each grid cell a suitability score ranging from 0 to 10. Then, we constructed cumulative models scoring each cell by summing the scores for all included environmental variables and dividing the sum by the number of variables included. Because the relative importance among variables to predicting presence of *A. houstonensis* is unknown, we used variations on this basic equation to design several model types.

Environmental Variable: Geology

We spatially identified geological formations across all counties using the United States Geological Survey (USGS) State Geologic Map Compilation (SGMC; Horton et al. 2017). To identify geologic formations with documented occurrence records, we used the spatially filtered dataset at both grid resolutions to identify all geological formations with documented *A. houstonensis* records (Table 1). We did not consider the Cook Mountain Formation to be suitable because the only spatially filtered record within the Cook Mountain Formation in both datasets was less than 300 m from the Sparta Sand Formation.

Table 1. Quantities of *A. houstonensis* occurrence records within each geological formation spatially filtered at two resolutions.

Geological Formation	N (30 m)	N (200 m)
Carizzo Sand	162	89
Reklaw Formation	84	60
Sparta Sand	73	59
Willis Formation	37	29
Calvert Bluff Formation	36	27
Queen City Sand	12	12
High gravel deposits	6	4
Weches Formation	5	4
Cook Mountain Formation	1	1

We considered the Carrizo Sand, Reklaw, Sparta Sand, Willis, Calvert Bluff, Queen City Sand, High Gravel Deposits, and Weches formations to be suitable. However, presence within formations was not consistent across the range of the species (Figure 5). For example, many positions were within the Calvert Bluff Formation in Bastrop and Lee counties, but large patches of the same formation in Milam and Robertson counties had no documented occurrence records. Similarly, most records in Leon, Robertson, and Burleson counties were within the Sparta Sand Formation, but there were no records within large patches of Sparta Sand in Bastrop and Lee counties. For this reason, we created two types of geology rasters. Raster G_a assigned a suitability score of 10 to each cell within contiguous formation patches with documented *A. houstonensis* records, a score of 5 for each cell within suitable formation patches without documented records, and a score of 0 for cells outside of suitable geologic formations. Raster G_o assigned a score of 10 for each cell within contiguous formation patches with documented *A. houstonensis* records and a score of 0 for all cells outside of those patches, even if within geologic formations identified as suitable within other portions of the species' range.

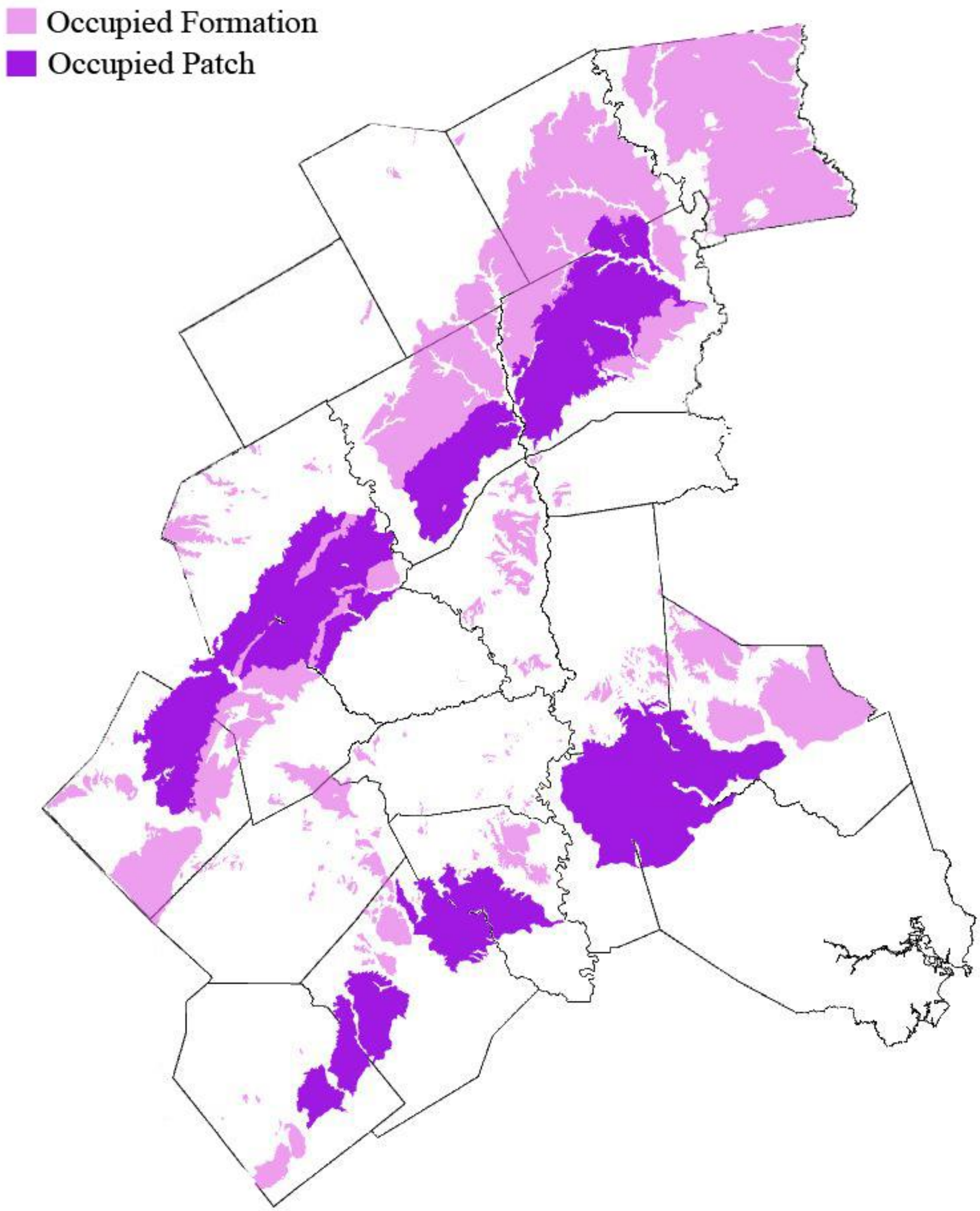

Figure 5. Geologic units with documented occurrences in the filtered *A. houstonensis* datasets.

Environmental Variable: Soil

The original Buzo models considered soils of suborders Ustalf and Udalf to be suitable, assigning them a suitability value of 10 and all other soils a suitability value of 1. Because some of the *A. houstonensis* occurrence records were within other soil suborders (Table 2), we considered all Natural Resource Conservation Service Soil Survey Geographic Database (NRCS SSURGO) soil map units with occurrence records in the 200-m dataset (Table 3; Figure 6) to be of high suitability with a value of 10, and all other soil map units to be unsuitable with a value of 0. This method can cause issues at county boundaries because soil groupings in NRCS datasets sometimes differ among counties, but the influence of county boundaries was minimal in all counties except Limestone County. Soils with components identical to those labeled “Crockett fine sandy loam” in neighboring counties were identified as “Crockett loam” in Limestone County. Although no *A. houstonensis* records occurred in Crockett loam, we included soils identified as Crockett loam in Limestone County because it was identical in composition and mapping to Crockett fine sandy loam in neighboring counties.

Table 2. Taxonomic soil suborders of all *A. houstonensis* occurrence records in the dataset spatially filtered to 200 m (n = 285).

Taxonomic Suborder	Records
Ustalfs	247
Udalfs	18
Psamments	8
Fluvents	5
Ustults	4
Aquents	2
Udults	1

Table 3. NRCS SSURGO soil map units of all *A. houstonensis* occurrence records in the dataset spatially filtered to 200 m (n = 285).

Soil	Records
Padina fine sand	55
Padina loamy fine sand	39
Silstid loamy fine sand	39
Eufala loamy fine sand	18
Jedd gravelly fine sandy loam	18
Edge gravelly fine sandy loam	13
Robco-Tanglewood complex	12
Tabor fine sandy loam	12
Depcor loamy fine sand	10
Edge fine sandy loam	9
Arenosa fine sand	8
Tremona fine sand	8
Tremona loamy fine sand	8
Sayers fine sandy loam	5
Catilla loamy fine sand	2
Chazos loamy fine sand	2
Crockett fine sandy loam	2
Hearne fine sandy loam	2
Melhomes loamy fine sand	2
Monaville loamy fine sand	2
Newulm loamy fine sand	2
Straber loamy fine sand	2
Wolfpen loamy fine sand	2
Boy loamy fine sand	1
Catilla loamy sand	1
Cheetham loamy sand	1
Edge - Gullied land complex	1
Fetzer loamy fine sand	1
Gasil fine sandy loam	1
Gasil loamy fine sand	1
Jedd fine sandy loam	1
Pickton loamy fine sand	1
Rader fine sandy loam	1
Robco loamy fine sand	1
Tenaha-Cuthbert complex	1

Vernia very gravelly loamy sand	1

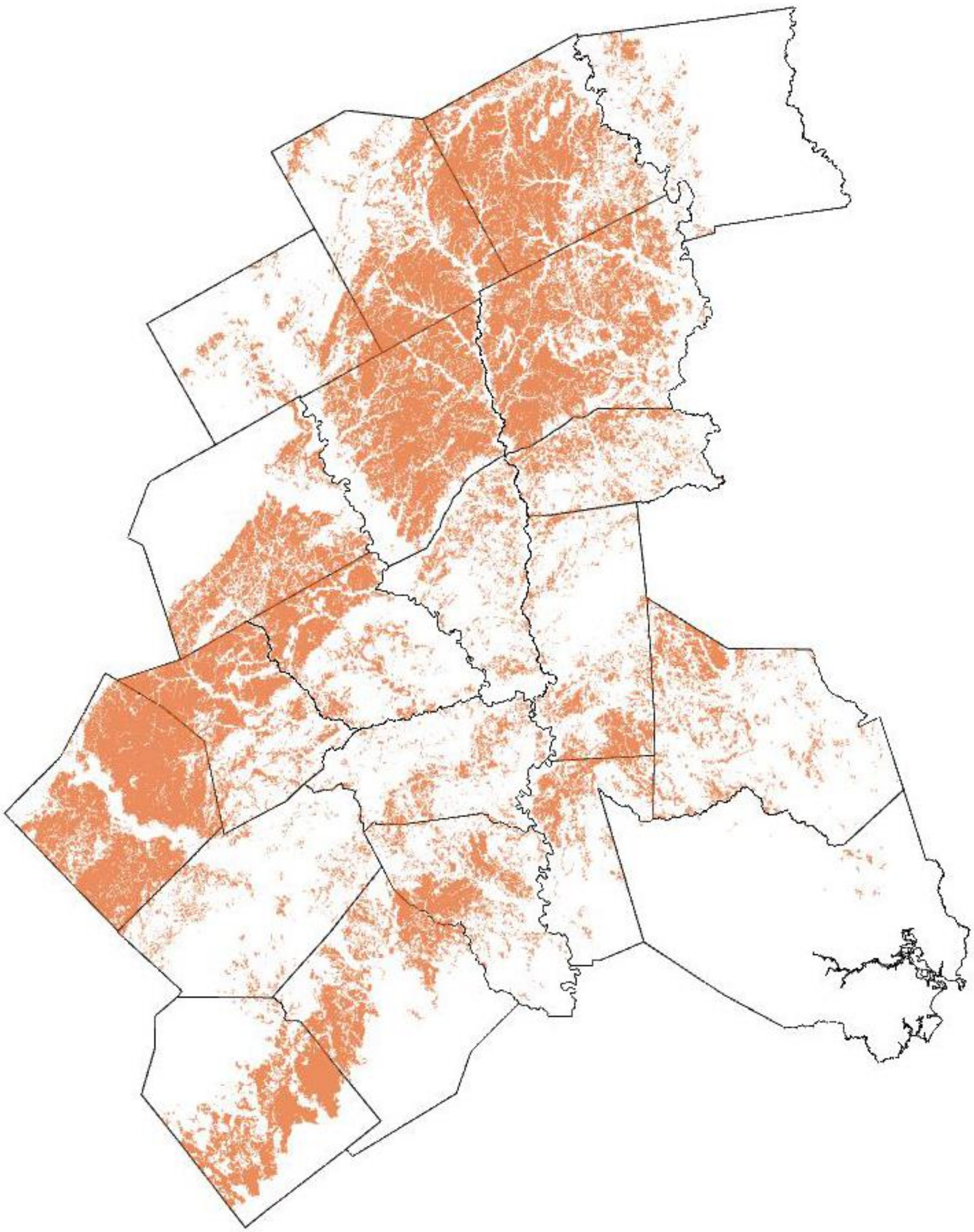

Figure 6. Soil map units with documented occurrences of *A. houstonensis* in the dataset filtered to 200 m.

Environmental Variable: Tree Canopy Cover

Occurrence records can provide crucial information on variable importance. However, many *A. houstonensis* records were from breeding ponds and it was not possible to know where the toads went when returning to terrestrial aestivation habitats. This factor, combined with the temporal variation among occurrence records and the mosaic heterogeneity of forested patches and clearings, made it impossible to quantify the importance of canopy at the 30-meter scale. We did not use occurrence records to calibrate tree canopy cover suitability, and instead assumed that expert elicitations used to inform the 2008 Buzo models were still applicable for *A. houstonensis*.

To provide the most current analysis of canopy possible, we downloaded 2020 multiband color infrared imagery from the National Agriculture Imagery Program (NAIP) at a resolution of 1 square meter. For each pixel, we used the red and near infrared bands to calculate the normalized difference vegetation index (NDVI) and used the green and near infrared bands to calculate the normalized difference water index (NDWI). We created a mask removing all pixels with an NDWI of 0.2 or higher, which removed open water, buildings, and some paved areas. We then removed areas with an NDVI below 0.3, leaving only pixels containing woody vegetation.

Because some shrubs and low-lying woody vegetation were included in the NAIP imagery analysis but do not provide suitable canopy cover for *A. houstonensis*, we used an additional mask generated from light detection and ranging (lidar) data. We downloaded USGS 2016-2018 lidar point clouds from the Texas Natural Resource Information System (TNRIS) and normalized ground returns using the package lidR in R (Roussel et al. 2020). After normalizing ground returns for point clouds at full resolution for each county, we created canopy height models at a 1-meter resolution.

Because previous efforts to model *A. houstonensis* habitat suitability identified that pines provide suitable canopy cover at a taller height than other trees (TPWD 2019), we used the Texas Ecological Mapping System (EMS) to identify areas as pine. Initially, we had identified as pine all areas in the following EMS units:

3001 Pineywoods: Pine Forest or Plantation
101 Bastrop Lost Pines: Loblolly Pine Forest
9305 Pine Plantation 1 to 3 meters tall
9301 Pine Plantation > 3 meters tall
121 Bastrop Lost Pines: Loblolly Pine Slope Forest
4001 Pineywoods: Longleaf or Loblolly Pine Flatwoods or Plantation
3011 Pineywoods: Dry Pine Forest or Plantation
3201 Pineywoods: Sandhill Pine Woodland
12005 Pineywoods: Longleaf Pine Woodland

Unfortunately, that approach did not work satisfactorily because of tree species heterogeneity within EMS units. In the final canopy models, we identified only areas explicitly identified as pine plantations (units 9301 and 9305) as pine monocultures. Because EMS rasters are provided with a 10-meter resolution, we resampled the data to 1 meter using the lidar grid. We created a height mask over the woody vegetation rasters by filtering the canopy height models with a threshold of 15 meters for pine monocultures and 10 meters for all other units.

The resulting imagery identified tree canopy cover at a 1-meter resolution (Figure 7). We created a 30-meter resolution grid and divided the number of canopy pixels within each grid cell by the total number of pixels within the cell, then multiplied by 100 to get the percent tree canopy cover. To generate final tree canopy cover scores (*C*), we used a ranking system similar to prior modeling efforts (TPWD 2019):

0% - 20% = 1
20% - 30% = 3
30% - 40% = 4
40% - 50% = 5
50% - 100% = 10

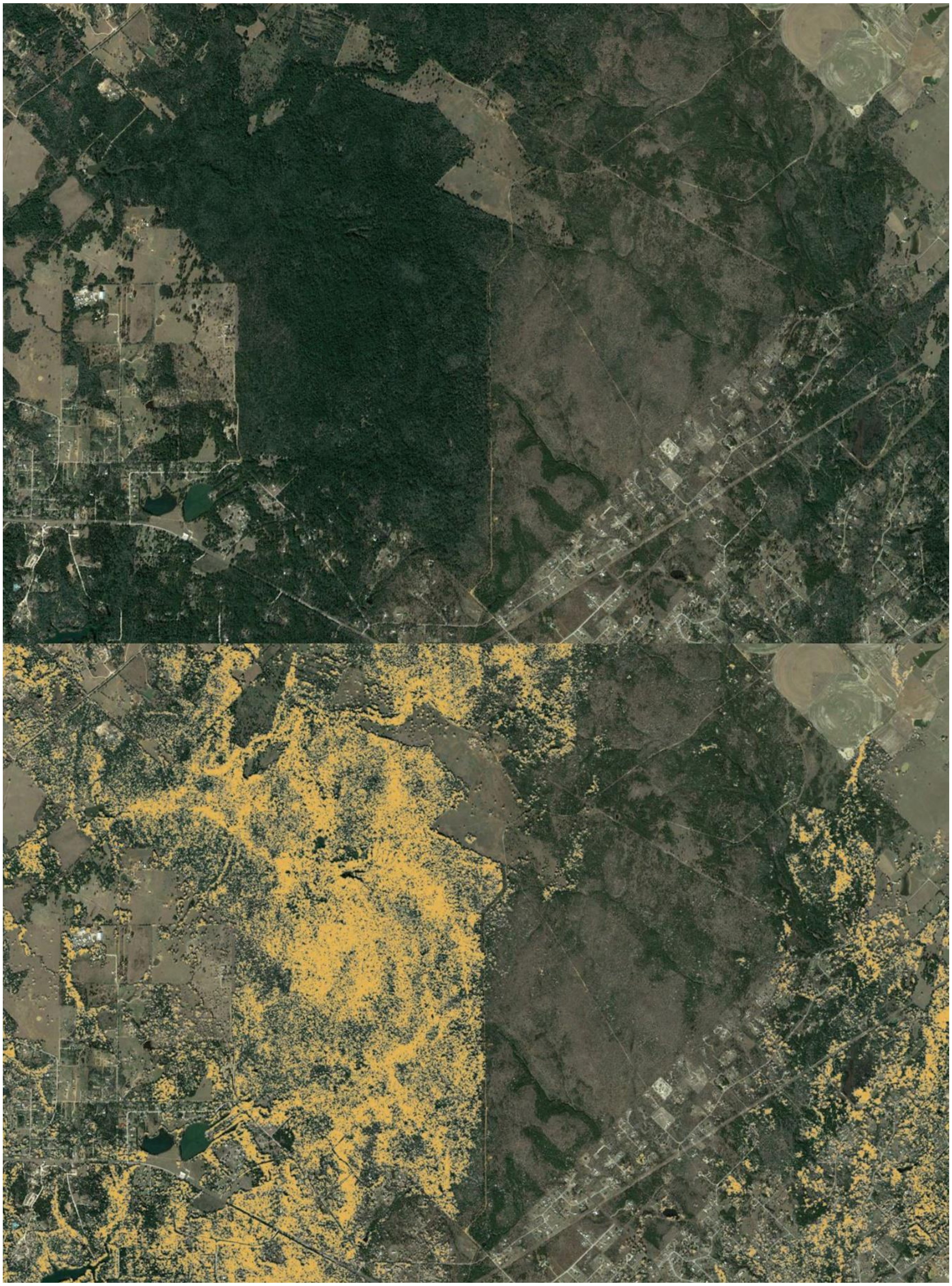

Figure 7. Image from Bastrop County (top) and same image with final 1-m resolution pixel filtering for tree canopy inclusion using NAIP imagery classification and lidar canopy height filtering (bottom).

Model 1: Occurrence-informed Presence Prediction Models

We generated three model designs intended to predict the presence of *A. houstonensis*. Although all model designs were informed by occurrence data via soil series inclusion, Model 1 was the most data-driven construction and most specific predictor of presence. In this design, only G_o was used to incorporate geology into the model, and areas outside of geologic formation patches with occurrence records were assumed to have zero probability of presence regardless of other environmental variables, because no records have been found outside of these patches beyond the aforementioned exceptions in more coastal formations. Soil and geology were treated as a combined substrate score in this design, and tree canopy cover scores were weighted evenly with the substrate scores. Model 1 cell scores were calculated using the equation,

$$M_1 = G_o\left(\frac{\frac{C}{2} + \frac{S}{4} + \frac{G_o}{4}}{10}\right)$$

Differences in assumptions of variable importance among model designs necessitated different scoring systems for each design. Model 1 was scored as follows:

$M_1 < 5.4$: No probability of presence
$M_1 = 5.4$ to 6.4 : Very low probability of presence
$M_1 = 6.4$ to 7.4 : Low probability of presence
$M_1 = 7.4$ to 9.0 : Medium probability of presence
$M_1 > 9.0$: High probability of presence

Model 2: Evenly Weighted Presence Prediction Models

Creating models with even weighting could be helpful retrospectively if future efforts quantify variation in the importance of environmental characteristics. Model 2 assumed soil, geology, and tree canopy cover to be of equal importance, and did not limit inclusion to formation patches with known occurrence records. Model 2 cell scores were calculated using the equation,

$$M_2 = \frac{C}{3} + \frac{S}{3} + \frac{G_a}{3}$$

Model 2 was scored as follows:

$M_2 < 4.5$: No probability of presence
$M_2 = 4.5$ to 6.0 : Very low probability of presence
$M_2 = 6.0$ to 8.0 : Low probability of presence
$M_2 = 8.0$ to 9.0 : Medium probability of presence

$M_2 > 9.0$: High probability of presence

Model 3: Integrated Substrate Presence Prediction Models

Our third model design integrated soil and geology into one substrate score, then weighted substrate scores evenly with tree canopy cover. Model 3 used G_a for the geology scores and did not limit inclusion to formation patches with known occurrence records. Model 3 cell scores were calculated using the equation,

$$M_3 = \frac{C}{2} + \frac{S}{4} + \frac{G_a}{4}$$

Model 3 was scored as follows:

$M_3 < 4.5$: No probability of presence
$M_3 = 4.5$ to 7.0 : Very low probability of presence
$M_3 = 7.0$ to 7.5 : Low probability of presence
$M_3 = 7.5$ to 9.0 : Medium probability of presence
$M_3 > 9.0$: High probability of presence

Model 4: Restoration and Reintroduction Potential

In addition to models generated for predicting species occurrence, we designed a fourth model to quantify the suitability of sites for habitat restoration and reintroduction. Model 4 assumed that geologic formations were only correlated to spatial trends in ecology influencing the history of distribution for the species and not indicative of actual suitability to species biology. The design incorporated only soil and tree canopy cover scores and was the most similar model to the 2008 Buzo models. The goal with Model 4 was to identify restoration and reintroduction potential but not direct suitability. The model design included no evaluation of hydrologic suitability and areas identified as having management potential would still need site evaluations to identify whether an adequate mosaic of suitable breeding wetlands is available or would have to be constructed. Model 4 cell scores were calculated using the equation,

$$M_4 = \frac{C}{2} + \frac{S}{2}$$

Model 4 was scored as follows:

$M_4 < 4.5$: No restoration potential
$M_4 = 4.5$ to 7.0 : Low restoration potential
$M_4 = 7.0$ to 7.5 : Medium restoration potential
$M_4 = 7.5$ to 9.0 : High restoration potential
$M_4 > 9.0$: Reintroduction potential, given appropriate hydrology

Updated Buzo Model Results

To date, we have compiled final R scripts and generated updated Buzo models for all thirteen counties (Tables 4 - 16, Figures 8 - 59). We attached model output rasters for all counties and environmental rasters for all but two counties as separate deliverables associated with this report.

Austin County

Table 4. Predicted areas in Austin County ranked by probability of presence (M_1, M_2, and M_3), restoration potential (M_4), and habitat suitability (Buzo 2008 model).

Model	Rank	Area (km^2)
M_1	None	1521.80
	Very Low	118.51
	Low	27.54
	Medium	15.17
	High	18.55
M_2	None	1403.05
	Very Low	80.04
	Low	182.36
	Medium	17.56
	High	18.55
M_3	None	1410.79
	Very Low	233.64
	Low	30.60
	Medium	7.99
	High	18.55
M_4	None	1271.01
	Low	306.70
	Medium	60.08
	High	21.81
	Reintroduction	41.97
Buzo (2008) Canopy + Soil Model	None	289.27
	Very Low	918.85
	Low	289.27
	Medium	102.09
	High	102.09

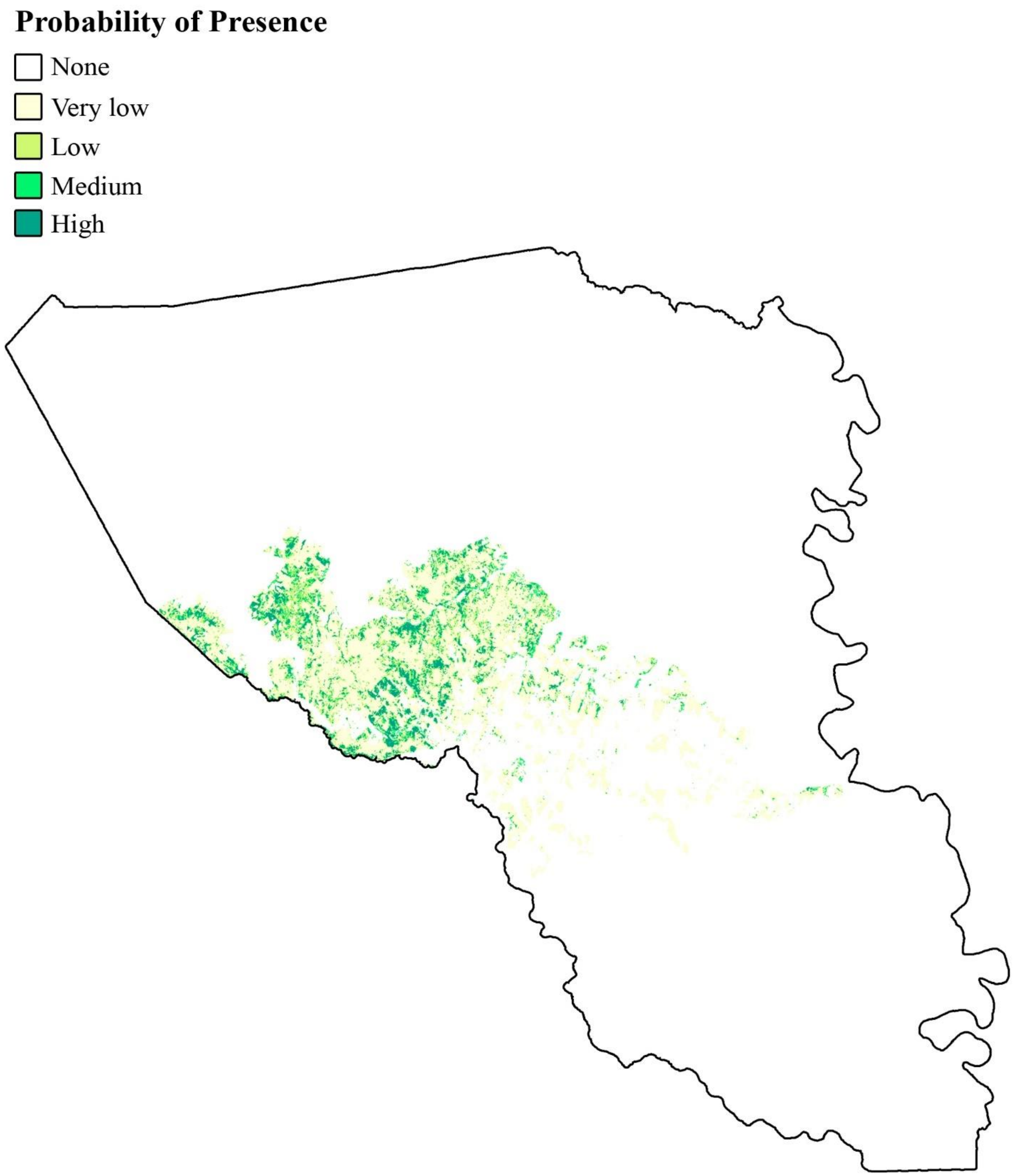

Figure 8. Model 1: occurrence-informed presence prediction model of Austin County.

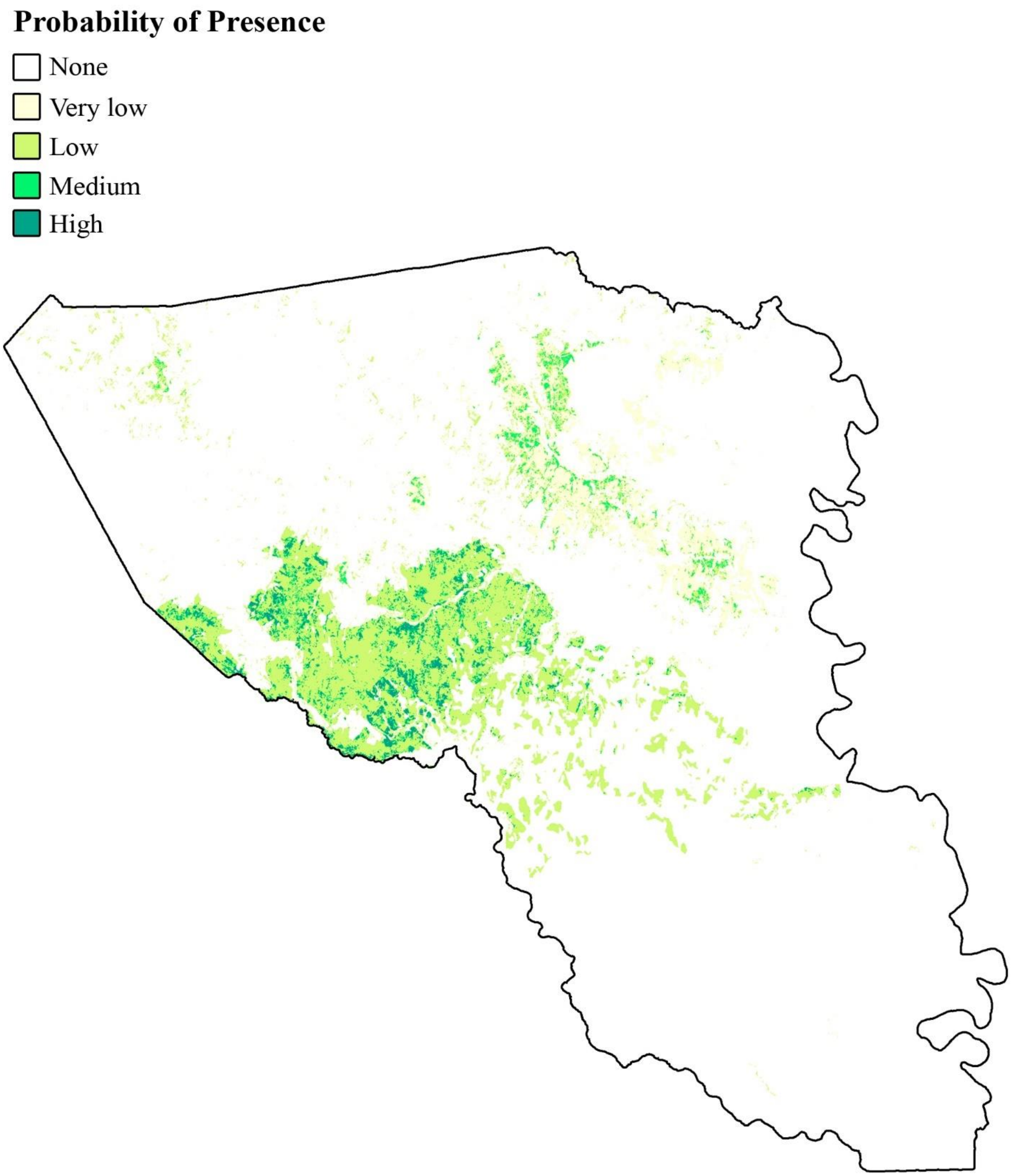

Figure 9. Model 2: evenly weighted presence prediction model of Austin County.

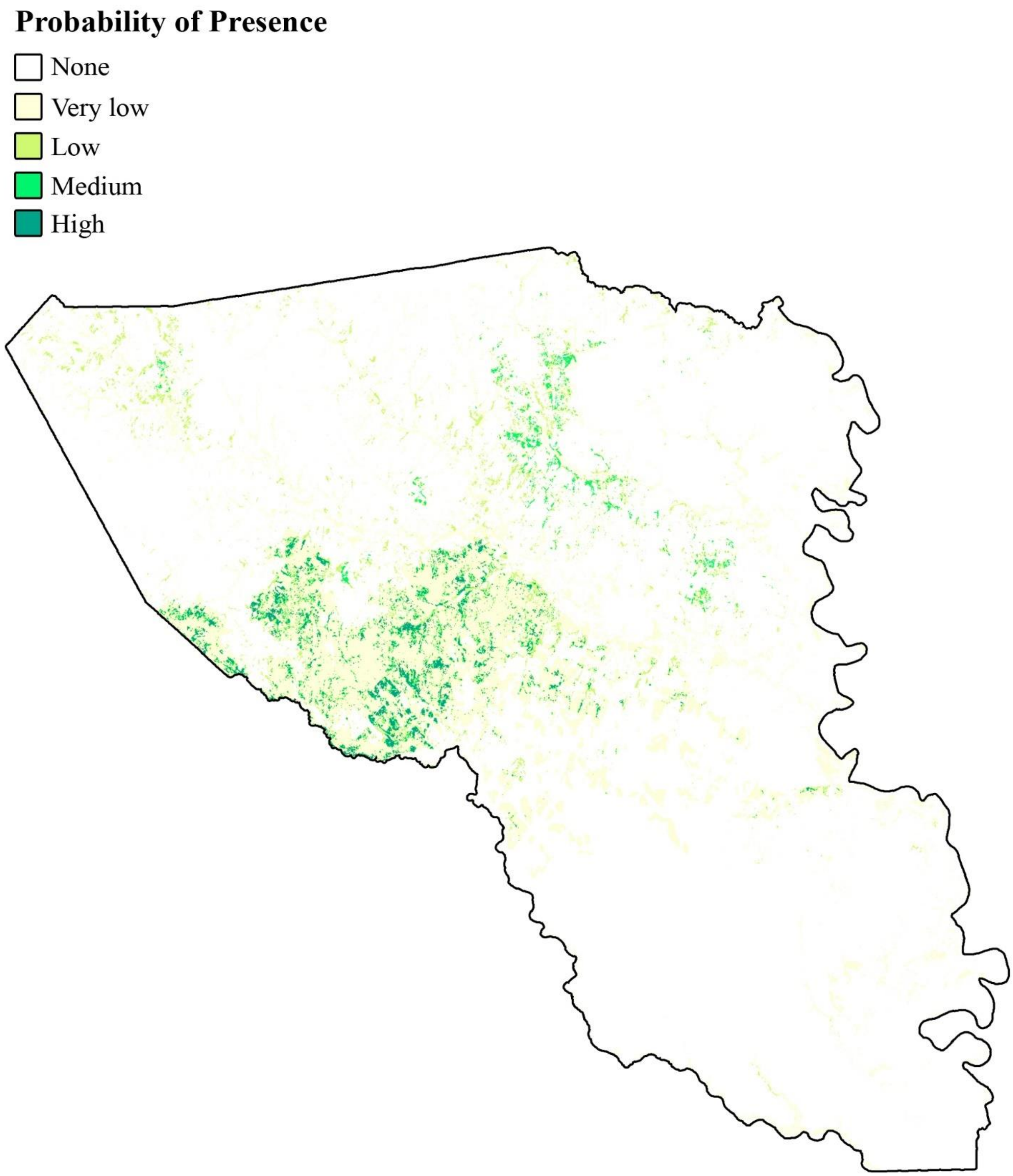

Figure 10. Model 3: integrated substrate presence prediction model of Austin County.

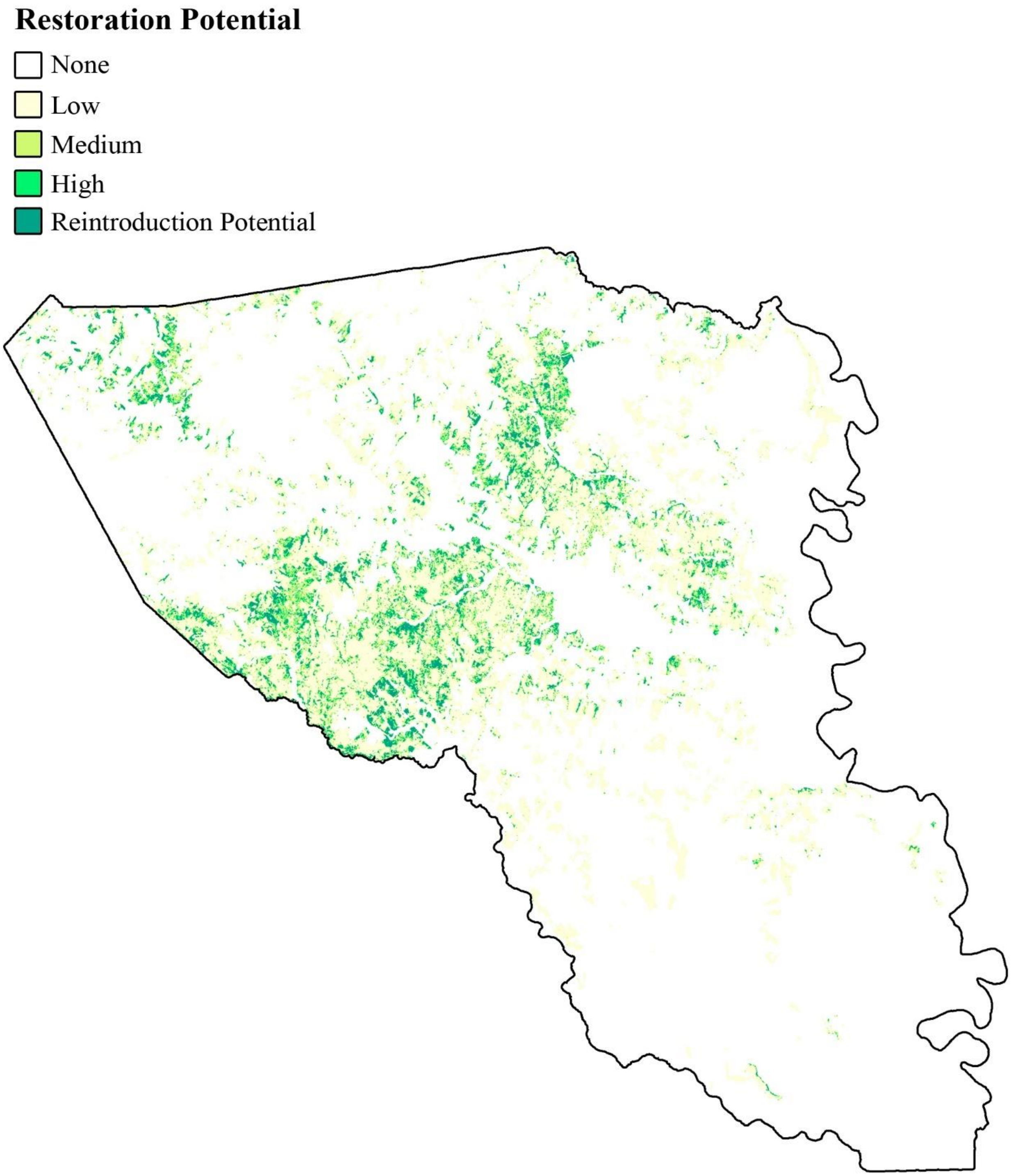

Figure 11. Model 4: restoration and reintroduction potential in Austin County.

Bastrop County

Table 5. Predicted areas in Bastrop County ranked by probability of presence (M_1, M_2, and M_3), restoration potential (M_4), and habitat suitability (Buzo 2008 model).

Model	Rank	Area (km^2)
M_1	None	1879.33
	Very Low	339.60
	Low	54.28
	Medium	17.79
	High	28.20
M_2	None	1302.28
	Very Low	446.75
	Low	500.49
	Medium	41.47
	High	28.20
M_3	None	1723.34
	Very Low	514.16
	Low	28.13
	Medium	25.37
	High	28.20
M_4	None	678.70
	Low	1361.00
	Medium	172.12
	High	43.46
	Reintroduction	63.90
Buzo (2008) Canopy + Soil Model	None	371.09
	Very Low	858.15
	Low	208.74
	Medium	603.03
	High	255.13

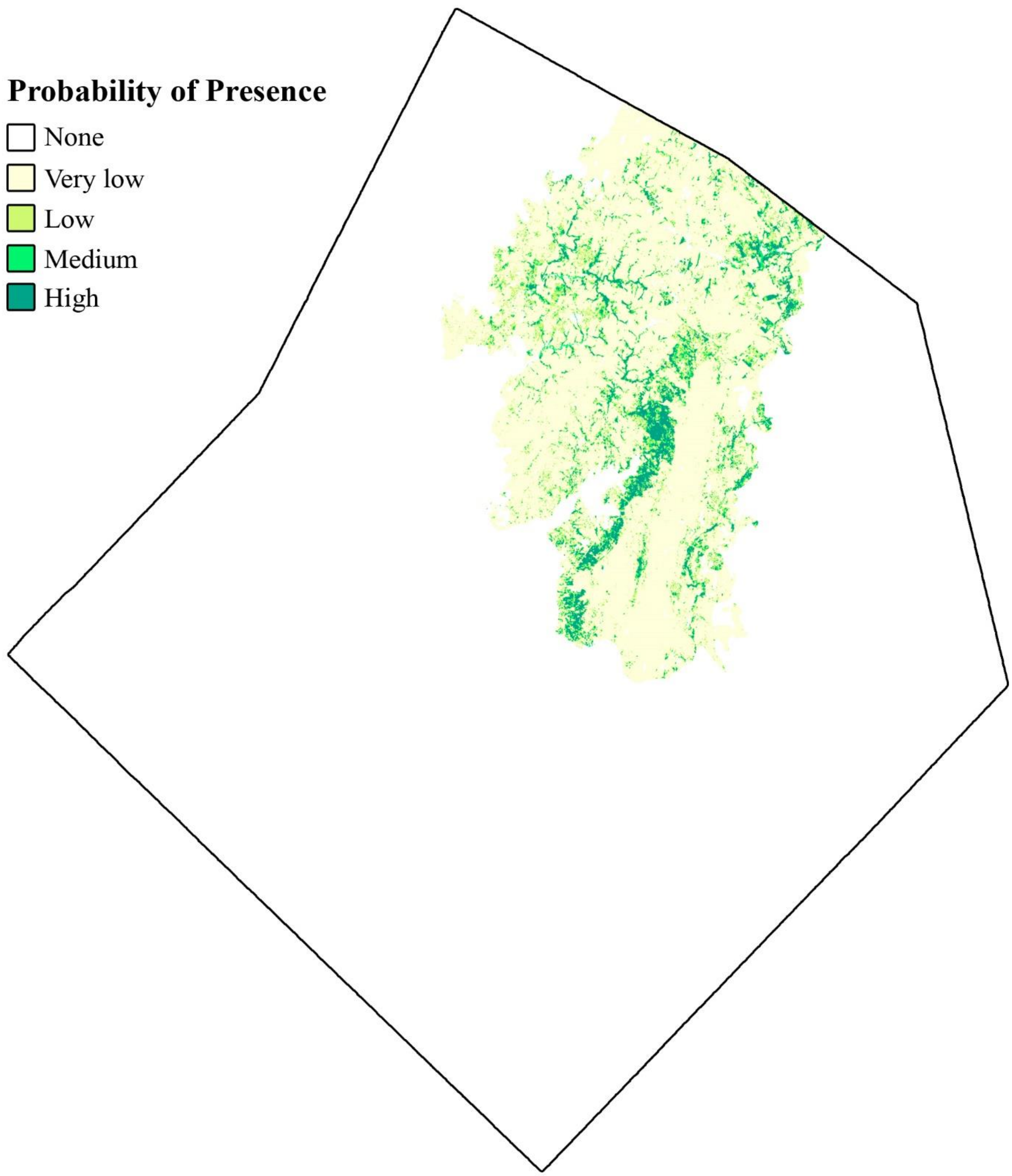

Figure 12. Model 1: occurrence-informed presence prediction model of Bastrop County.

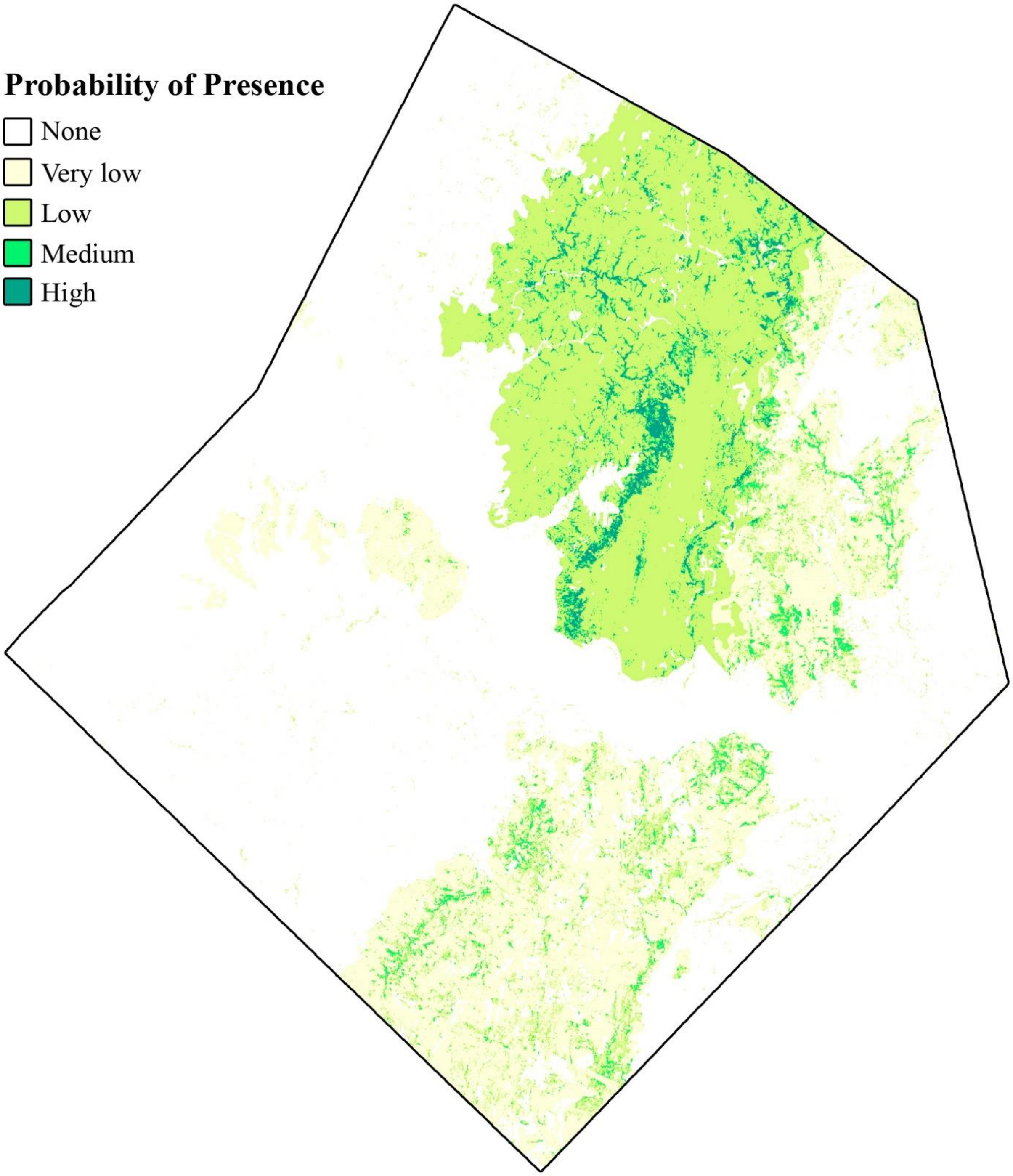

Figure 13. Model 2: evenly weighted presence prediction model of Bastrop County.

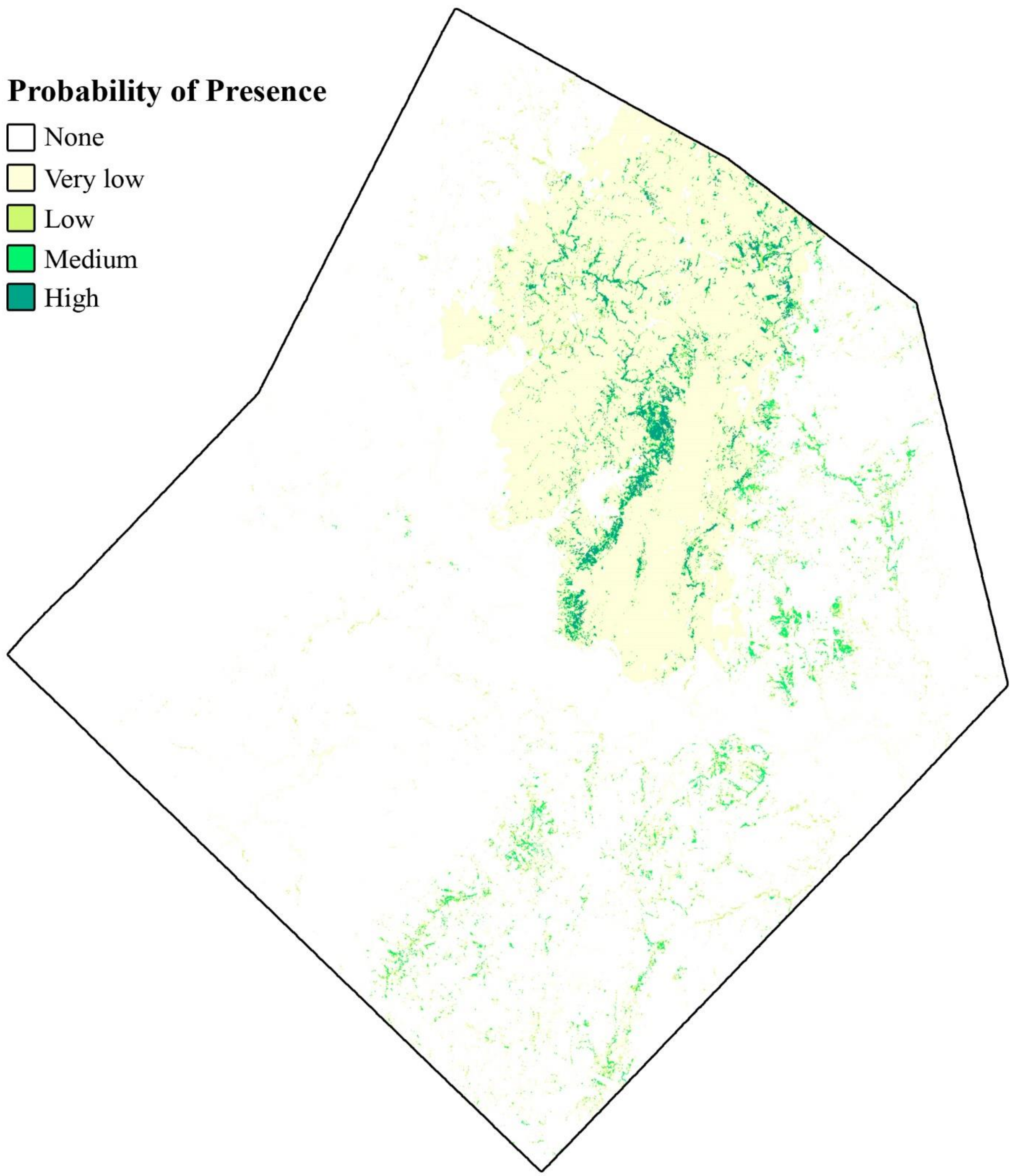

Figure 14. Model 3: integrated substrate presence prediction model of Bastrop County.

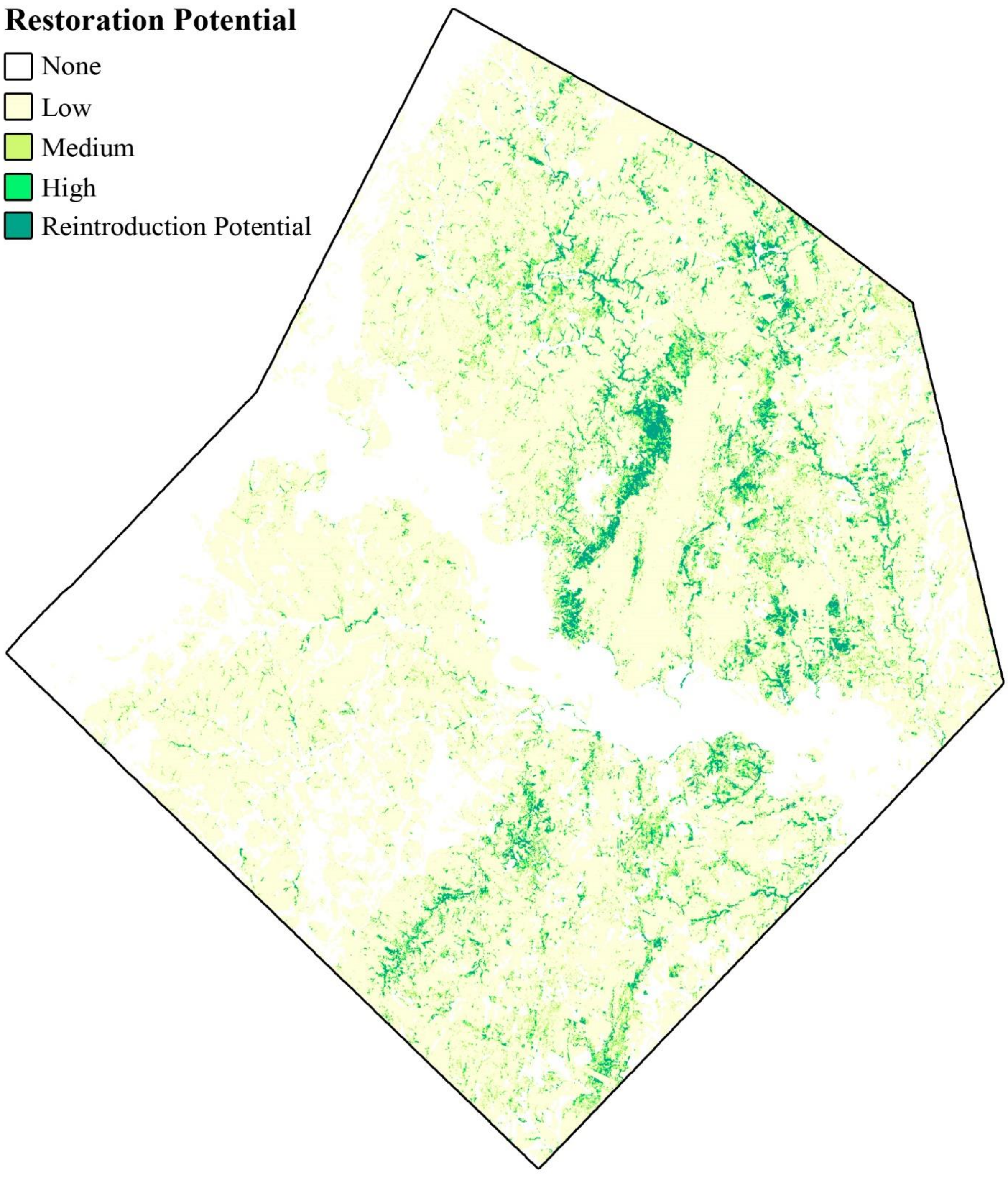

Figure 15. Model 4: restoration and reintroduction potential in Bastrop County.

Brazos County

Table 6. Predicted areas in Brazos County ranked by probability of presence (M_1, M_2, and M_3), restoration potential (M_4), and habitat suitability (Buzo 2008 model).

Model	Rank	Area (km^2)
M_1	None	1532.62
	Very Low	0.00
	Low	0.00
	Medium	0.00
	High	0.00
M_2	None	1418.69
	Very Low	86.70
	Low	24.07
	Medium	3.17
	High	0.00
M_3	None	1422.02
	Very Low	95.30
	Low	12.14
	Medium	3.17
	High	0.00
M_4	None	1271.27
	Low	201.92
	Medium	33.19
	High	10.94
	Reintroduction	15.31
Buzo (2008) Canopy + Soil Model	None	NA
	Very Low	NA
	Low	NA
	Medium	NA
	High	NA

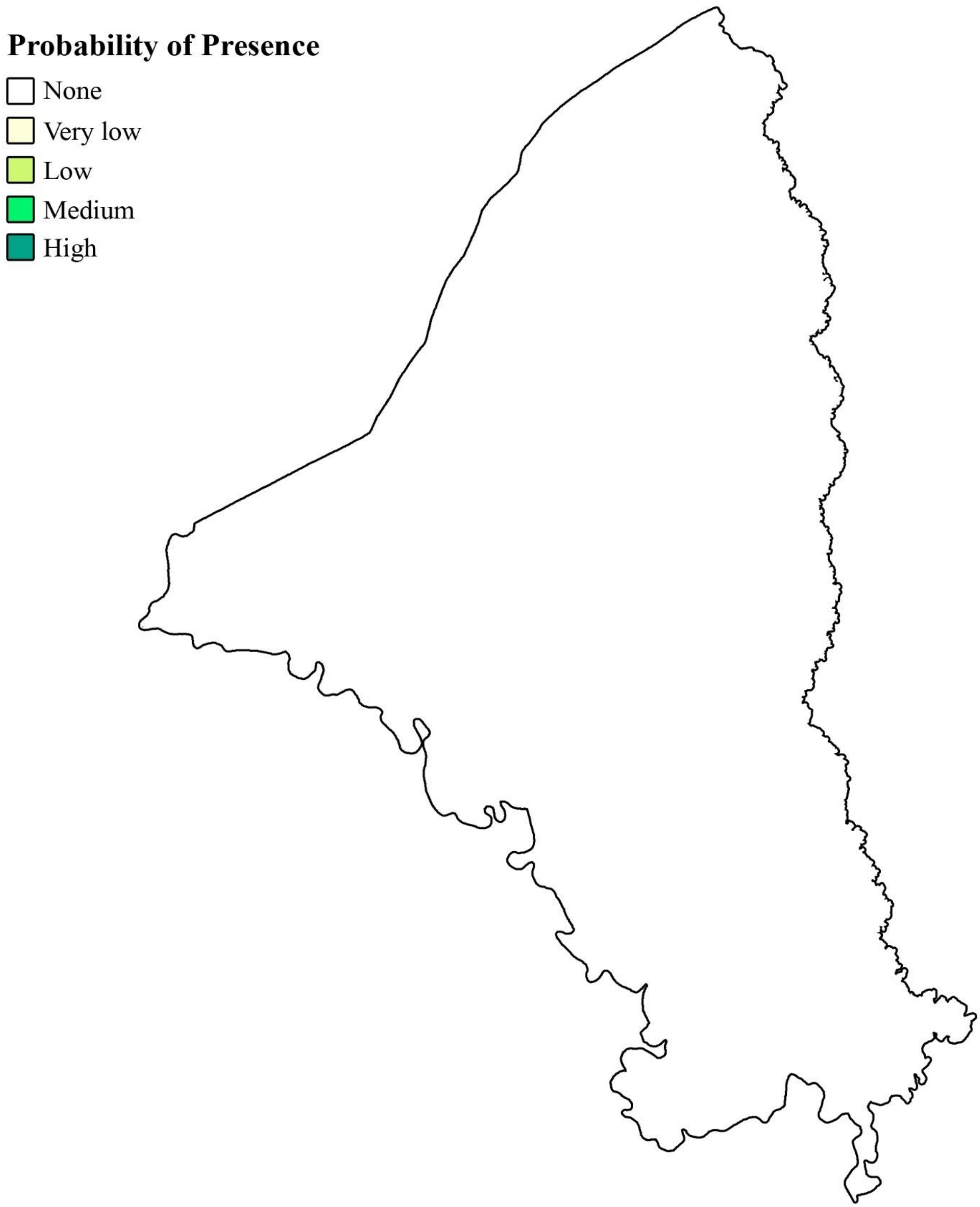

Figure 16. Model 1: occurrence-informed presence prediction model of Brazos County.

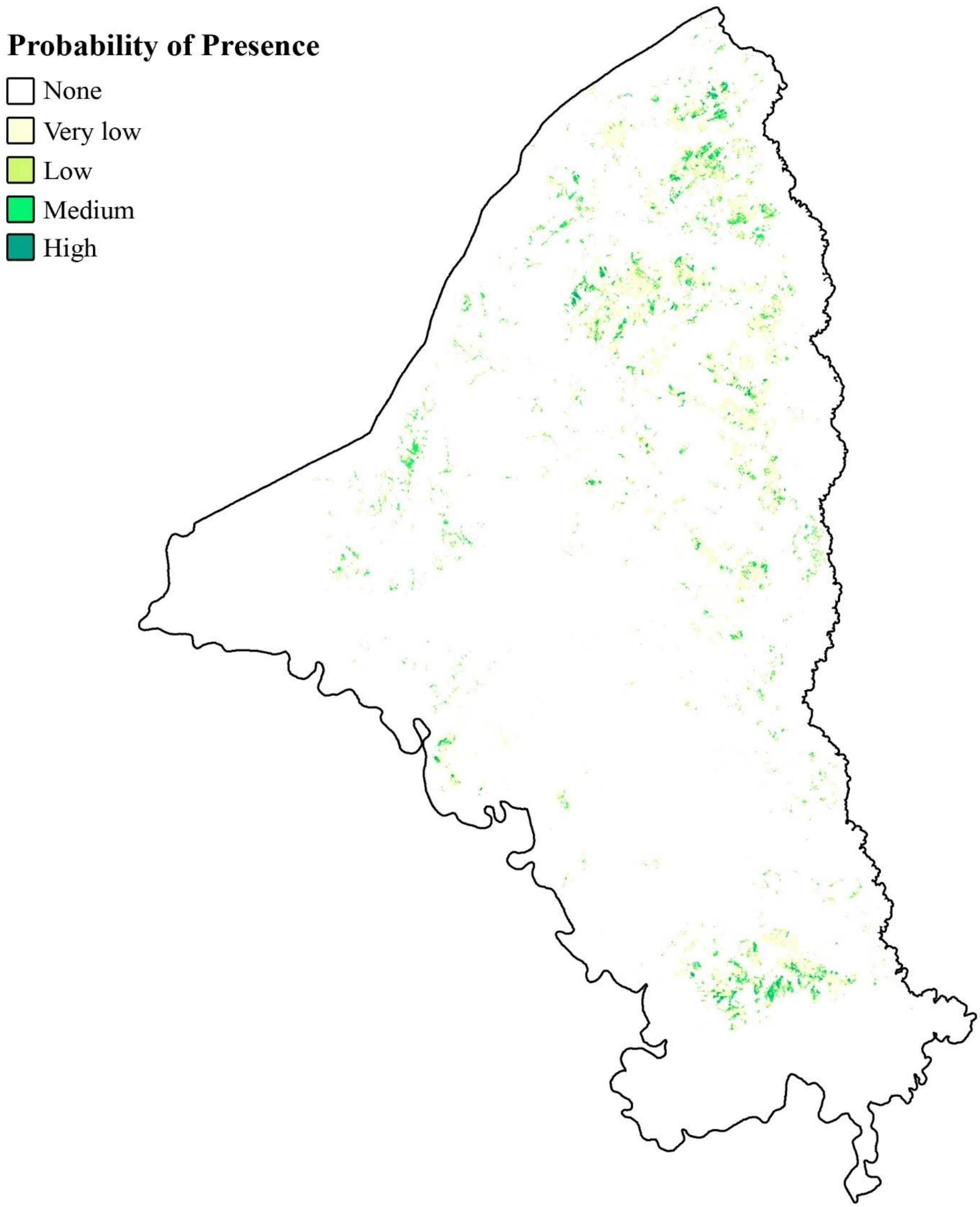

Figure 17. Model 2: evenly weighted presence prediction model of Brazos County.

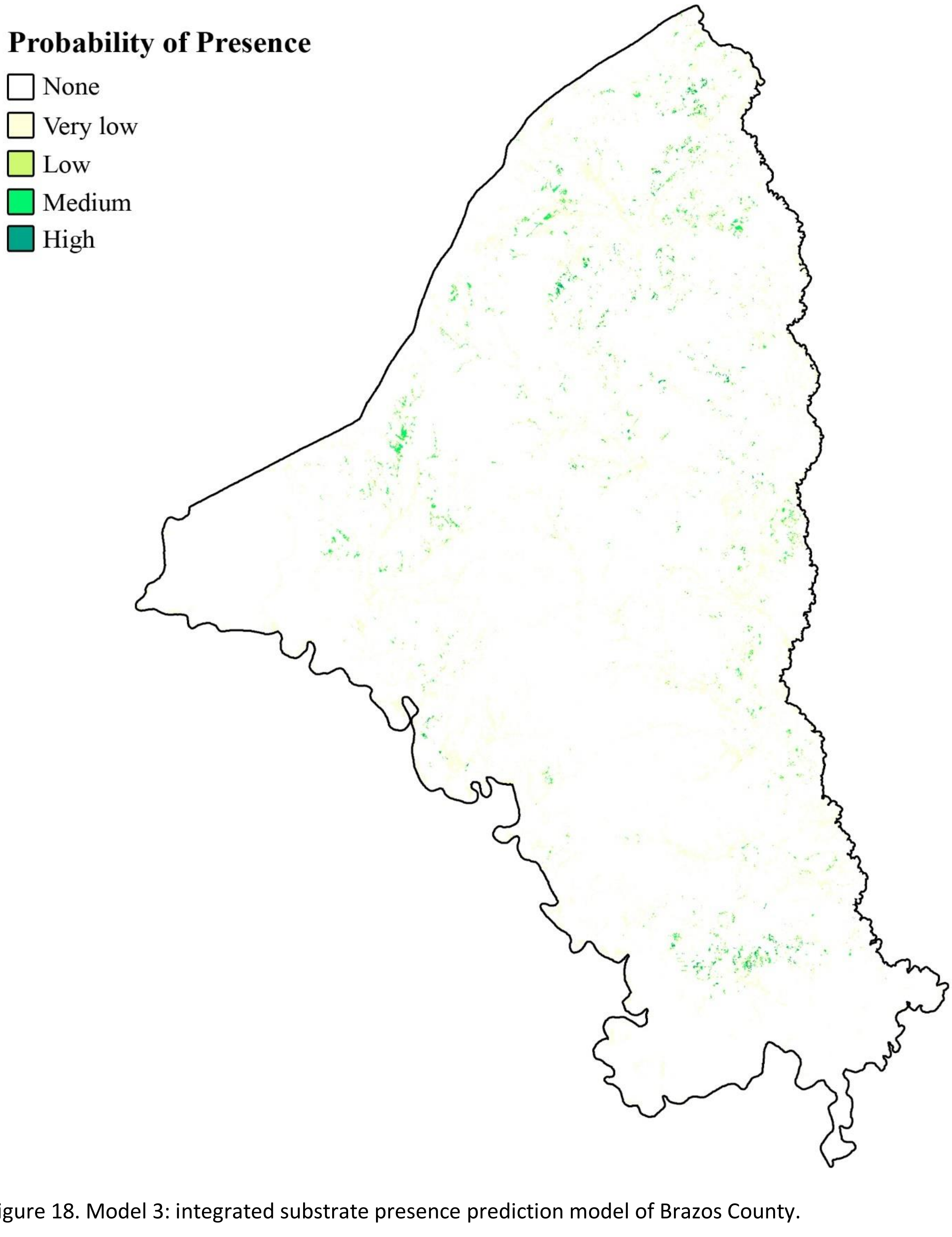

Figure 18. Model 3: integrated substrate presence prediction model of Brazos County.

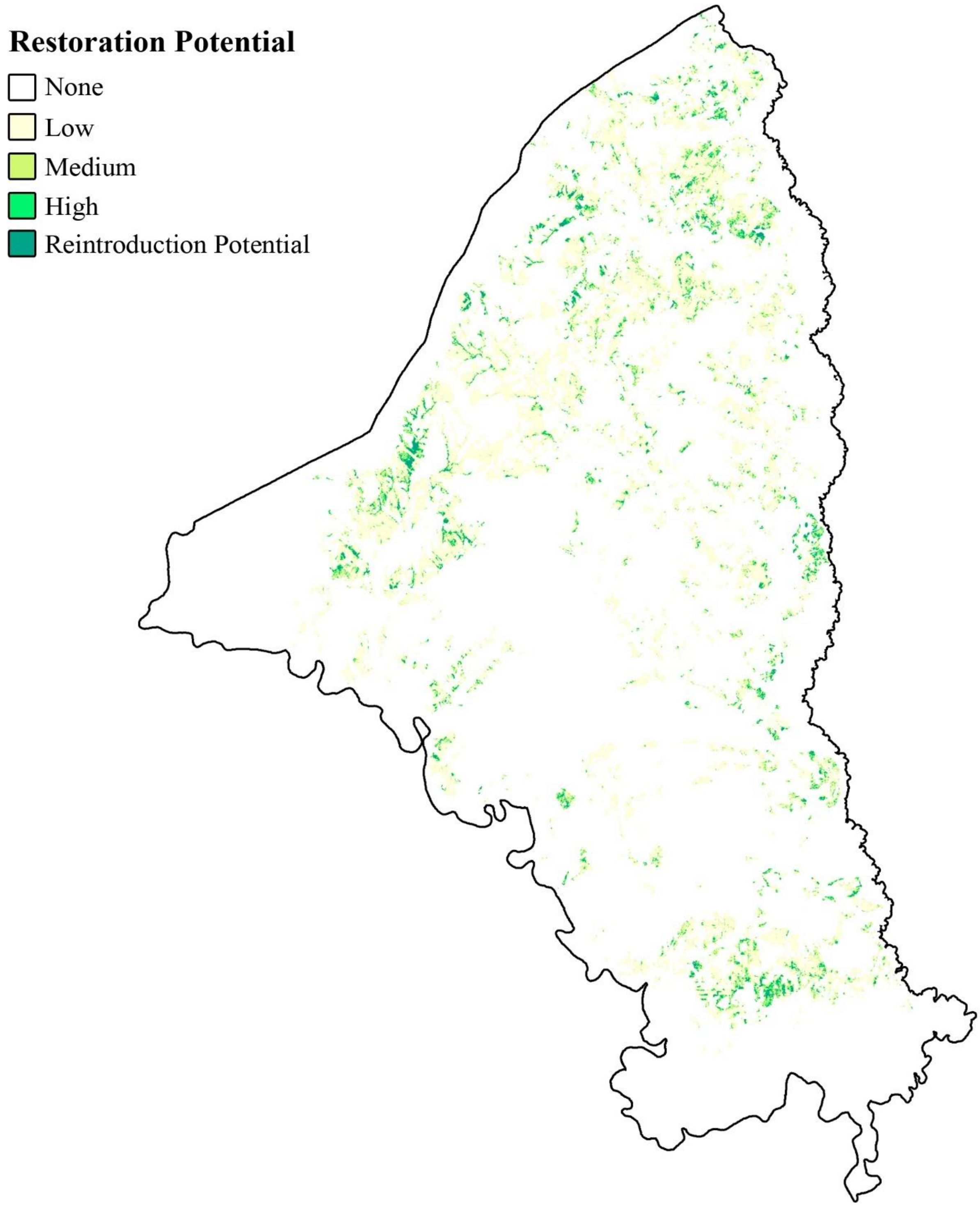

Figure 19. Model 4: restoration and reintroduction potential in Brazos County.

Burleson County

Table 7. Predicted areas in Burleson County ranked by probability of presence (M_1, M_2, and M_3), restoration potential (M_4), and habitat suitability (Buzo 2008 model).

Model	Rank	Area (km^2)
M_1	None	1471.00
	Very Low	174.65
	Low	51.29
	Medium	27.89
	High	29.11
M_2	None	1357.16
	Very Low	77.89
	Low	263.32
	Medium	26.45
	High	29.11
M_3	None	1375.01
	Very Low	300.95
	Low	39.97
	Medium	8.90
	High	29.11
M_4	None	1208.16
	Low	374.91
	Medium	90.28
	High	30.50
	Reintroduction	50.08
Buzo (2008) Canopy + Soil Model	None	105.24
	Very Low	1192.68
	Low	157.85
	Medium	245.55
	High	52.62

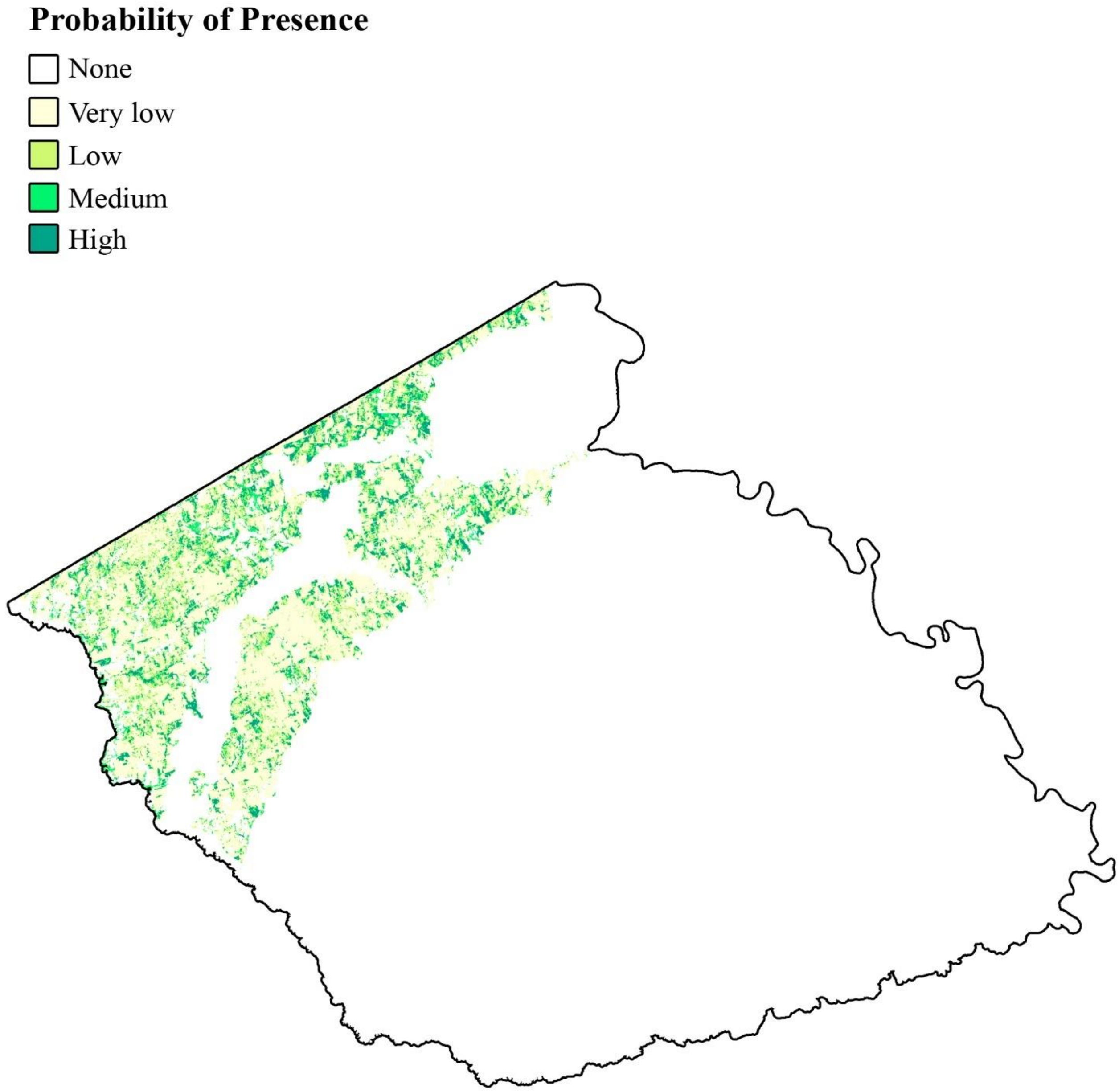

Figure 20. Model 1: occurrence-informed presence prediction model of Burleson County.

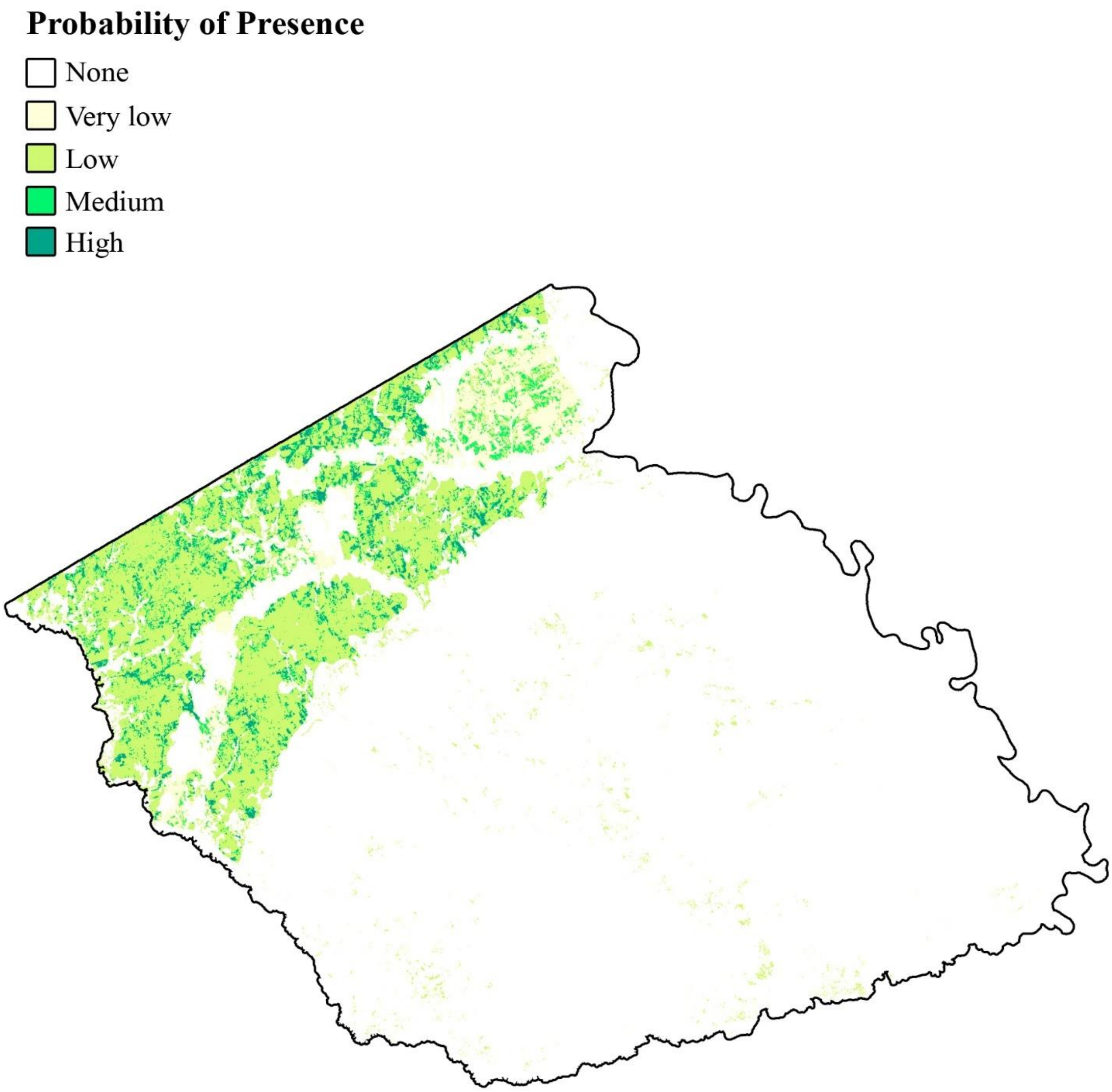

Figure 21. Model 2: evenly weighted presence prediction model of Burleson County.

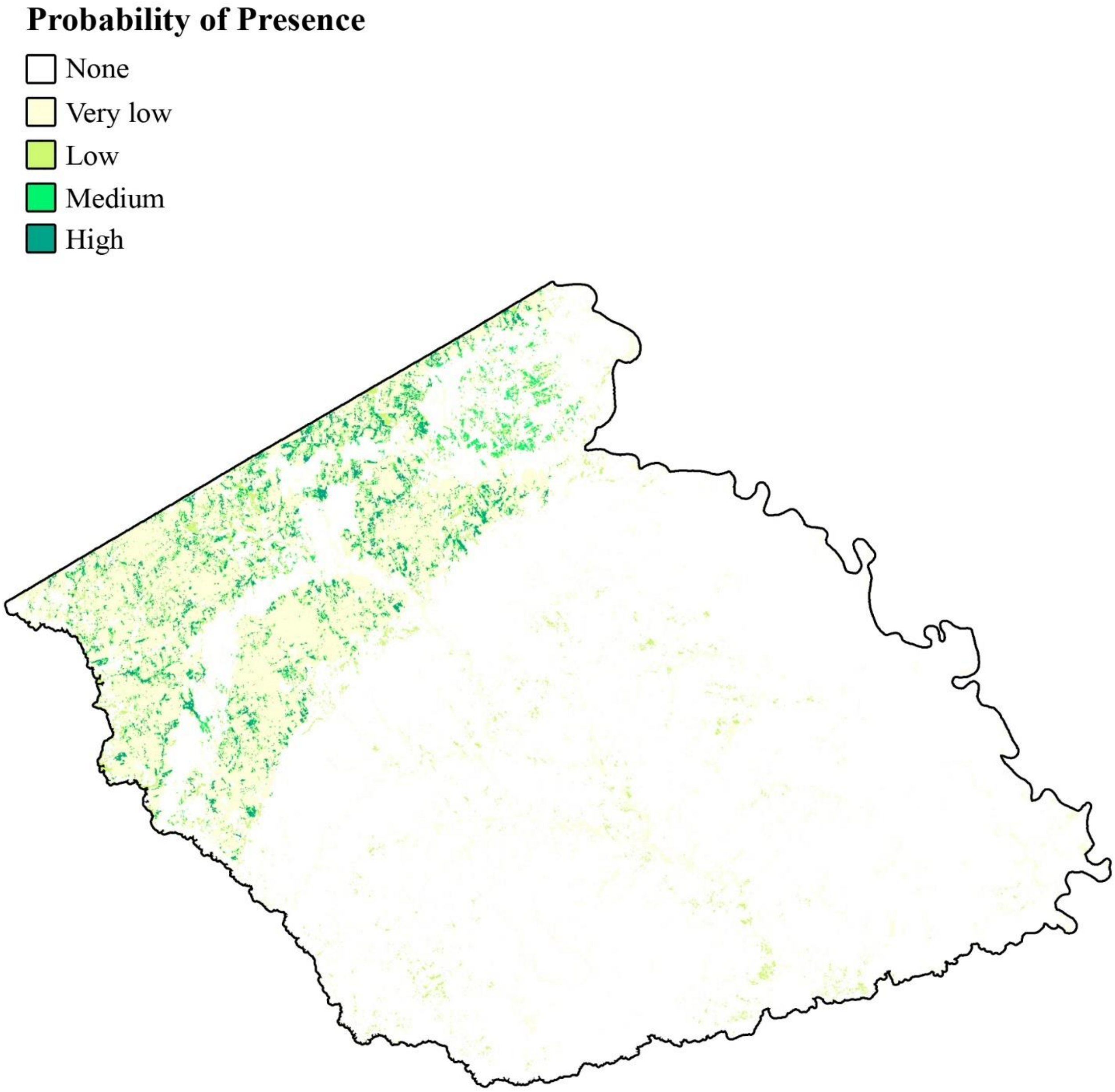

Figure 22. Model 3: integrated substrate presence prediction model of Burleson County.

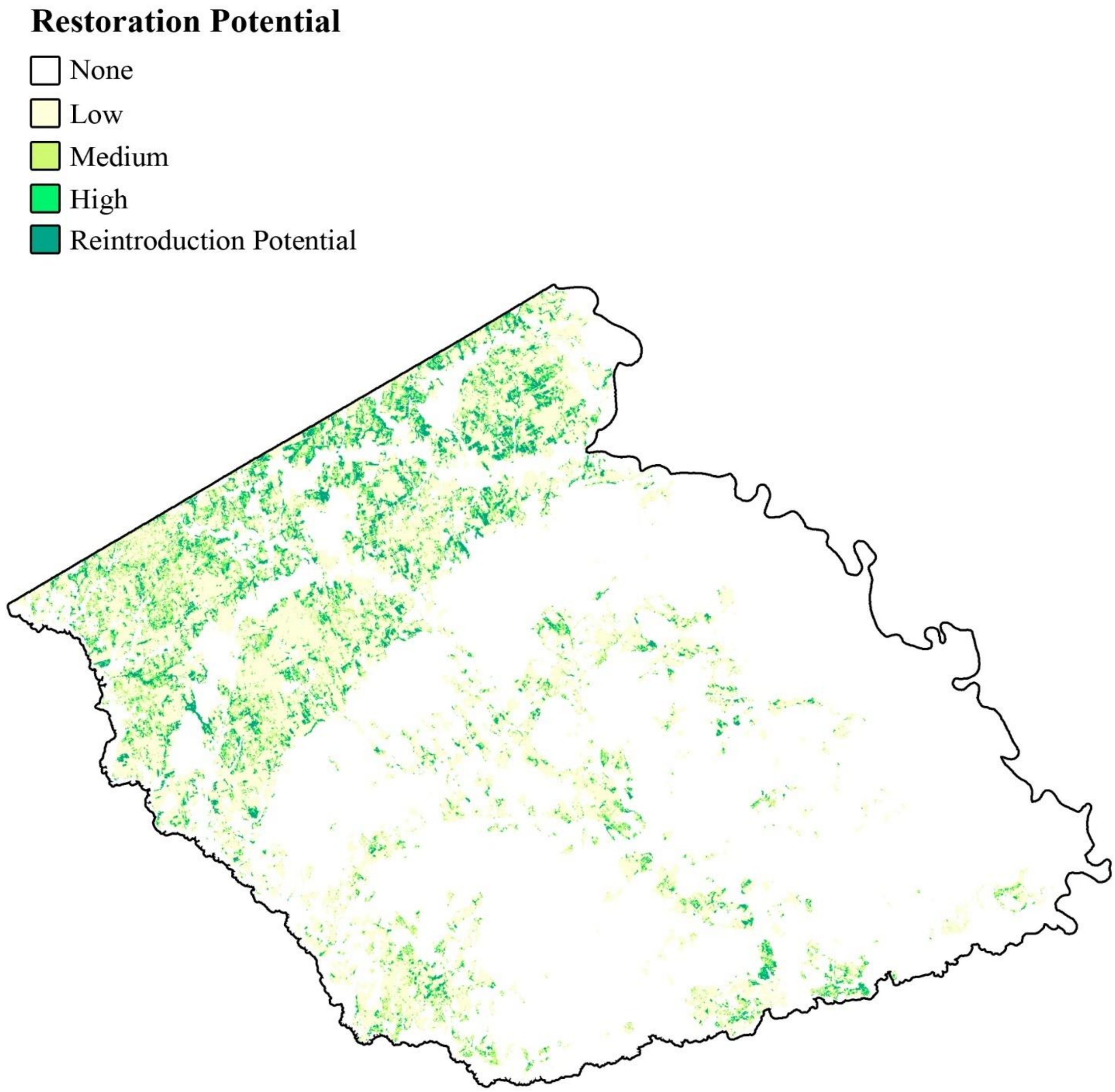

Figure 23. Model 4: restoration and reintroduction potential in Burleson County.

Colorado County

Table 8. Predicted areas in Colorado County ranked by probability of presence (M_1, M_2, and M_3), restoration potential (M_4), and habitat suitability (Buzo 2008 model).

Model	Rank	Area (km^2)
M_1	None	2140.62
	Very Low	273.01
	Low	54.49
	Medium	26.24
	High	29.04
M_2	None	2049.99
	Very Low	71.10
	Low	354.42
	Medium	18.85
	High	29.04
M_3	None	2049.28
	Very Low	408.55
	Low	33.97
	Medium	2.56
	High	29.04
M_4	None	1983.30
	Low	397.90
	Medium	79.50
	High	23.38
	Reintroduction	39.33
Buzo (2008) Canopy + Soil Model	None	328.04
	Very Low	1261.70
	Low	479.45
	Medium	277.57
	High	176.64

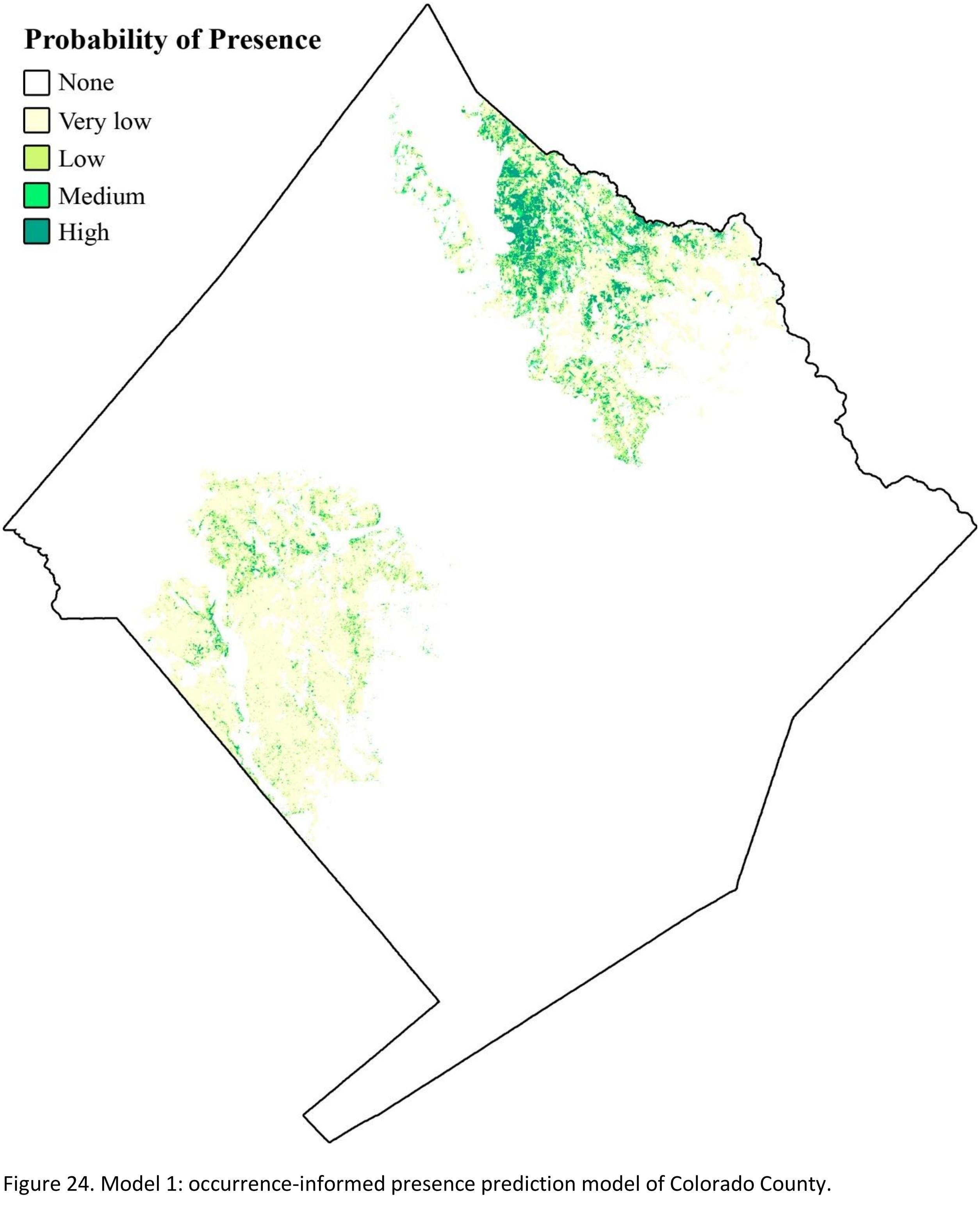

Figure 24. Model 1: occurrence-informed presence prediction model of Colorado County.

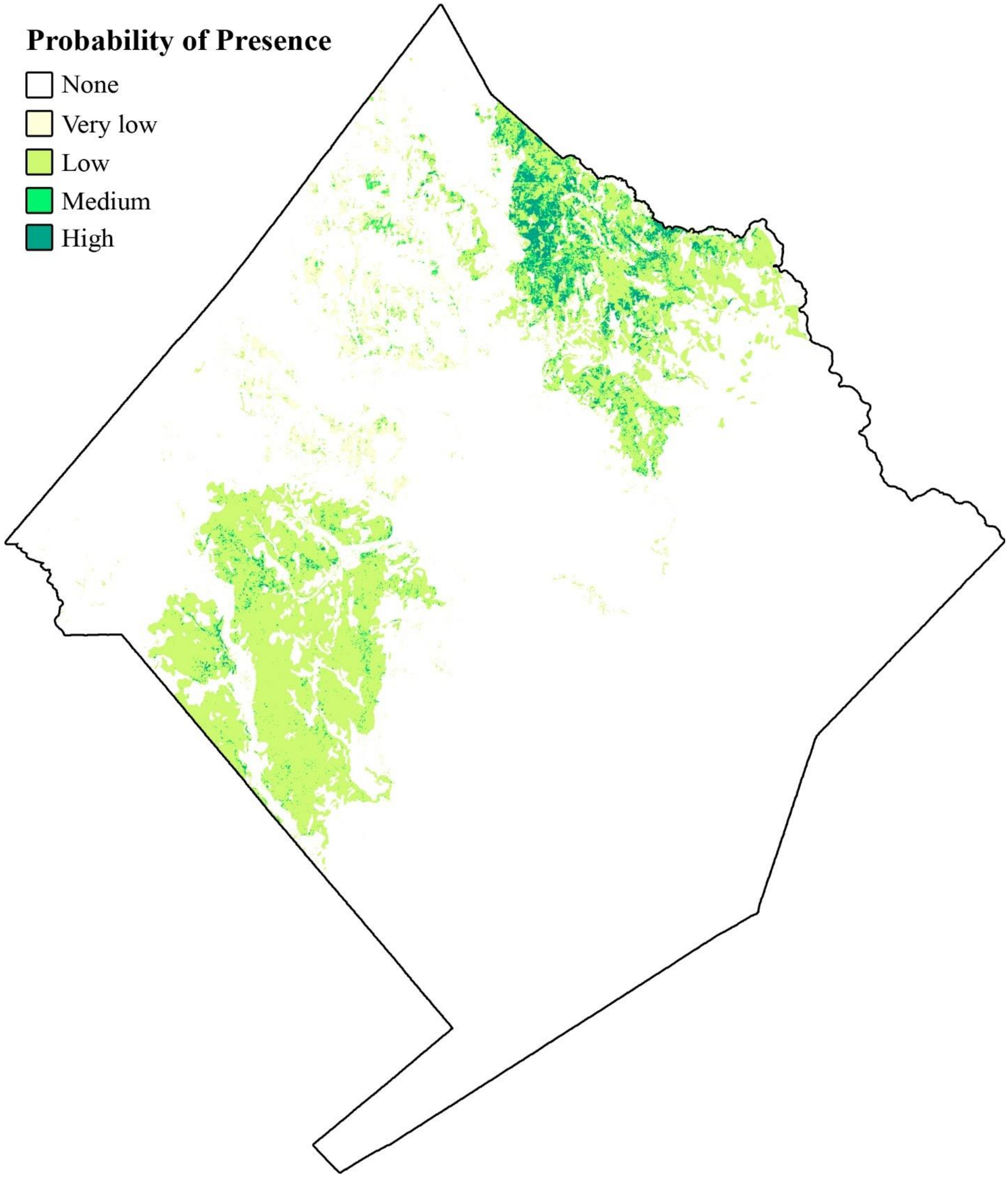

Figure 25. Model 2: evenly weighted presence prediction model of Colorado County.

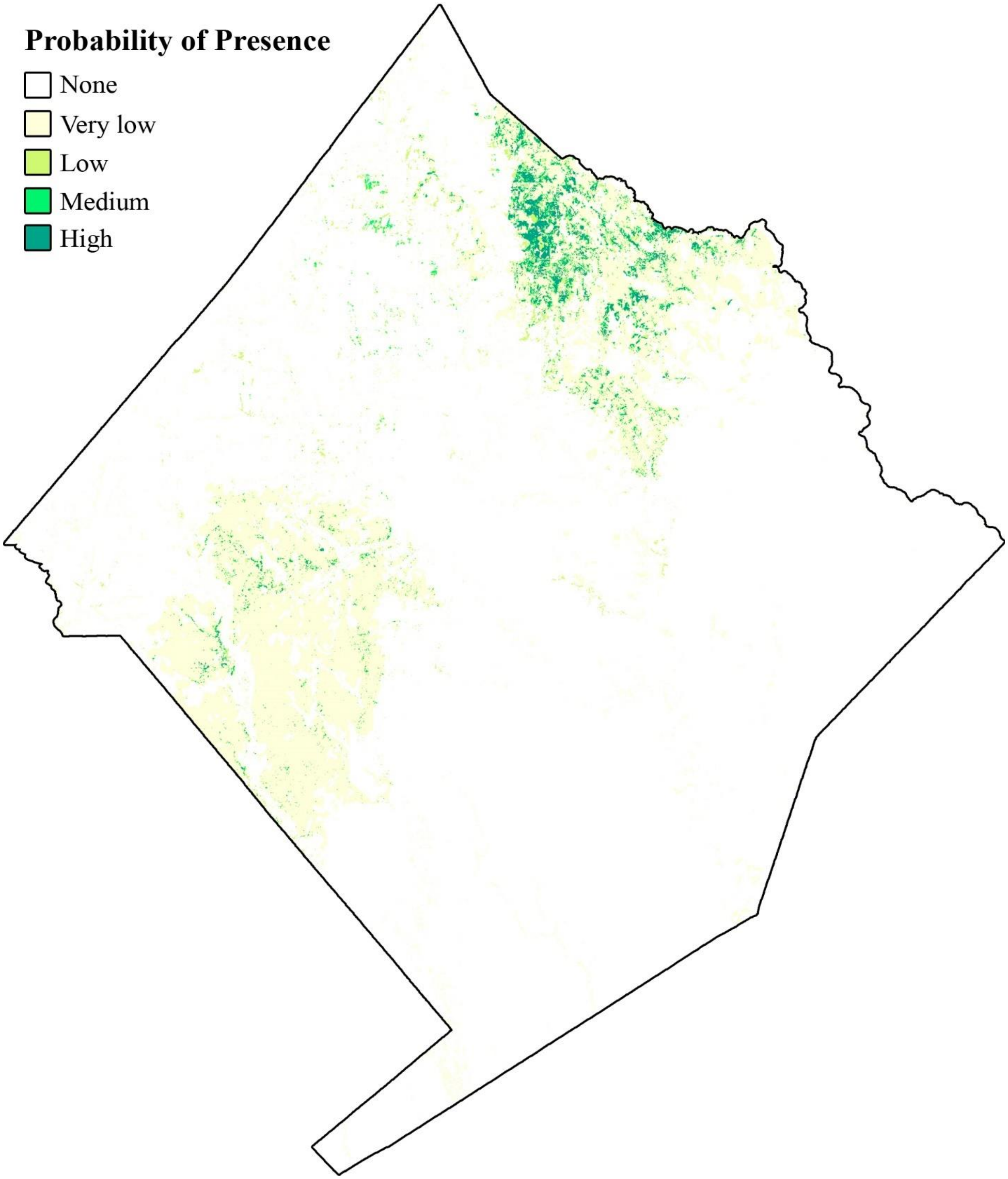

Figure 26. Model 3: integrated substrate presence prediction model of Colorado County.

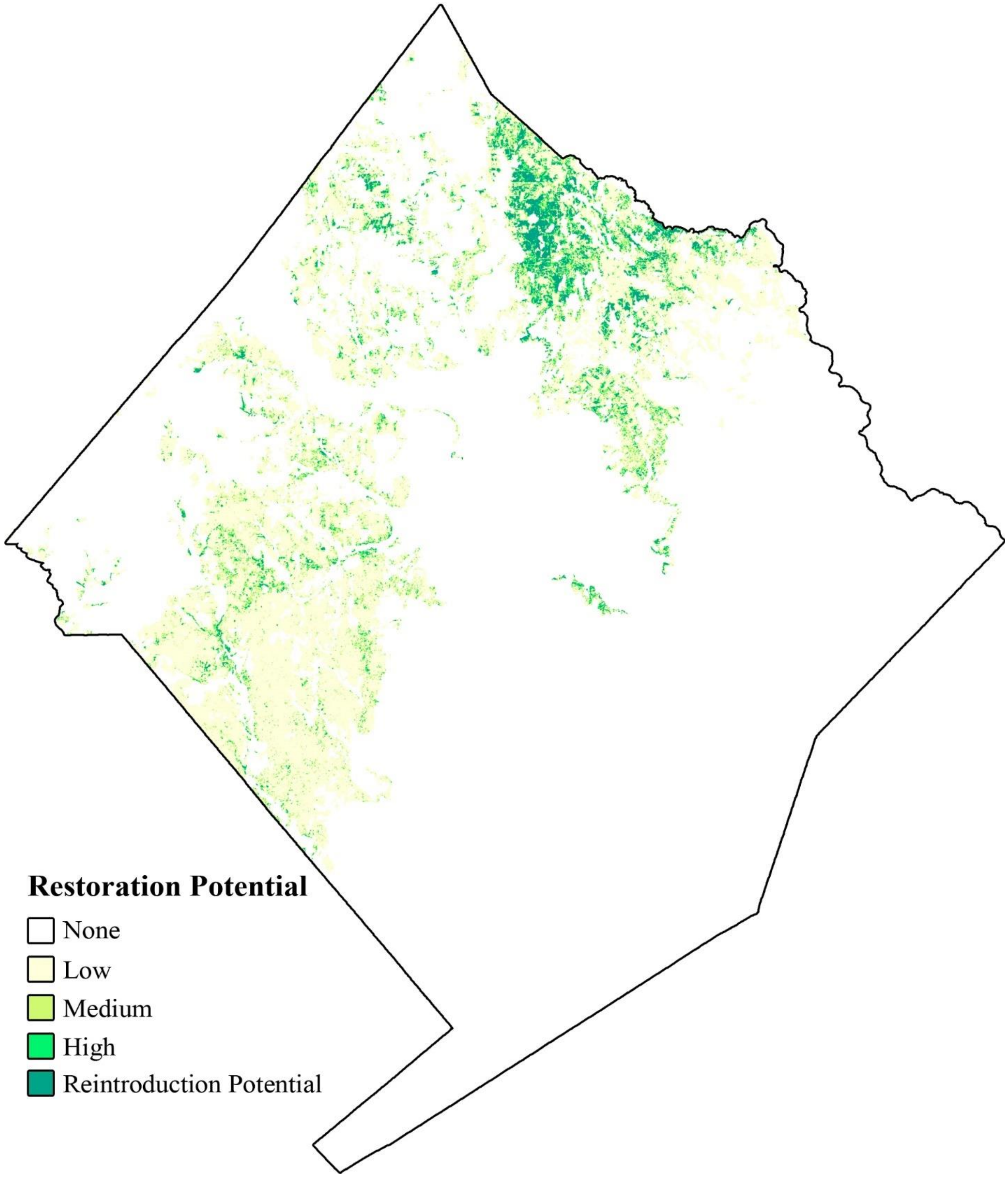

Figure 27. Model 4: restoration and reintroduction potential in Colorado County.

Freestone County

Table 9. Predicted areas in Freestone County ranked by probability of presence (M_1, M_2, and M_3), restoration potential (M_4), and habitat suitability (Buzo 2008 model).

Model	Rank	Area (km^2)
M_1	None	2262.39
	Very Low	33.23
	Low	8.57
	Medium	4.51
	High	3.88
M_2	None	1199.06
	Very Low	756.55
	Low	234.28
	Medium	118.81
	High	3.88
M_3	None	1745.63
	Very Low	397.09
	Low	49.43
	Medium	116.54
	High	3.88
M_4	None	957.85
	Low	967.91
	Medium	158.21
	High	63.26
	Reintroduction	165.34
Buzo (2008) Canopy + Soil Model	None	NA
	Very Low	NA
	Low	NA
	Medium	NA
	High	NA

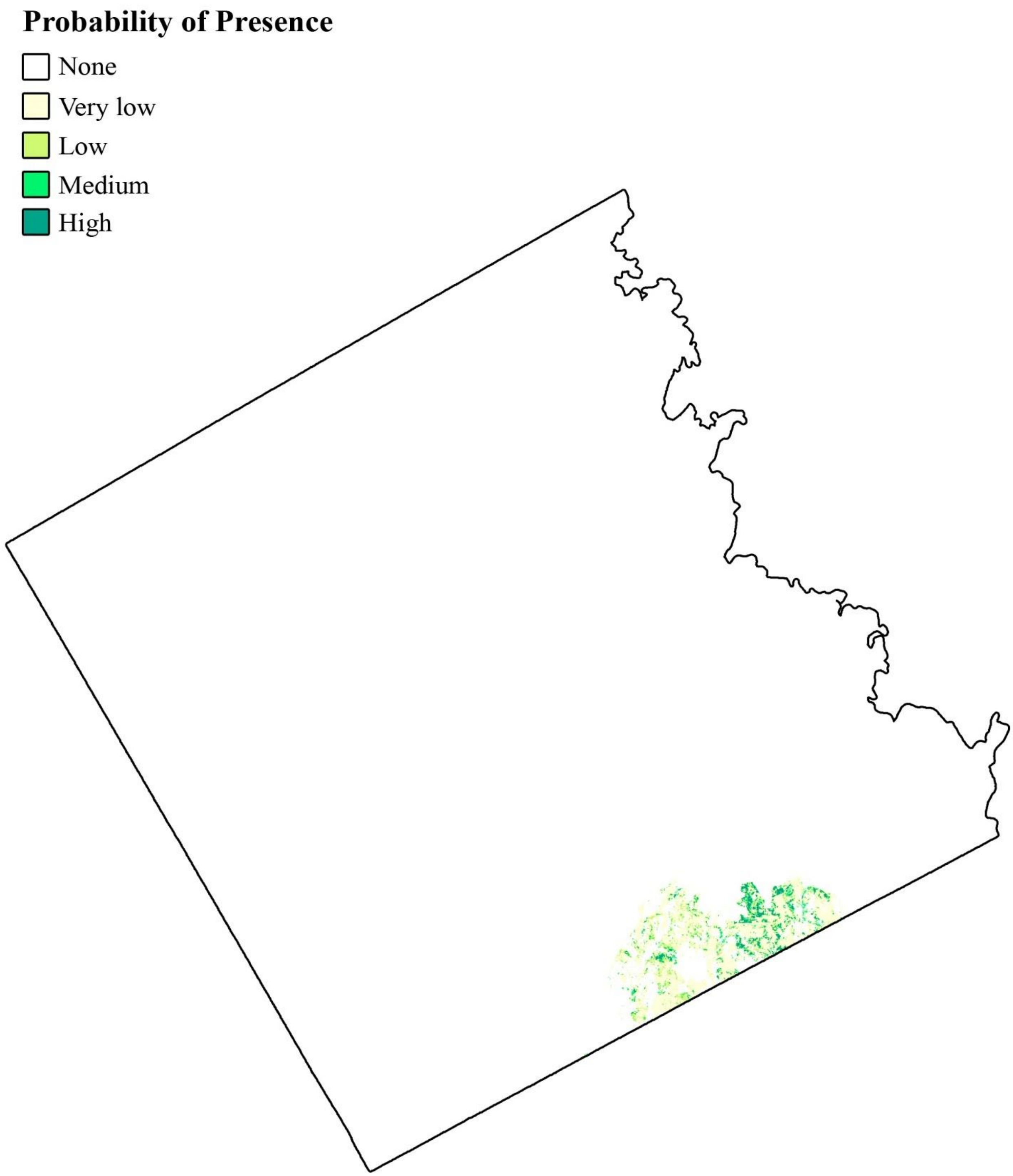

Figure 28. Model 1: occurrence-informed presence prediction model of Freestone County.

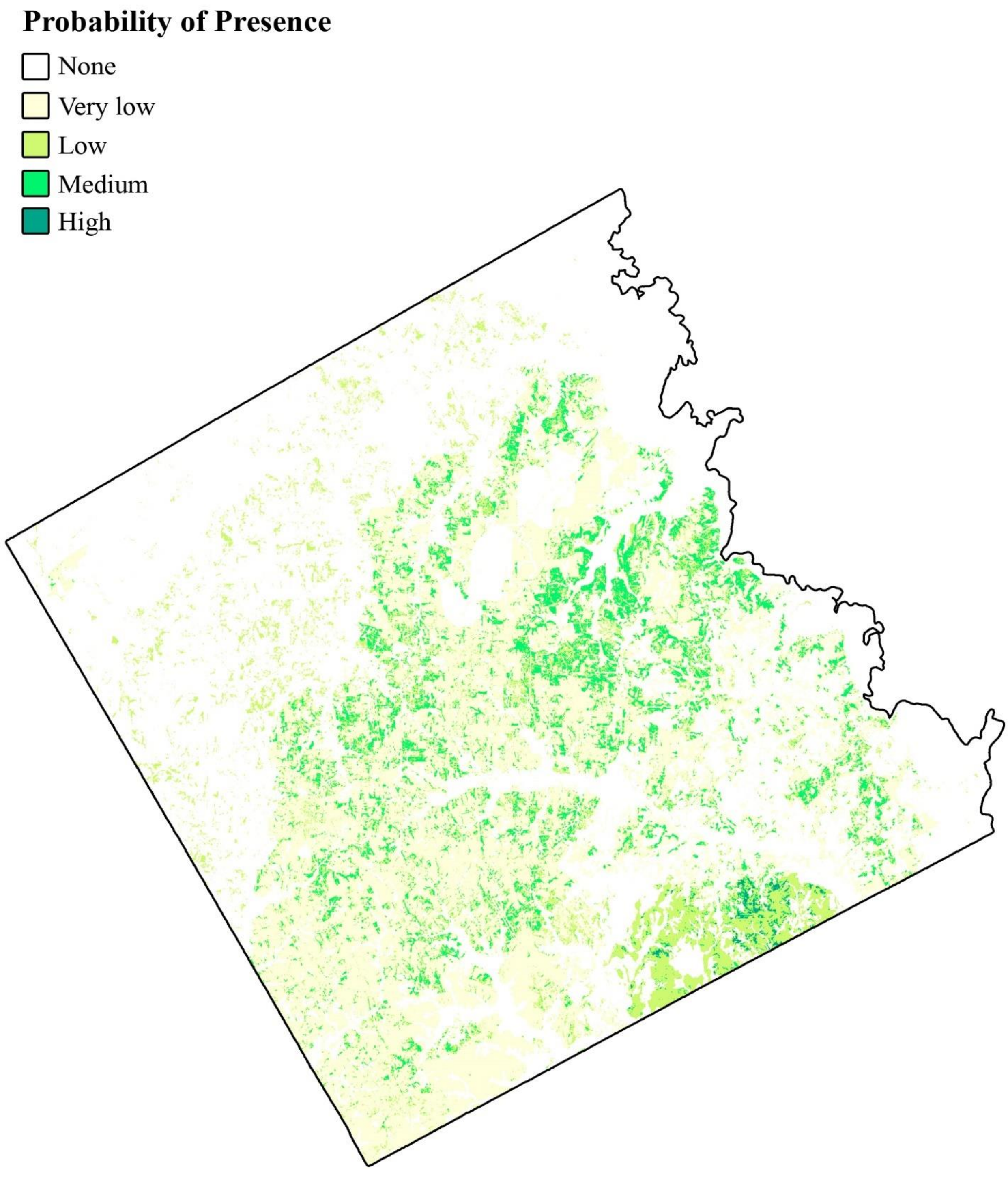

Figure 29. Model 2: evenly weighted presence prediction model of Freestone County.

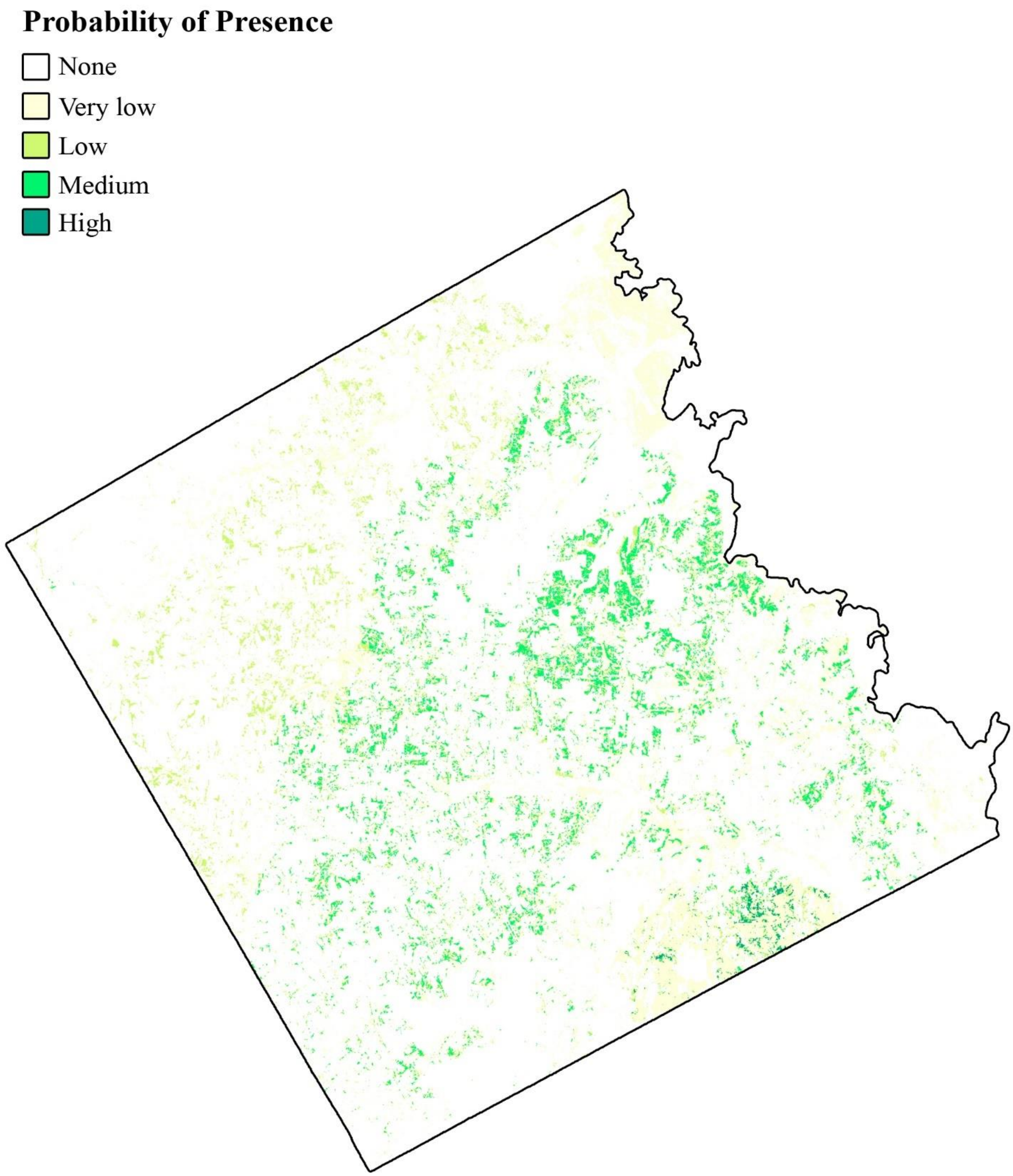

Figure 30. Model 3: integrated substrate presence prediction model of Freestone County.

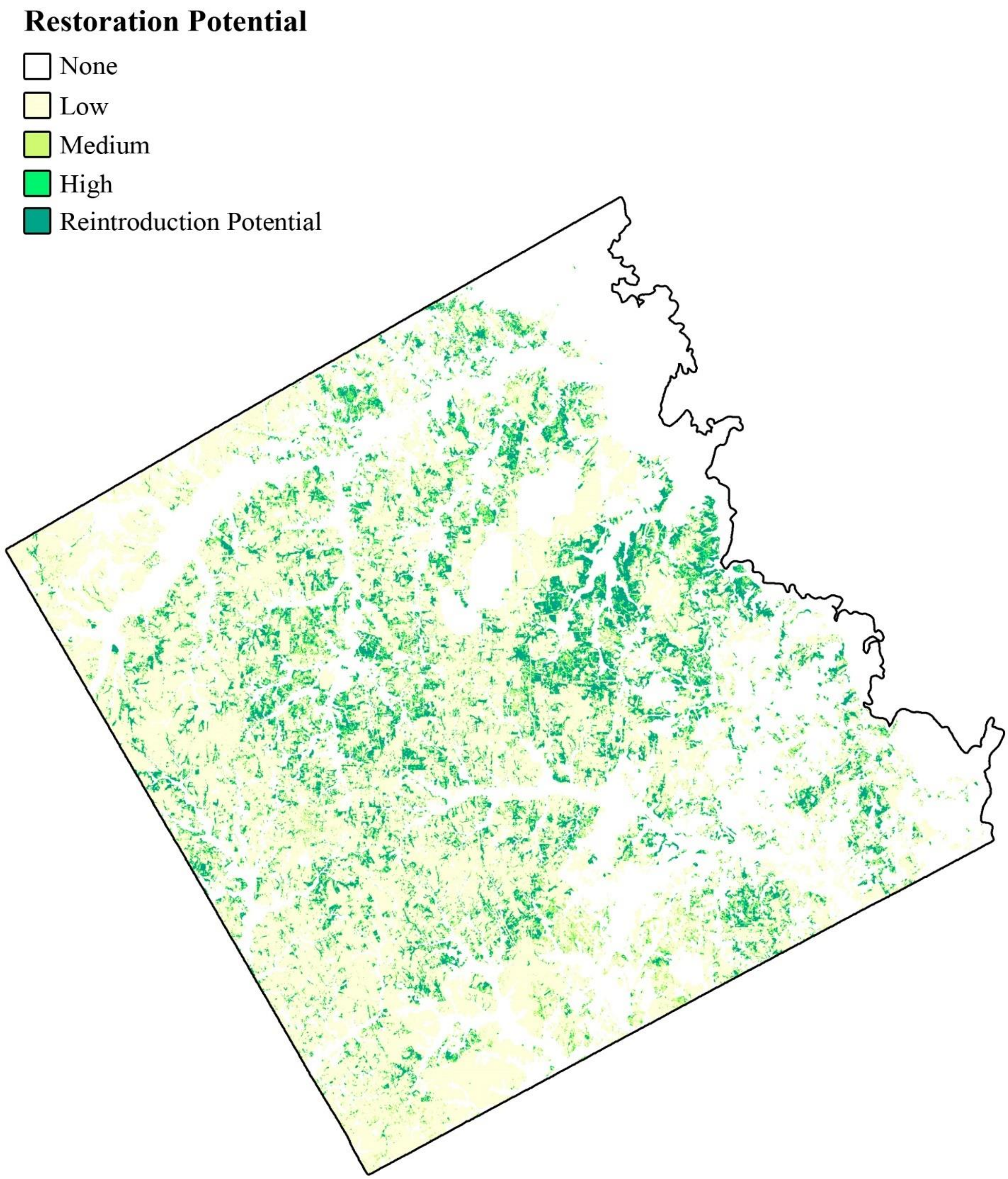

Figure 31. Model 4: restoration and reintroduction potential in Freestone County.

Harris County

Table 10. Predicted areas in Harris County ranked by probability of presence (M_1, M_2, and M_3), restoration potential (M_4), and habitat suitability (Buzo 2008 model).

Model	Rank	Area (km^2)
M_1	None	4517.04
	Very Low	0.84
	Low	0.18
	Medium	13.32
	High	0.20
M_2	None	4499.54
	Very Low	14.03
	Low	17.73
	Medium	0.07
	High	0.20
M_3	None	4247.66
	Very Low	266.94
	Low	16.79
	Medium	0.00
	High	0.20
M_4	None	4516.05
	Low	9.18
	Medium	1.88
	High	0.81
	Reintroduction	3.66
Buzo (2008) Canopy + Soil Model	None	861.00
	Very Low	2764.26
	Low	543.79
	Medium	317.21
	High	90.63

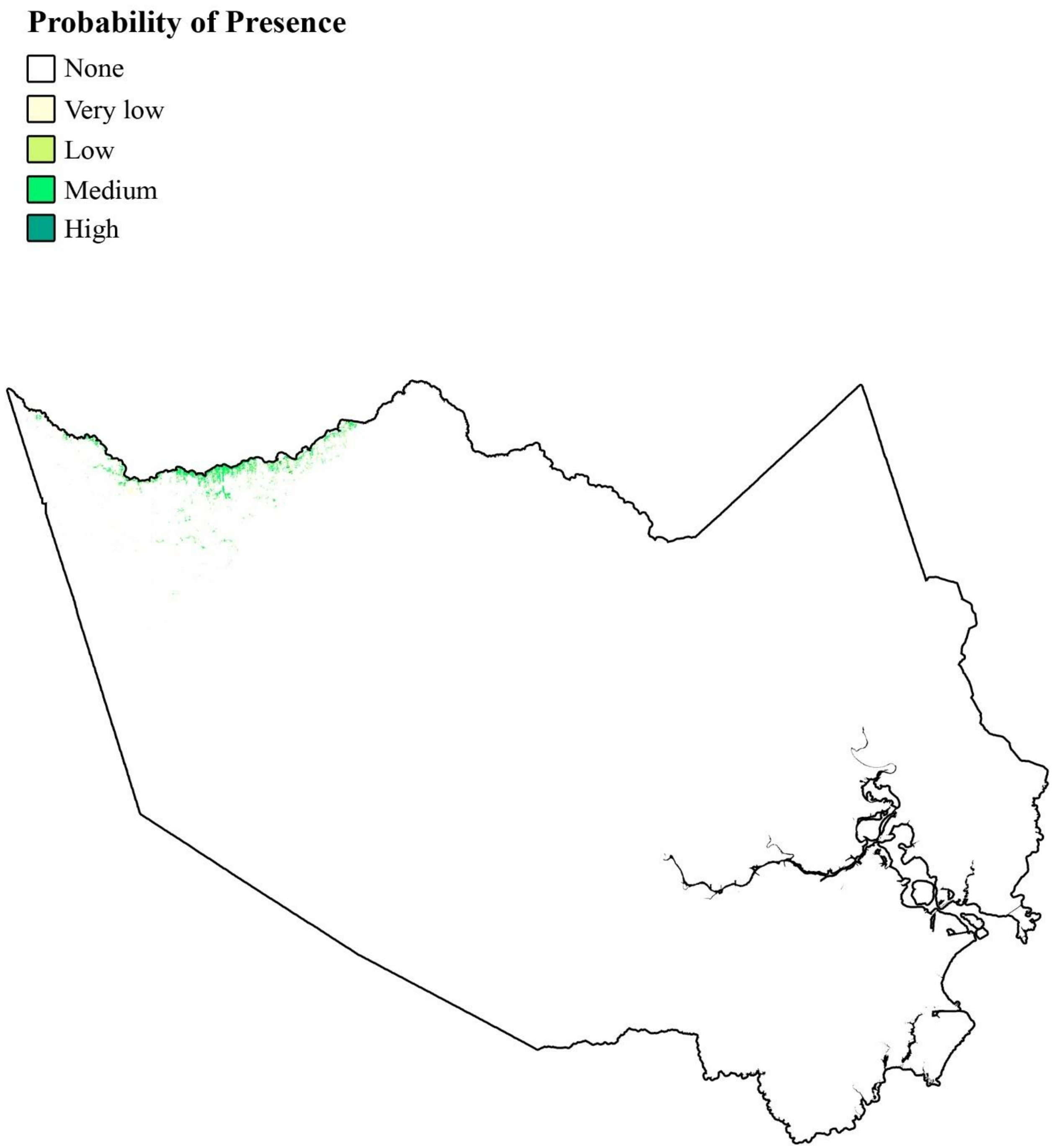

Figure 32. Model 1: occurrence-informed presence prediction model of Harris County.

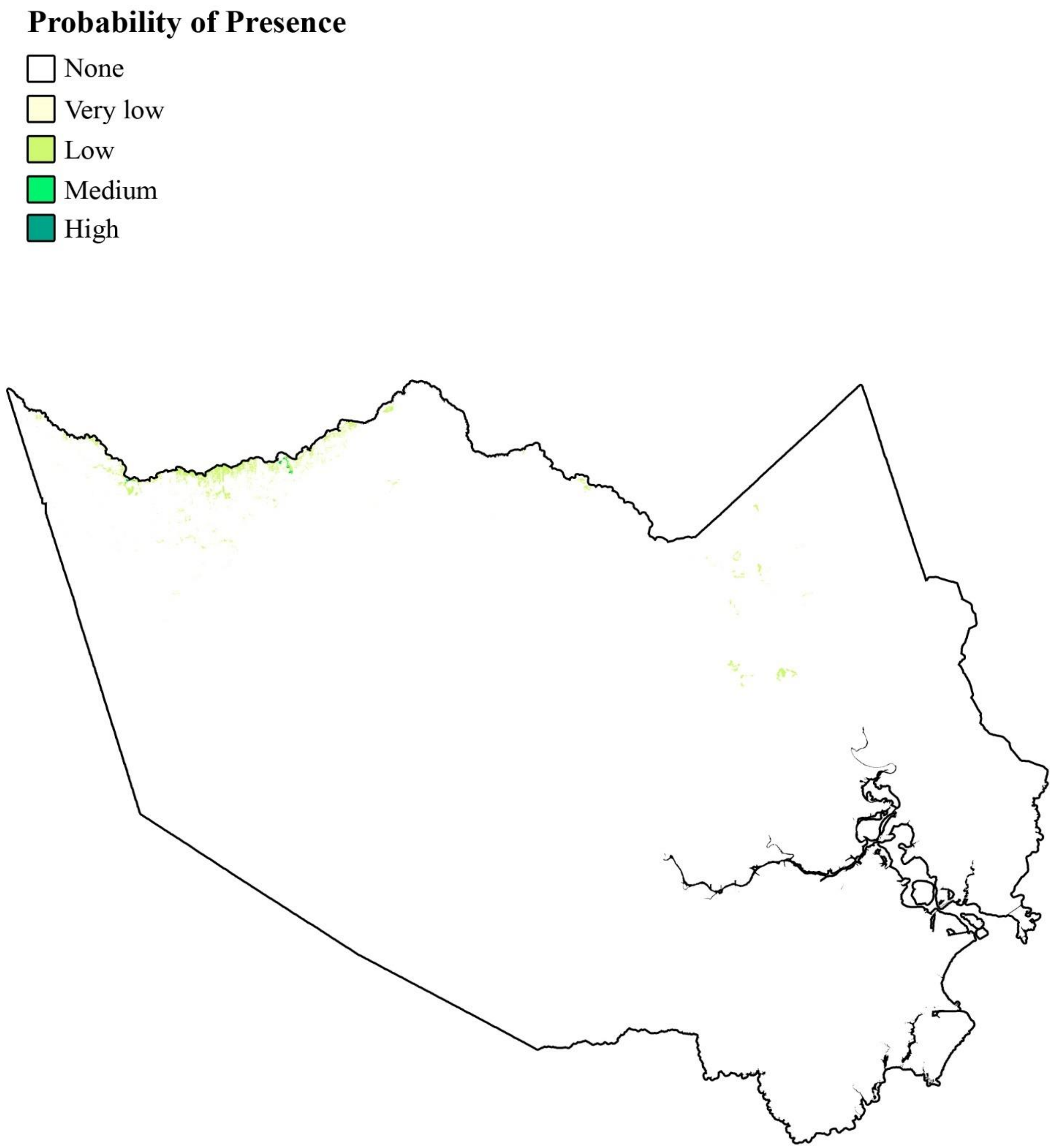

Figure 33. Model 2: evenly weighted presence prediction model of Harris County.

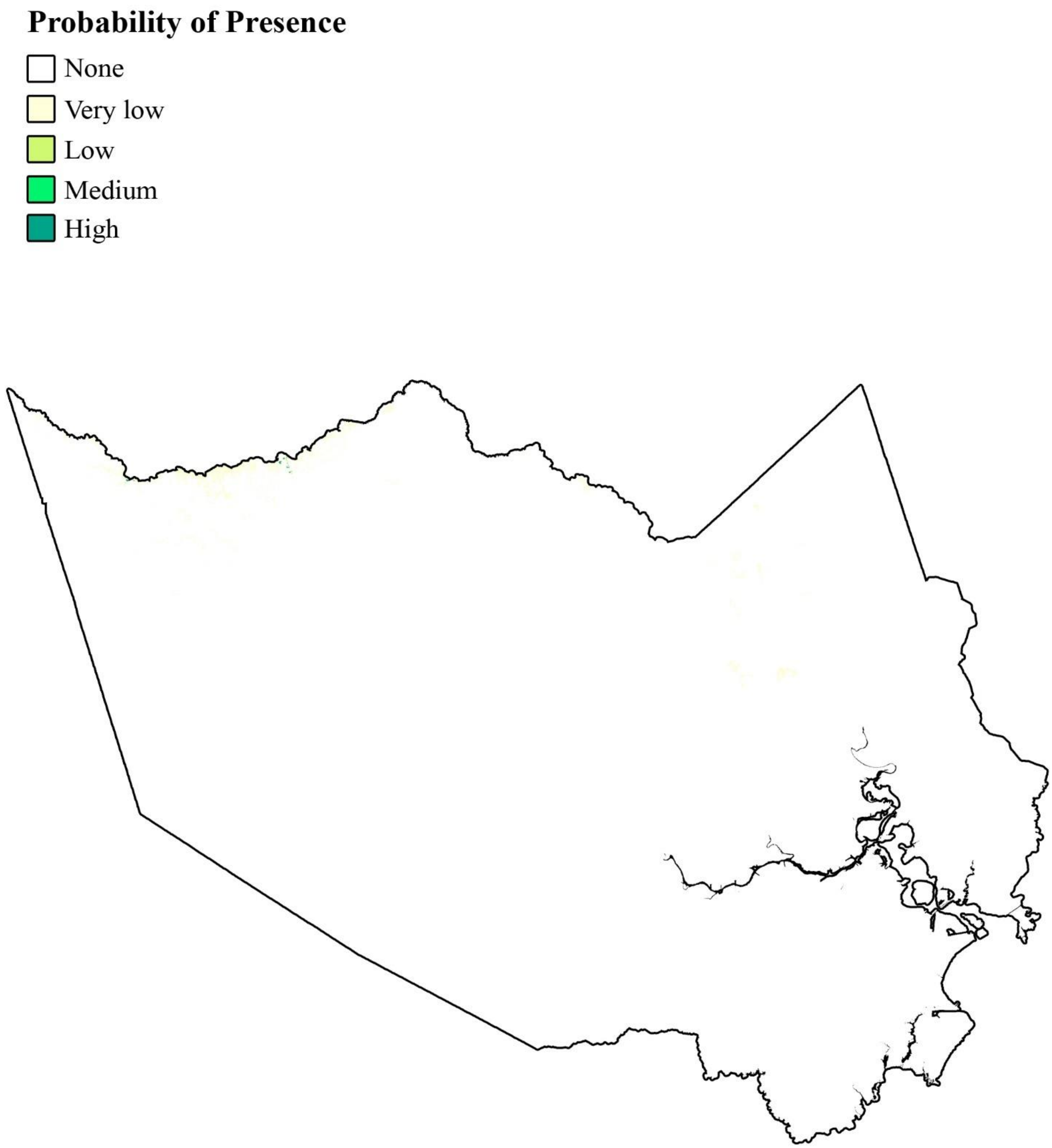

Figure 34. Model 3: integrated substrate presence prediction model of Harris County.

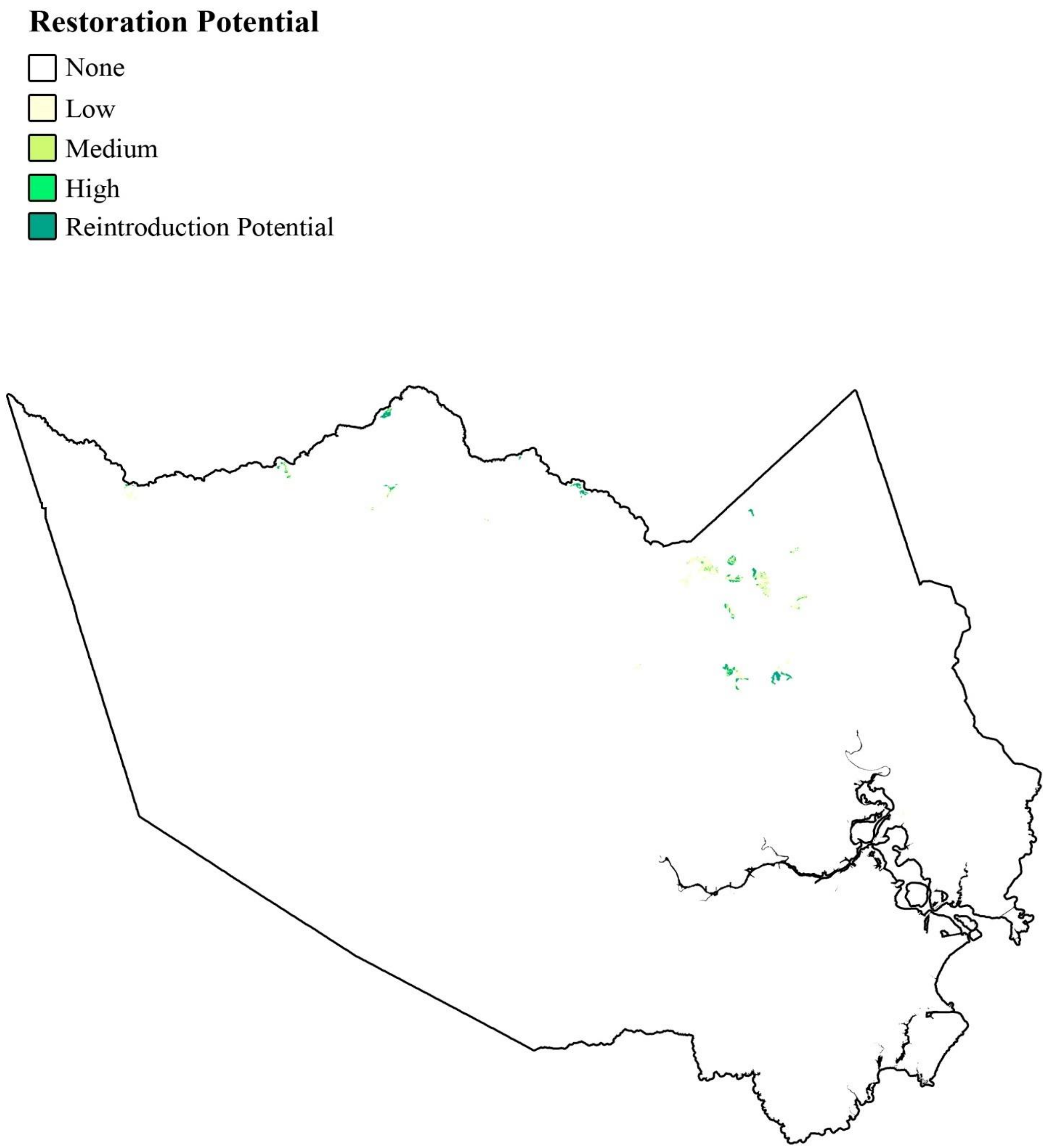

Figure 35. Model 4: restoration and reintroduction potential in Harris County.

Lavaca County

Table 11. Predicted areas in Lavaca County ranked by probability of presence (M_1, M_2, and M_3), restoration potential (M_4), and habitat suitability (Buzo 2008 model).

Model	Rank	Area (km^2)
	None	2293.20
	Very Low	188.92
M_1	Low	19.96
	Medium	7.24
	High	4.61
	None	2153.00
	Very Low	113.39
M_2	Low	237.49
	Medium	5.42
	High	4.61
	None	2184.82
	Very Low	297.15
M_3	Low	25.84
	Medium	1.49
	High	4.61
	None	1799.77
	Low	603.32
M_4	Medium	69.21
	High	16.92
	Reintroduction	24.70
Buzo	None	477.65
(2008)	Very Low	1055.85
Canopy +	Low	226.25
Soil	Medium	553.06
Model	High	201.11

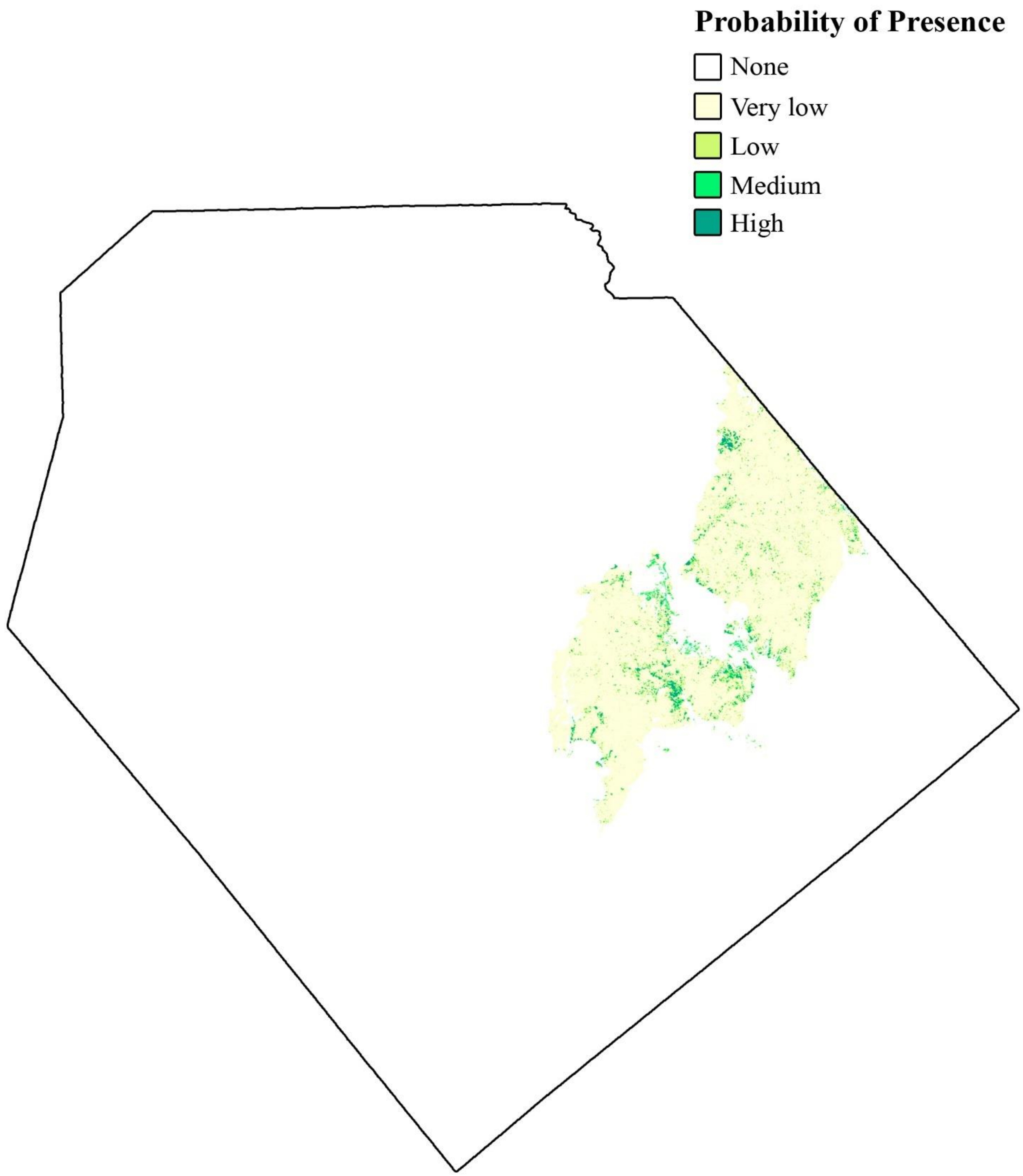

Figure 36. Model 1: occurrence-informed presence prediction model of Lavaca County.

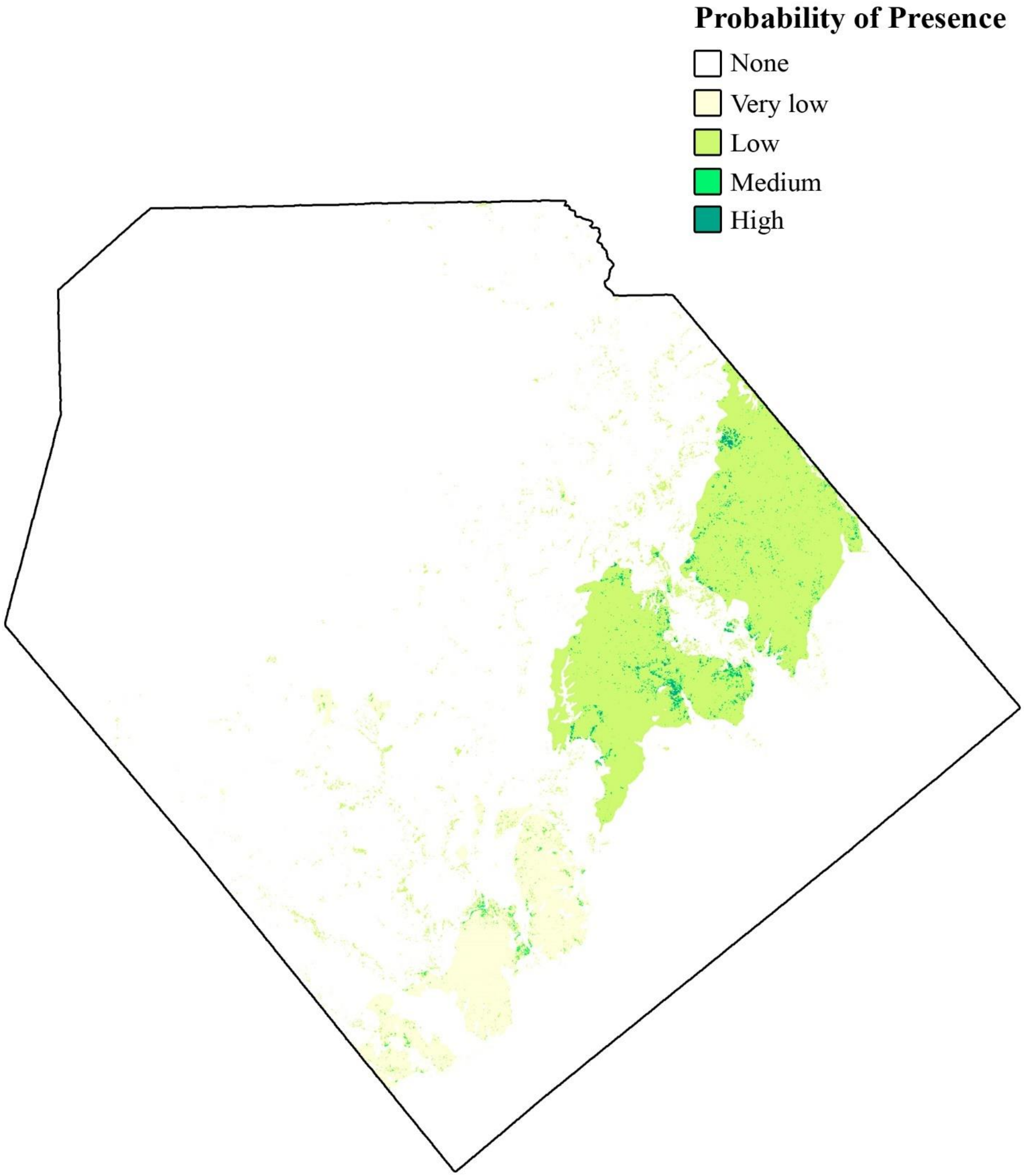

Figure 37. Model 2: evenly weighted presence prediction model of Lavaca County.

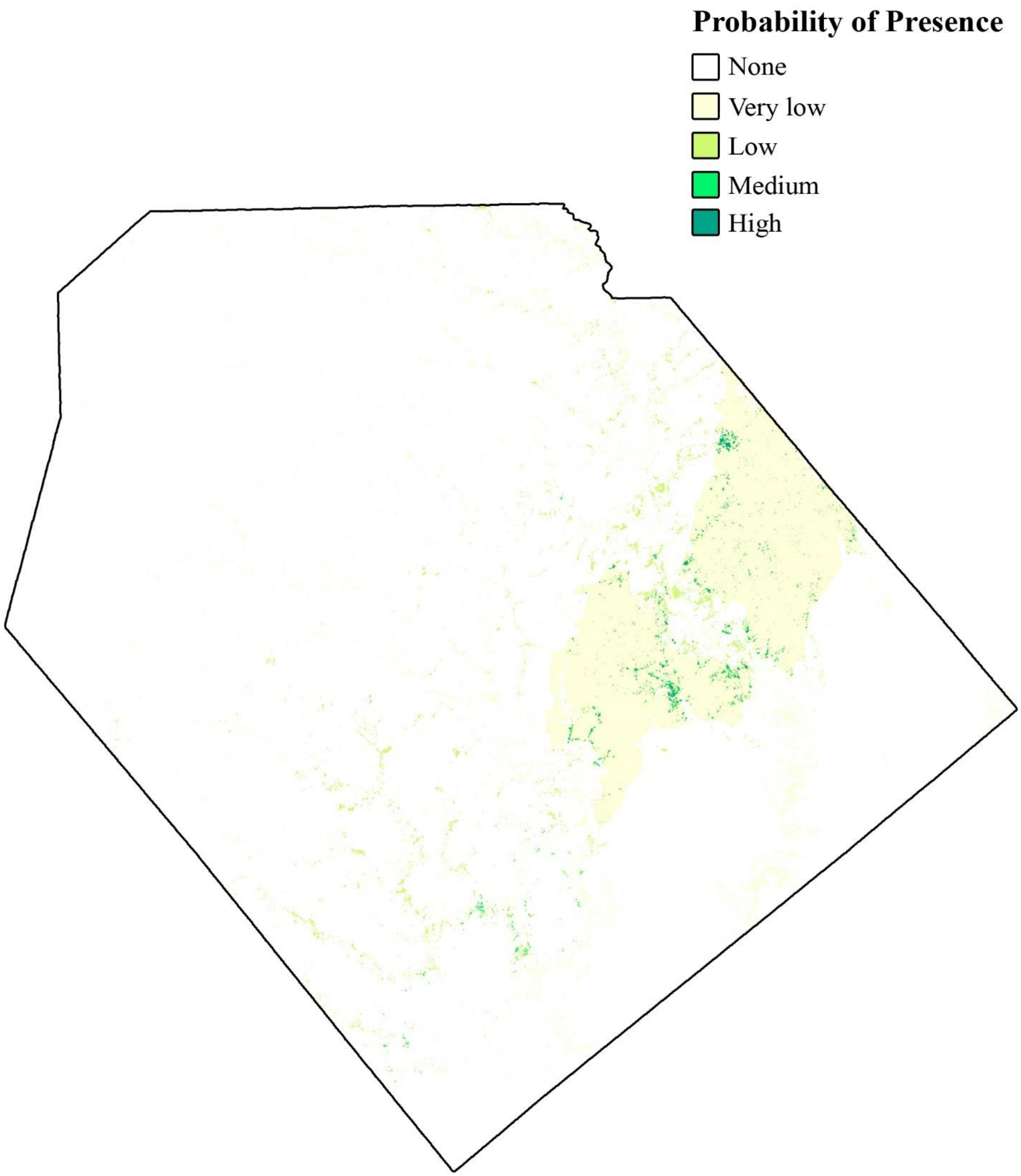

Figure 38. Model 3: integrated substrate presence prediction model of Lavaca County.

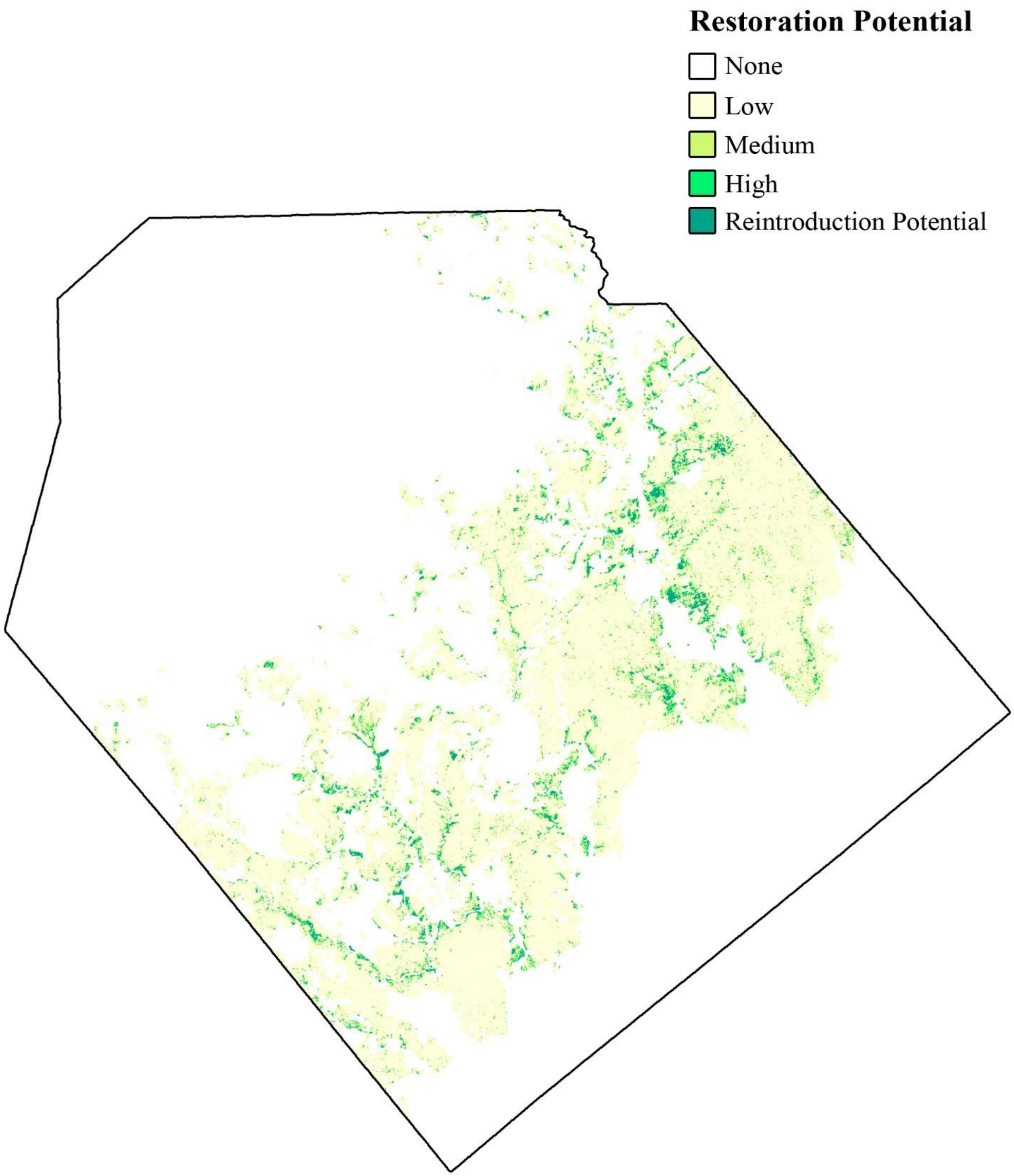

Figure 39. Model 4: restoration and reintroduction potential in Lavaca County.

Lee County

Table 12. Predicted areas in Lee County ranked by probability of presence (M_1, M_2, and M_3), restoration potential (M_4), and habitat suitability (Buzo 2008 model).

Model	Rank	Area (km^2)
	None	1333.45
	Very Low	241.08
M_1	Low	37.23
	Medium	17.89
	High	12.91
	None	1057.51
	Very Low	228.27
M_2	Low	325.54
	Medium	18.33
	High	12.91
	None	1255.42
	Very Low	343.51
M_3	Low	22.01
	Medium	8.71
	High	12.91
	None	847.53
	Low	665.81
M_4	Medium	82.79
	High	20.69
	Reintroduction	25.74
Buzo (2008) Canopy + Soil Model	None	114.98
	Very Low	936.26
	Low	65.70
	Medium	492.77
	High	49.28

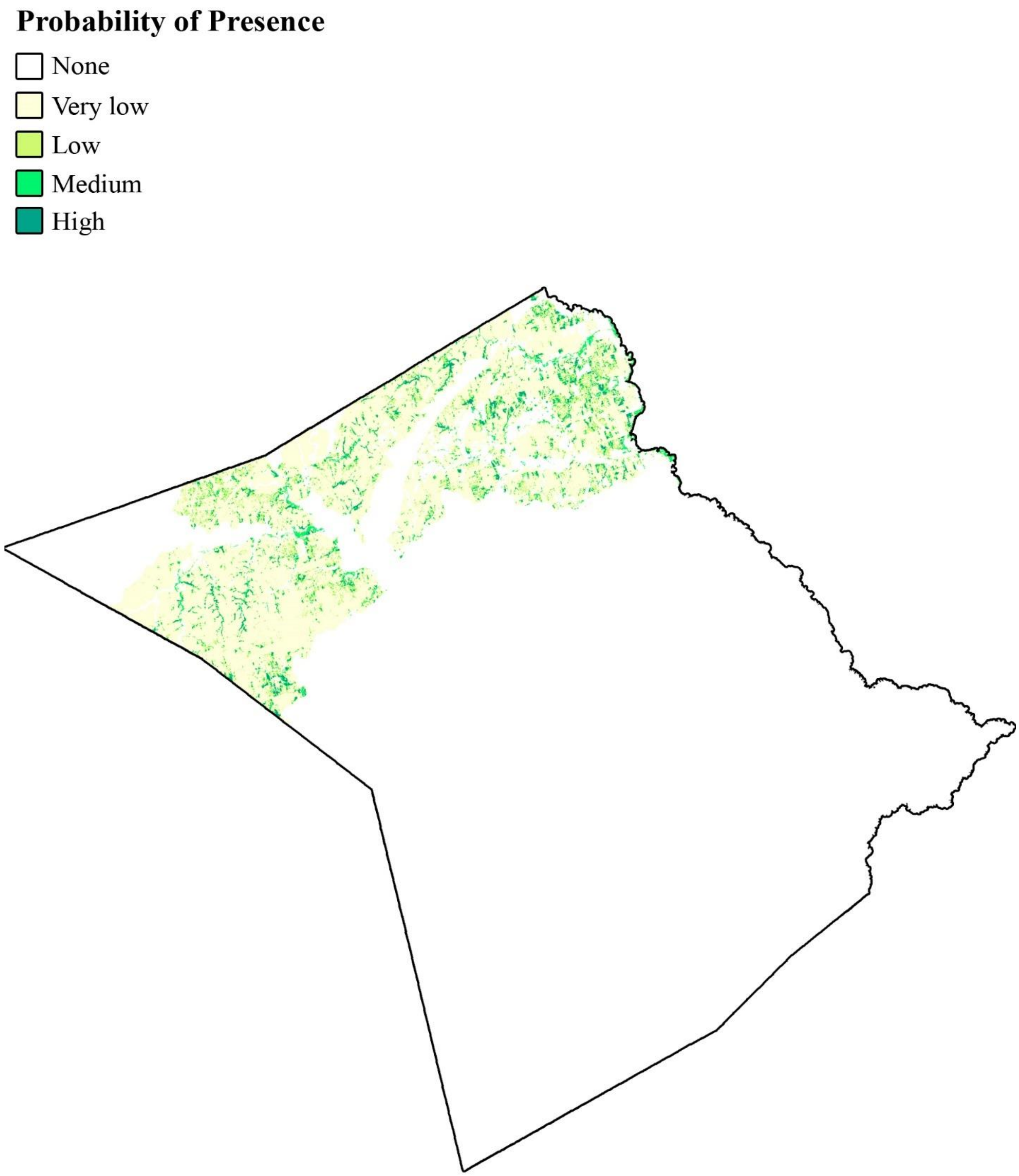

Figure 40. Model 1: occurrence-informed presence prediction model of Lee County.

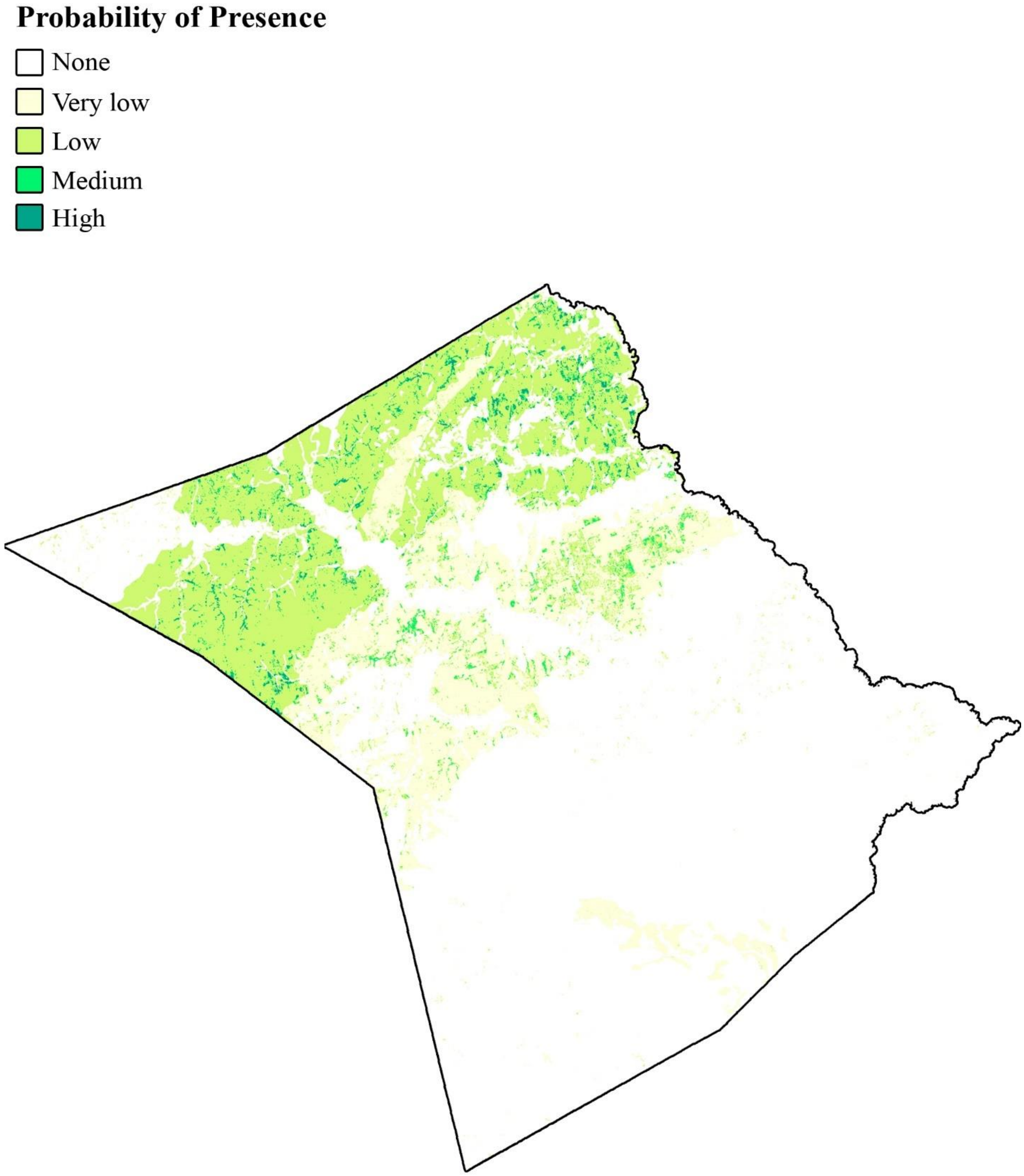

Figure 41. Model 2: evenly weighted presence prediction model of Lee County.

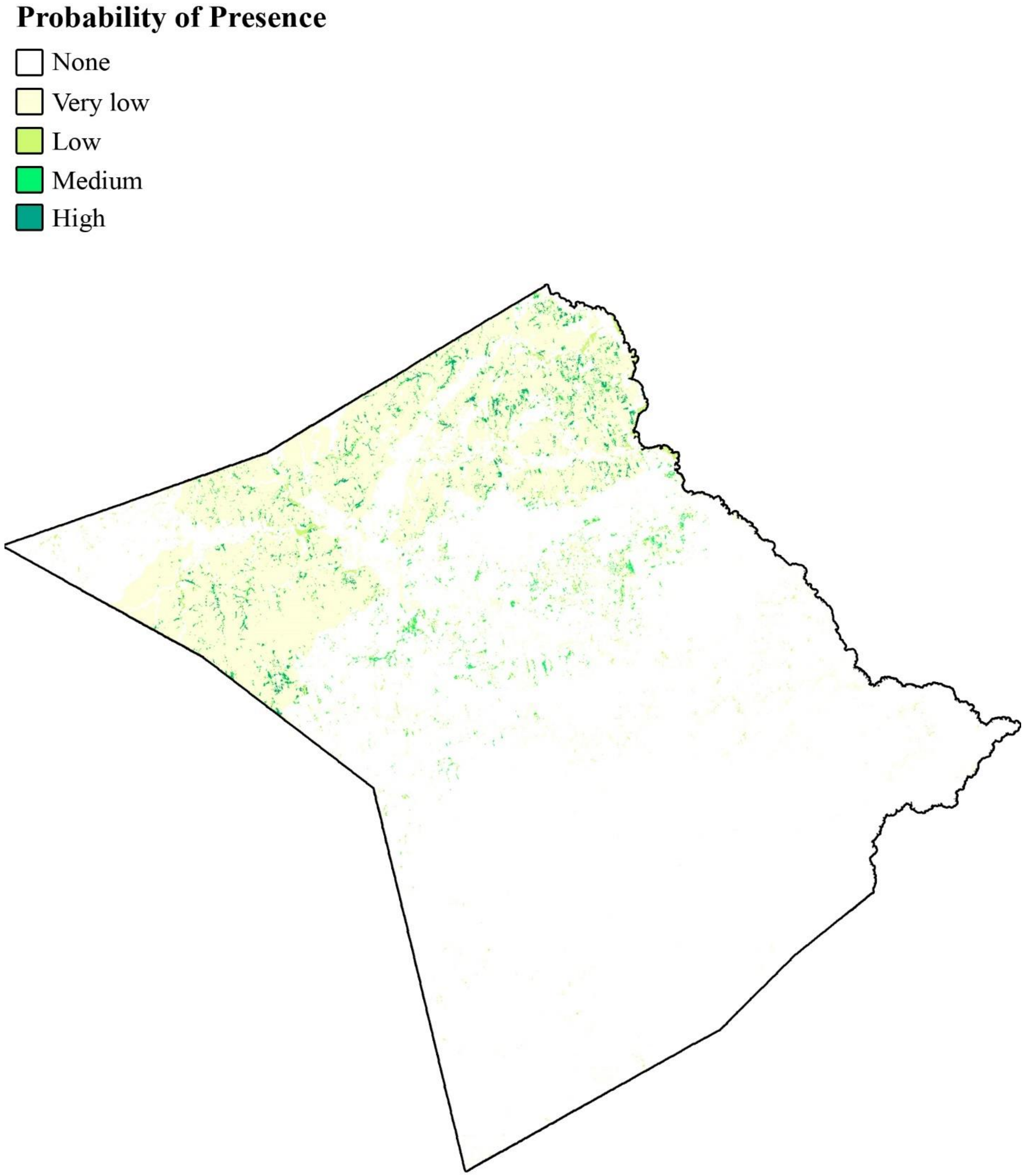

Figure 42. Model 3: integrated substrate presence prediction model of Lee County.

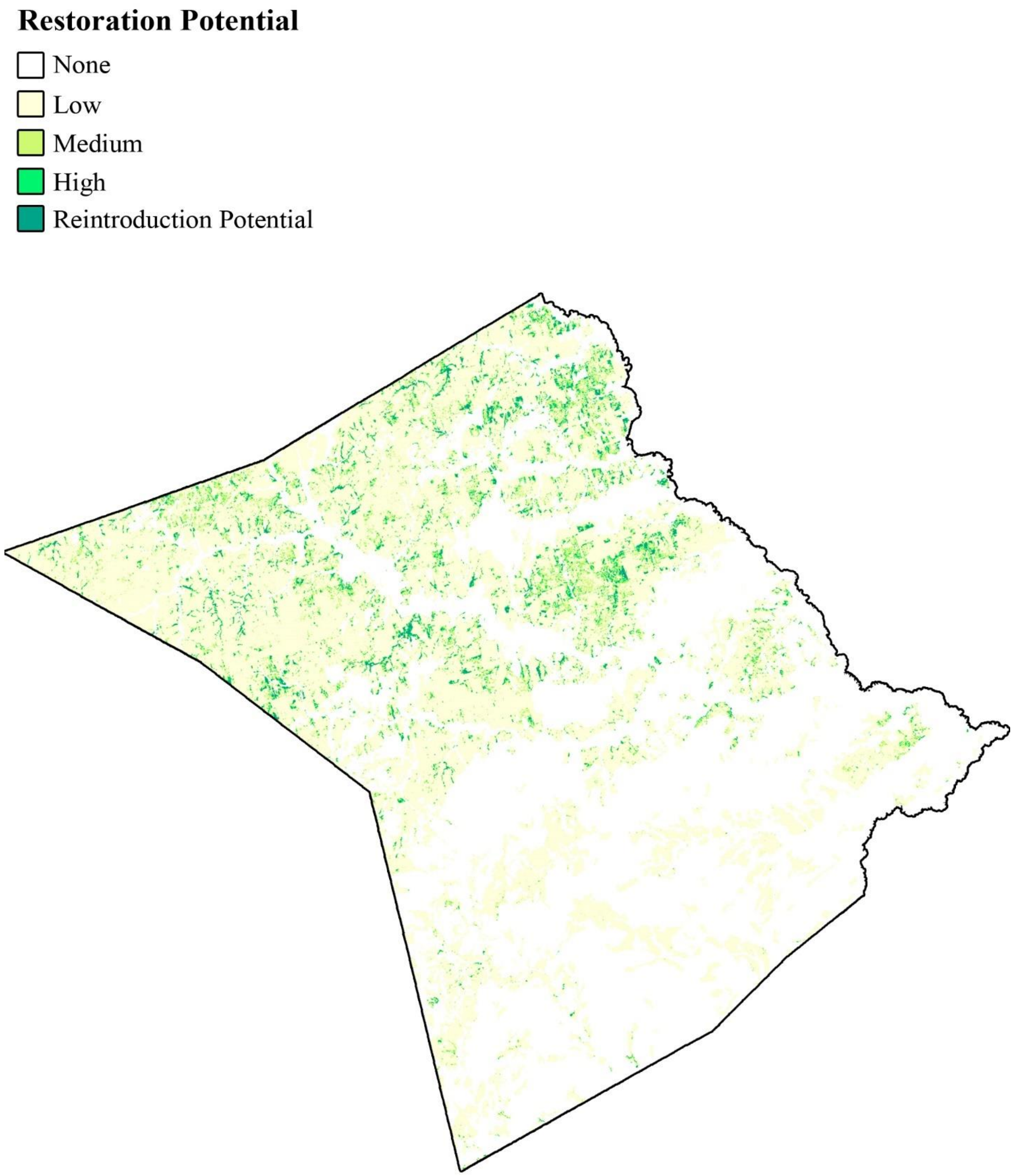

Figure 43. Model 4: restoration and reintroduction potential in Lee County.

Leon County

Table 13. Predicted areas in Leon County ranked by probability of presence (M_1, M_2, and M_3), restoration potential (M_4), and habitat suitability (Buzo 2008 model).

Model	Rank	Area (km^2)
M_1	None	1882.97
	Very Low	418.01
	Low	163.23
	Medium	175.09
	High	162.90
M_2	None	1295.21
	Very Low	375.92
	Low	801.55
	Medium	166.63
	High	162.90
M_3	None	1474.19
	Very Low	874.14
	Low	213.09
	Medium	77.88
	High	162.90
M_4	None	1315.92
	Low	809.68
	Medium	261.25
	High	136.58
	Reintroduction	278.78
Buzo (2008) Canopy + Soil Model	None	392.31
	Very Low	1625.28
	Low	336.26
	Medium	364.29
	High	84.07

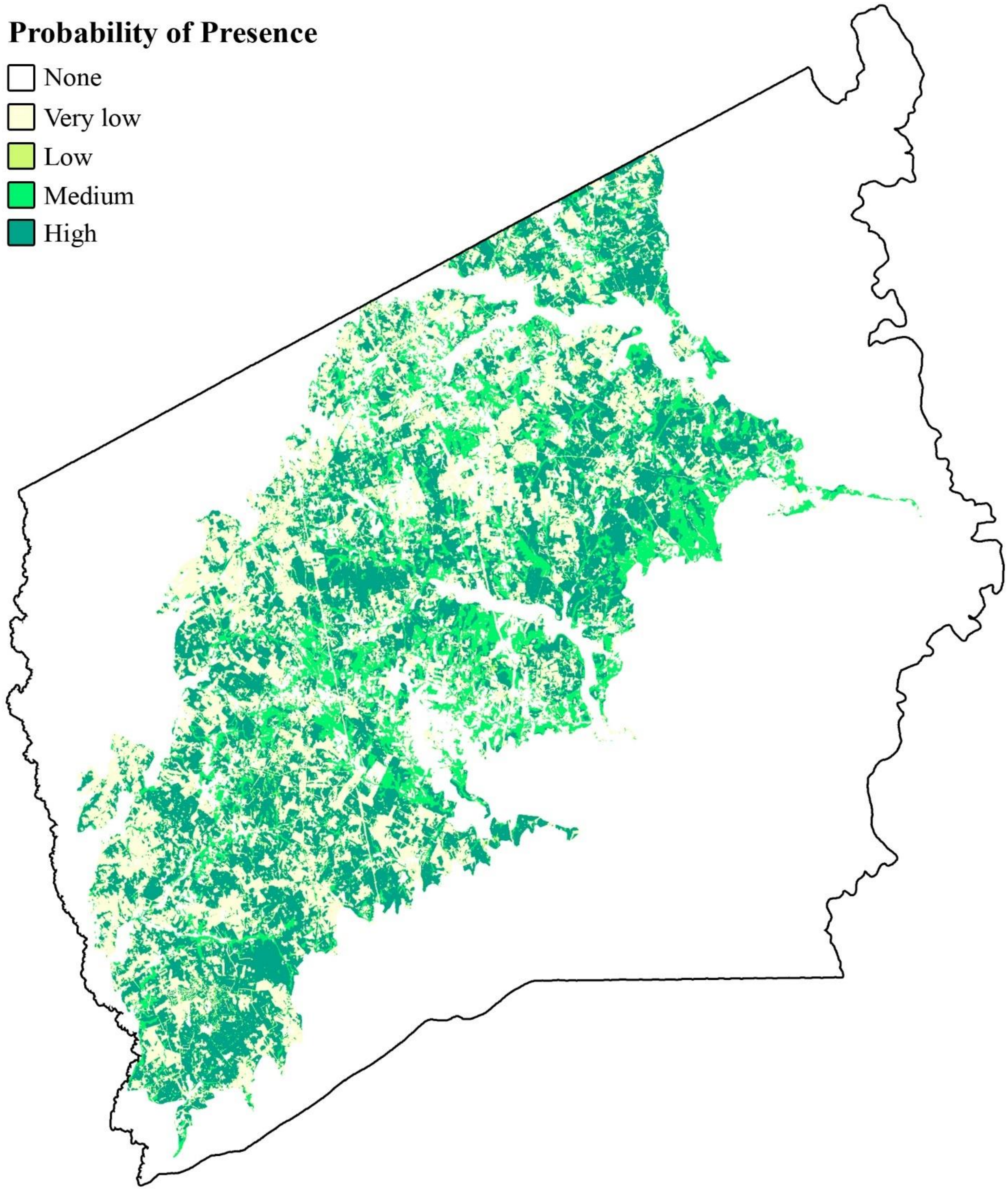

Figure 44. Model 1: occurrence-informed presence prediction model of Leon County.

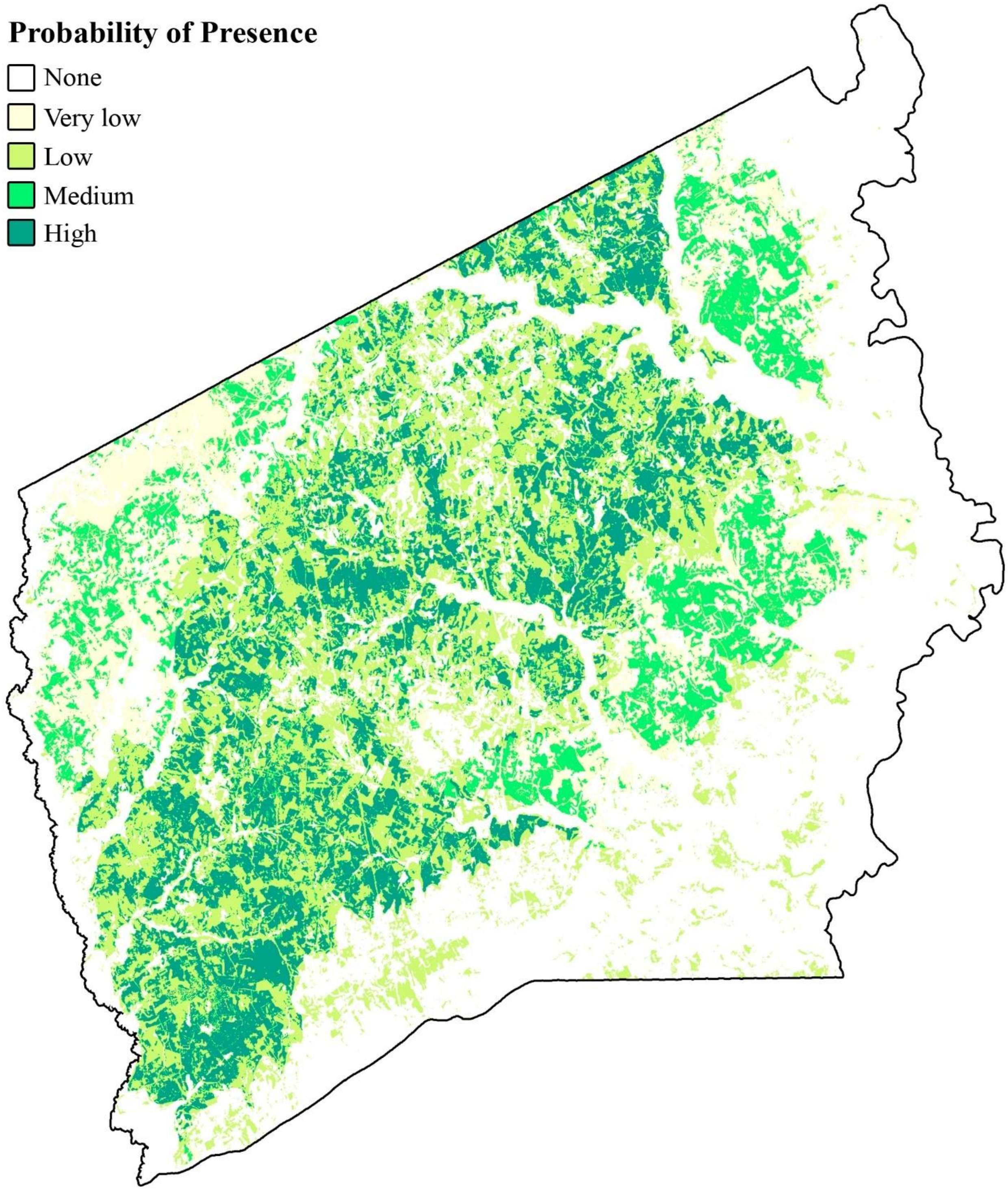

Figure 45. Model 2: evenly weighted presence prediction model of Leon County.

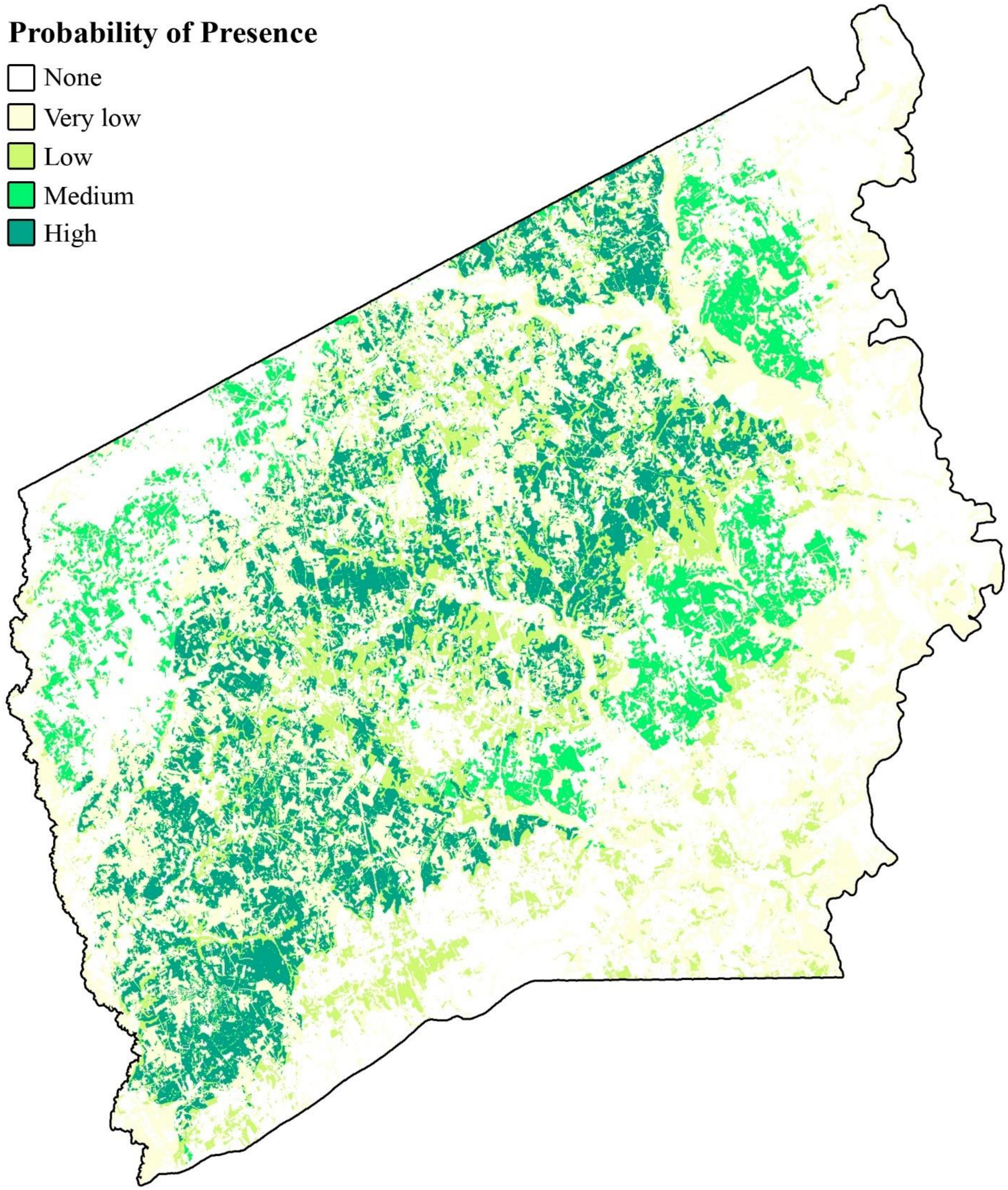

Figure 46. Model 3: integrated substrate presence prediction model of Leon County.

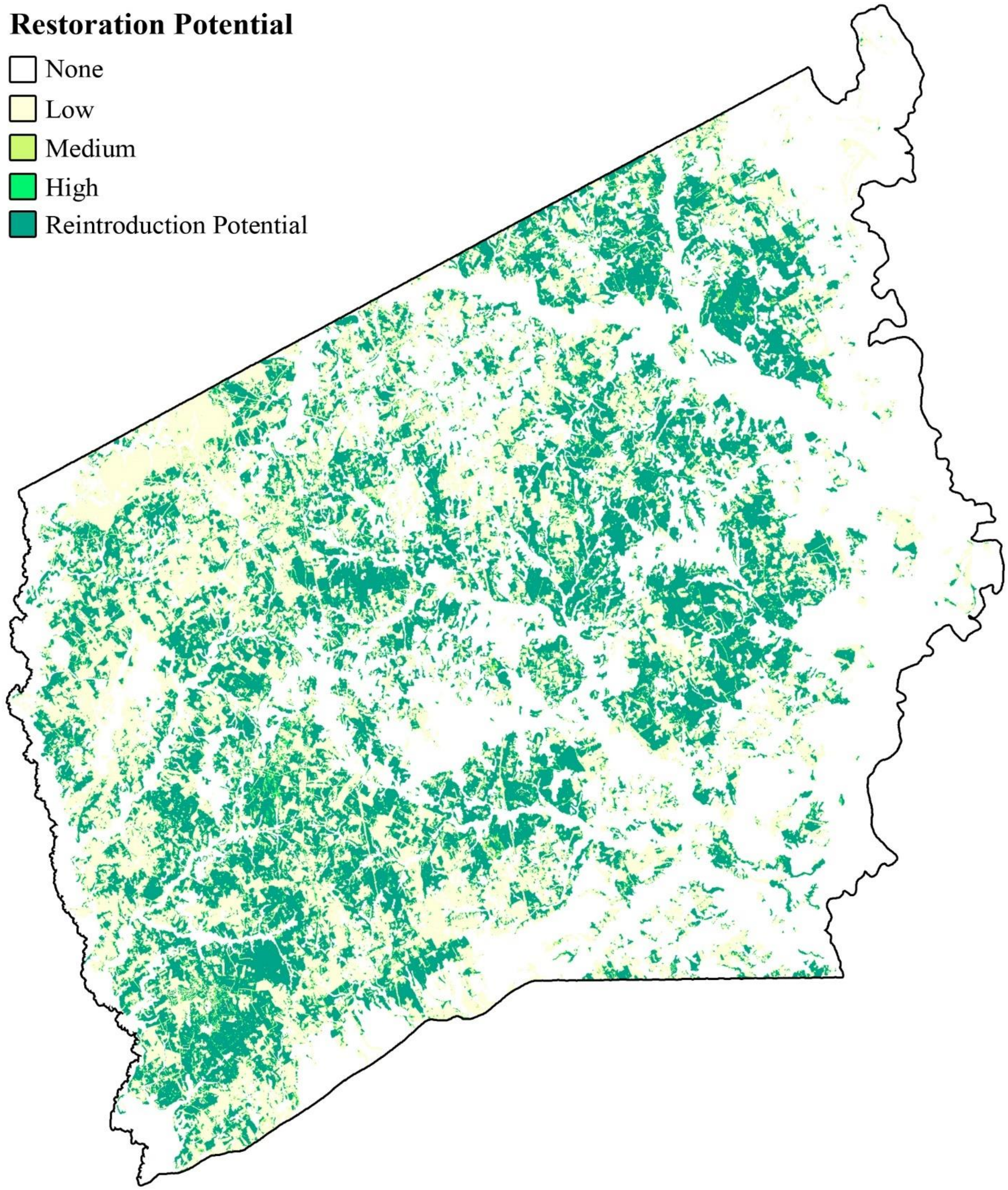

Figure 47. Model 4: restoration and reintroduction potential in Leon County.

Milam County

Table 14. Predicted areas in Milam County ranked by probability of presence (M_1, M_2, and M_3), restoration potential (M_4), and habitat suitability (Buzo 2008 model).

Model	Rank	Area (km^2)
M_1	None	2252.15
	Very Low	268.65
	Low	56.92
	Medium	42.92
	High	23.89
M_2	None	2129.88
	Very Low	93.33
	Low	376.89
	Medium	20.53
	High	23.89
M_3	None	2146.83
	Very Low	412.21
	Low	58.83
	Medium	2.76
	High	23.89
M_4	None	1871.93
	Low	592.13
	Medium	106.08
	High	31.82
	Reintroduction	42.56
Buzo (2008) Canopy + Soil Model	None	132.23
	Very Low	1560.27
	Low	185.12
	Medium	608.24
	High	132.23

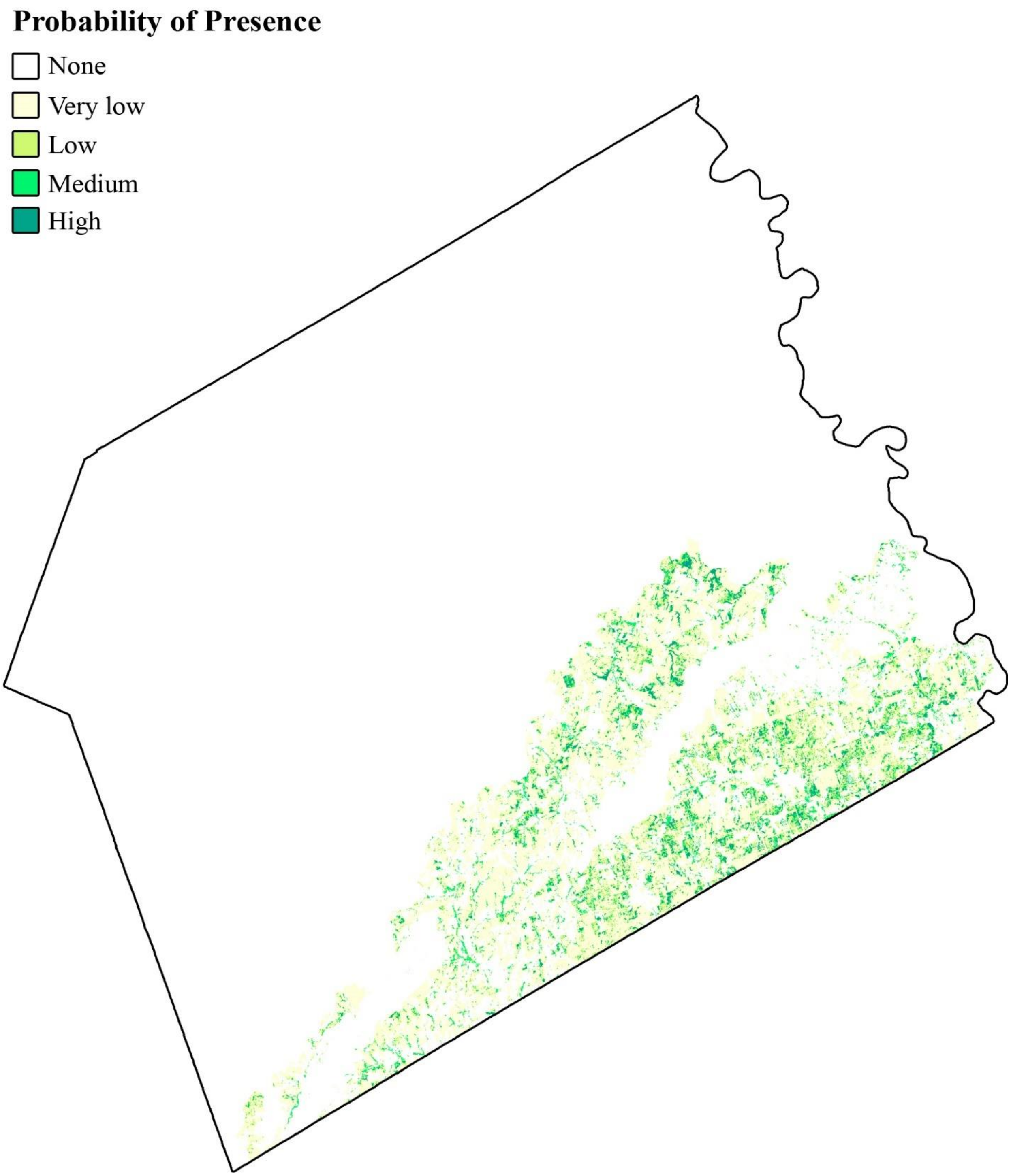

Figure 48. Model 1: occurrence-informed presence prediction model of Milam County.

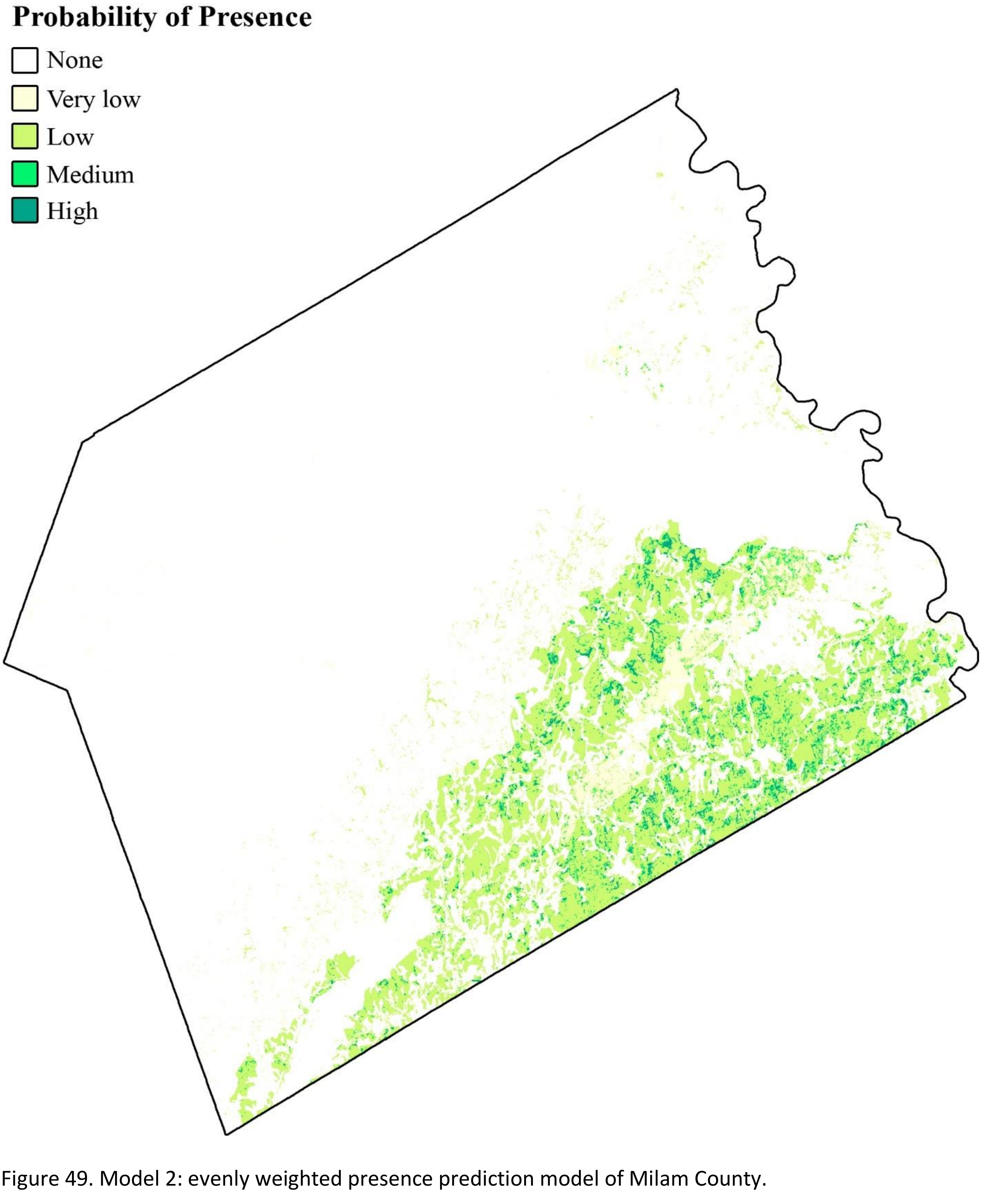

Figure 49. Model 2: evenly weighted presence prediction model of Milam County.

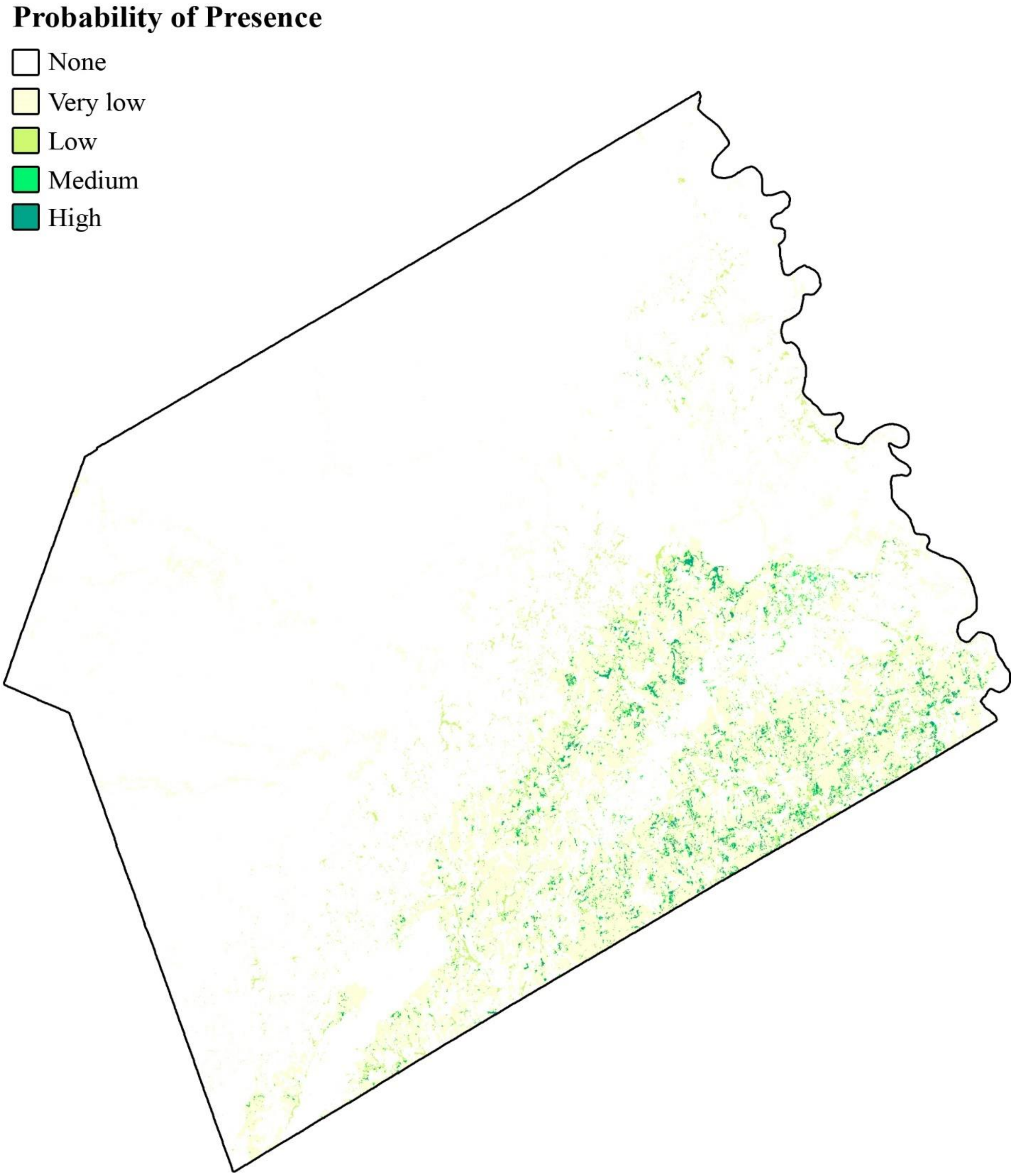

Figure 50. Model 3: integrated substrate presence prediction model of Milam County.

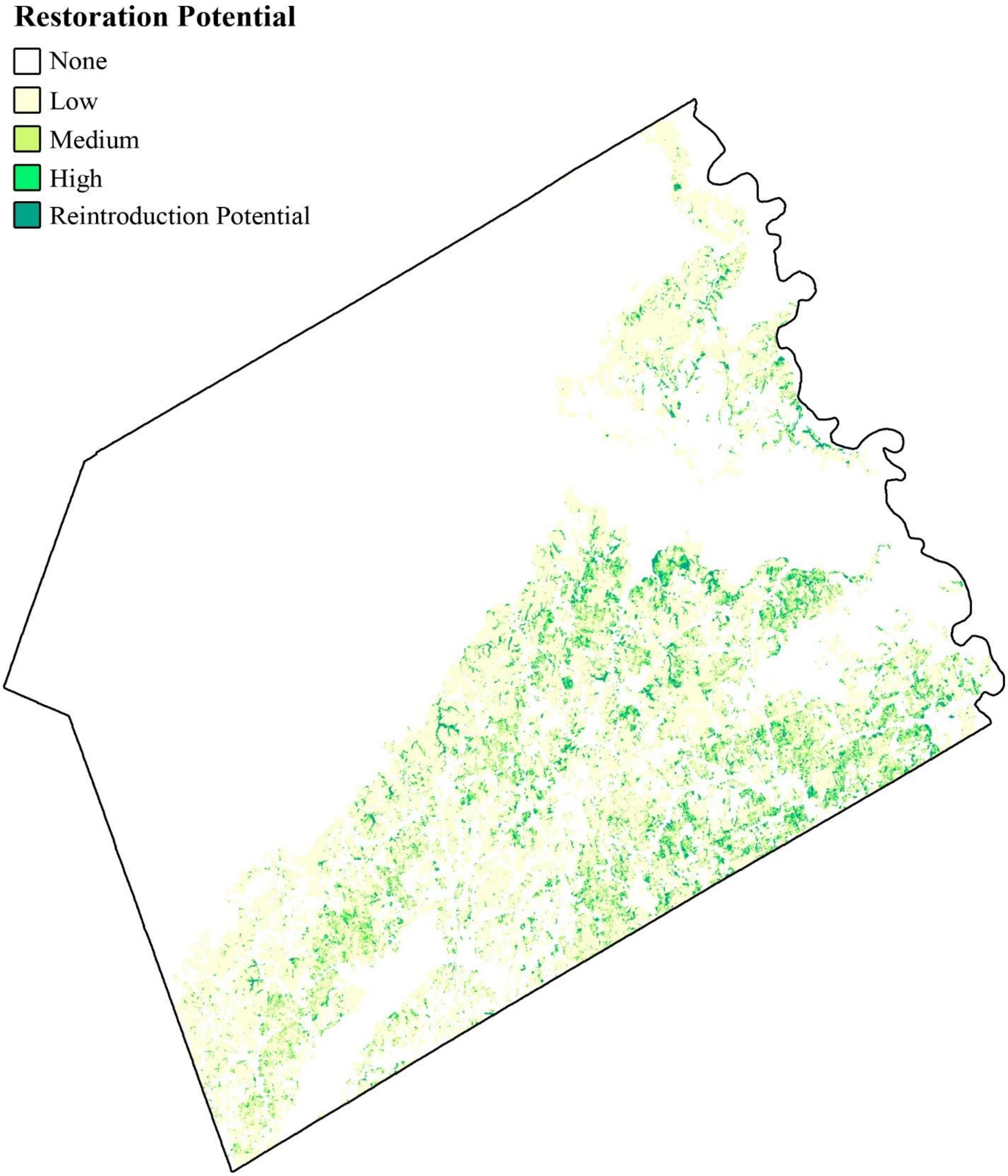

Figure 51. Model 4: restoration and reintroduction potential in Milam County.

Robertson County

Table 15. Predicted areas in Robertson County ranked by probability of presence (M_1, M_2, and M_3), restoration potential (M_4), and habitat suitability (Buzo 2008 model).

Model	Rank	Area (km^2)
M_1	None	1777.42
	Very Low	275.40
	Low	83.88
	Medium	51.17
	High	55.64
M_2	None	1011.65
	Very Low	567.77
	Low	508.25
	Medium	100.20
	High	55.64
M_3	None	1501.73
	Very Low	548.21
	Low	71.09
	Medium	66.84
	High	55.64
M_4	None	898.88
	Low	941.72
	Medium	186.33
	High	74.18
	Reintroduction	142.40
Buzo (2008) Canopy + Soil Model	None	67.31
	Very Low	1189.06
	Low	269.22
	Medium	538.44
	High	179.48

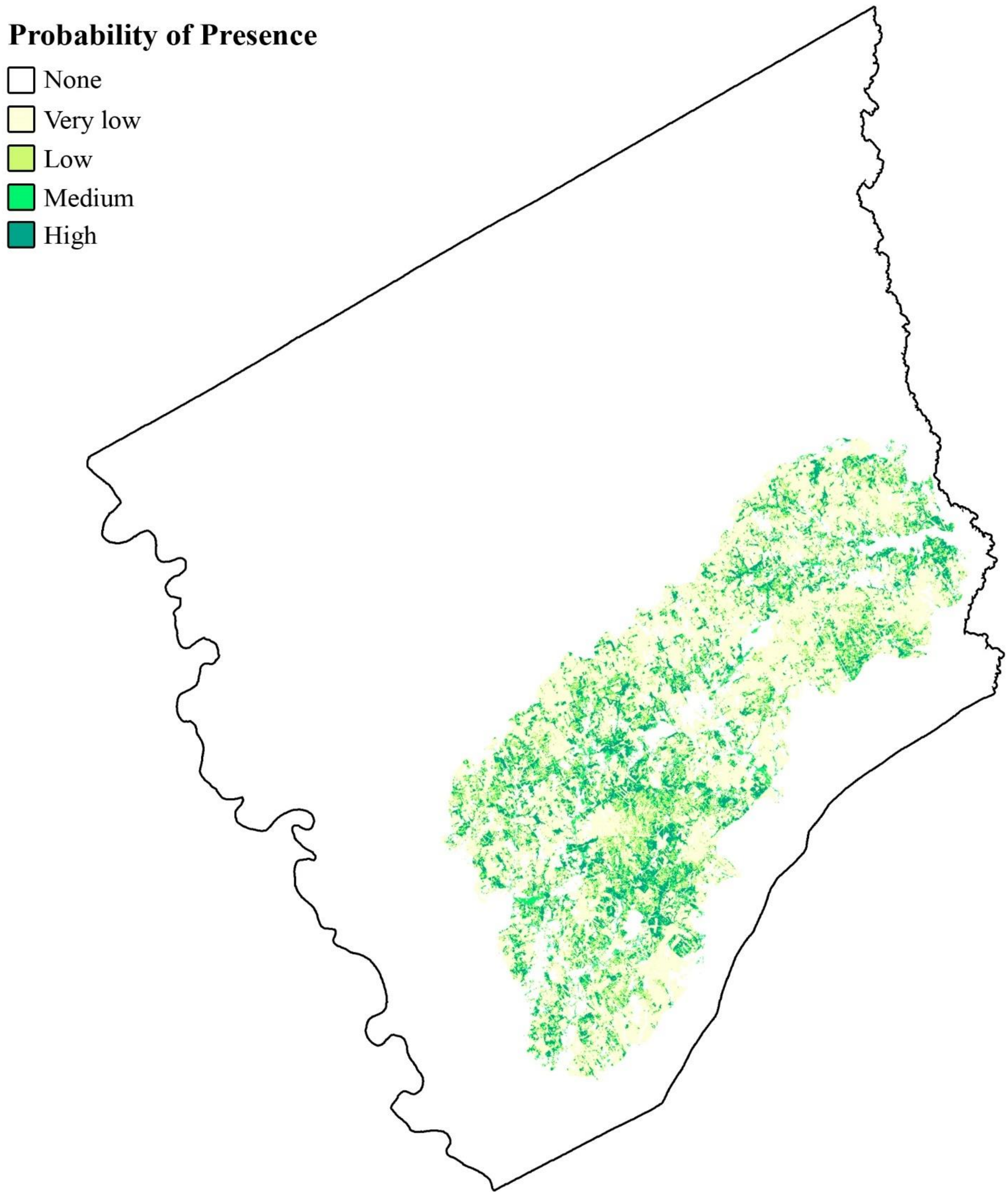

Figure 52. Model 1: occurrence-informed presence prediction model of Robertson County.

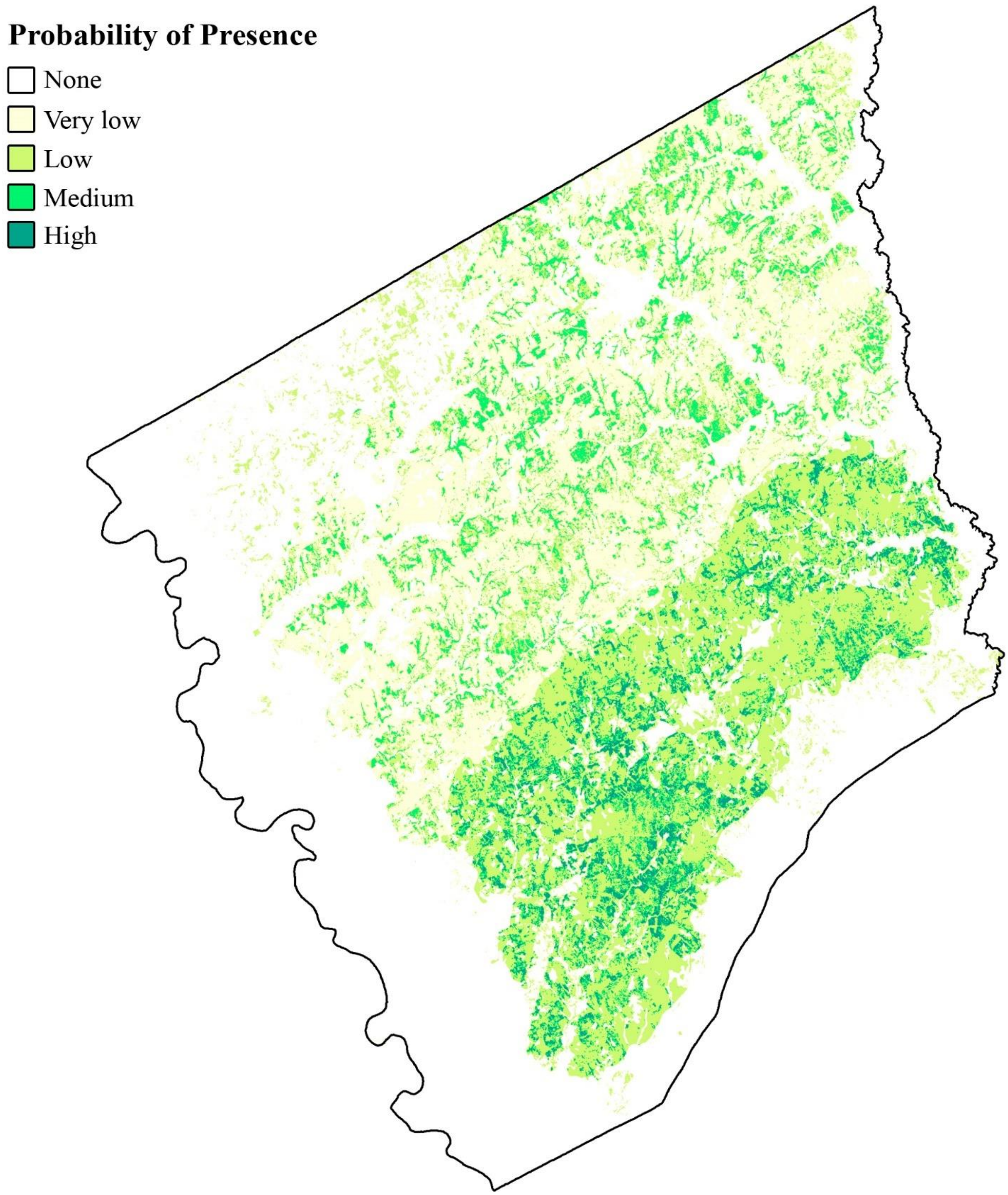

Figure 53. Model 2: evenly weighted presence prediction model of Robertson County.

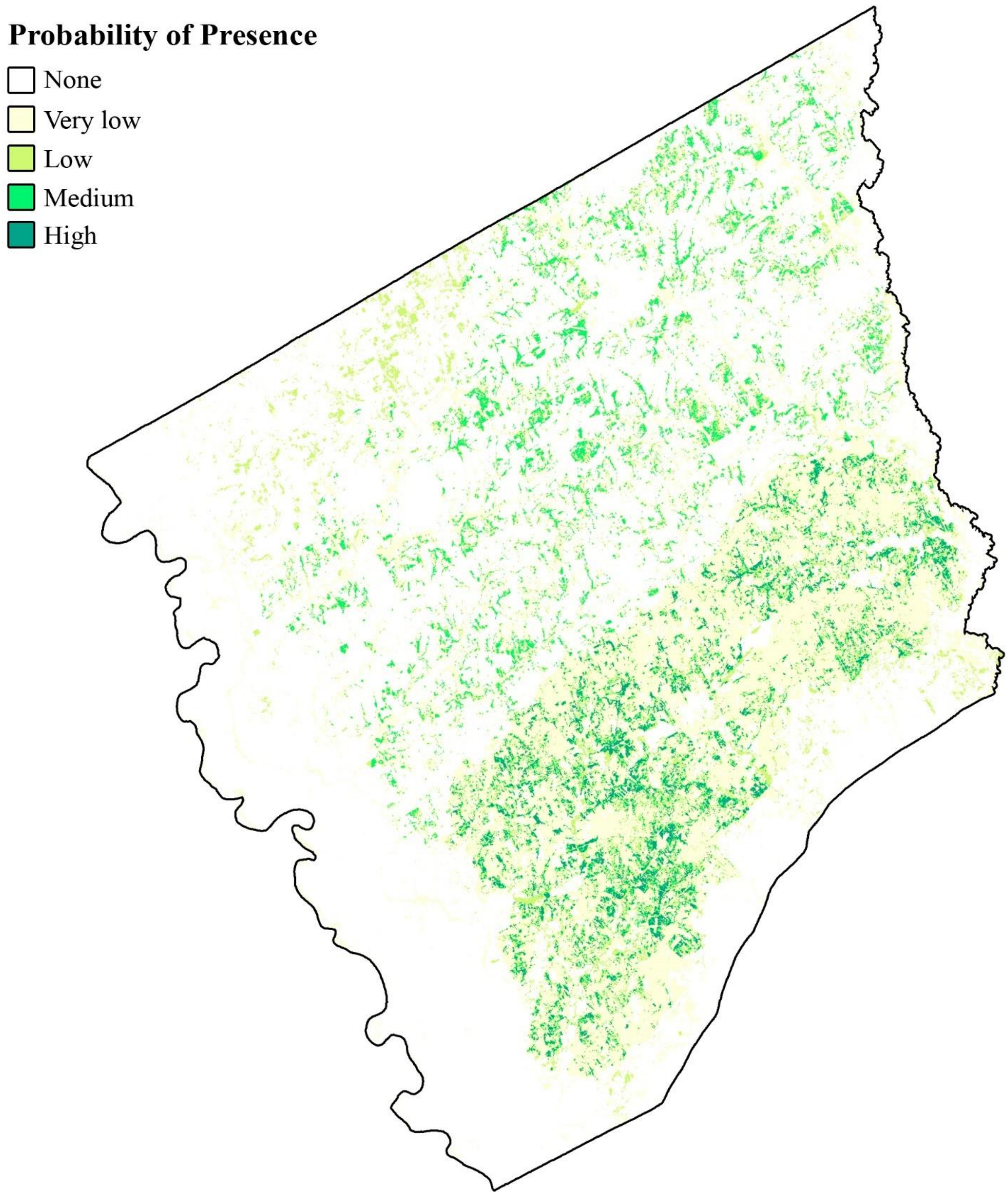

Figure 54. Model 3: integrated substrate presence prediction model of Robertson County.

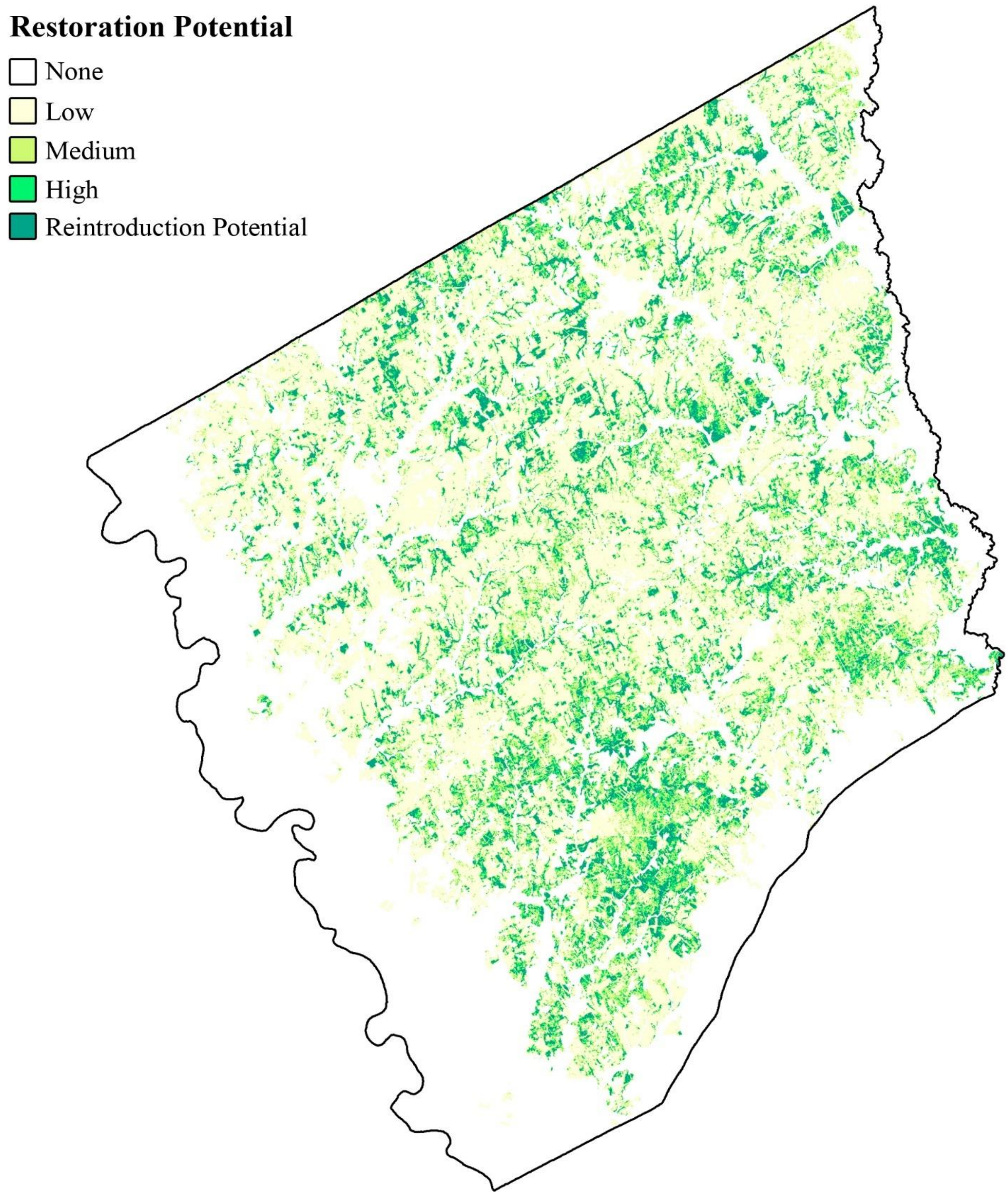

Figure 55. Model 4: restoration and reintroduction potential in Robertson County.

Waller County

Table 16. Predicted areas in Waller County ranked by probability of presence (M_1, M_2, and M_3), restoration potential (M_4), and habitat suitability (Buzo 2008 model).

Model	Rank	Area (km^2)
	None	1104.23
	Very Low	139.55
M_1	Low	22.79
	Medium	46.87
	High	28.94
	None	1065.58
	Very Low	35.08
M_2	Low	203.58
	Medium	9.21
	High	28.94
	None	1056.02
	Very Low	207.00
M_3	Low	50.44
	Medium	0.00
	High	28.94
	None	1092.72
	Low	176.82
M_4	Medium	29.08
	High	11.26
	Reintroduction	32.51
Buzo (2008) Canopy + Soil Model	None	NA
	Very Low	NA
	Low	NA
	Medium	NA
	High	NA

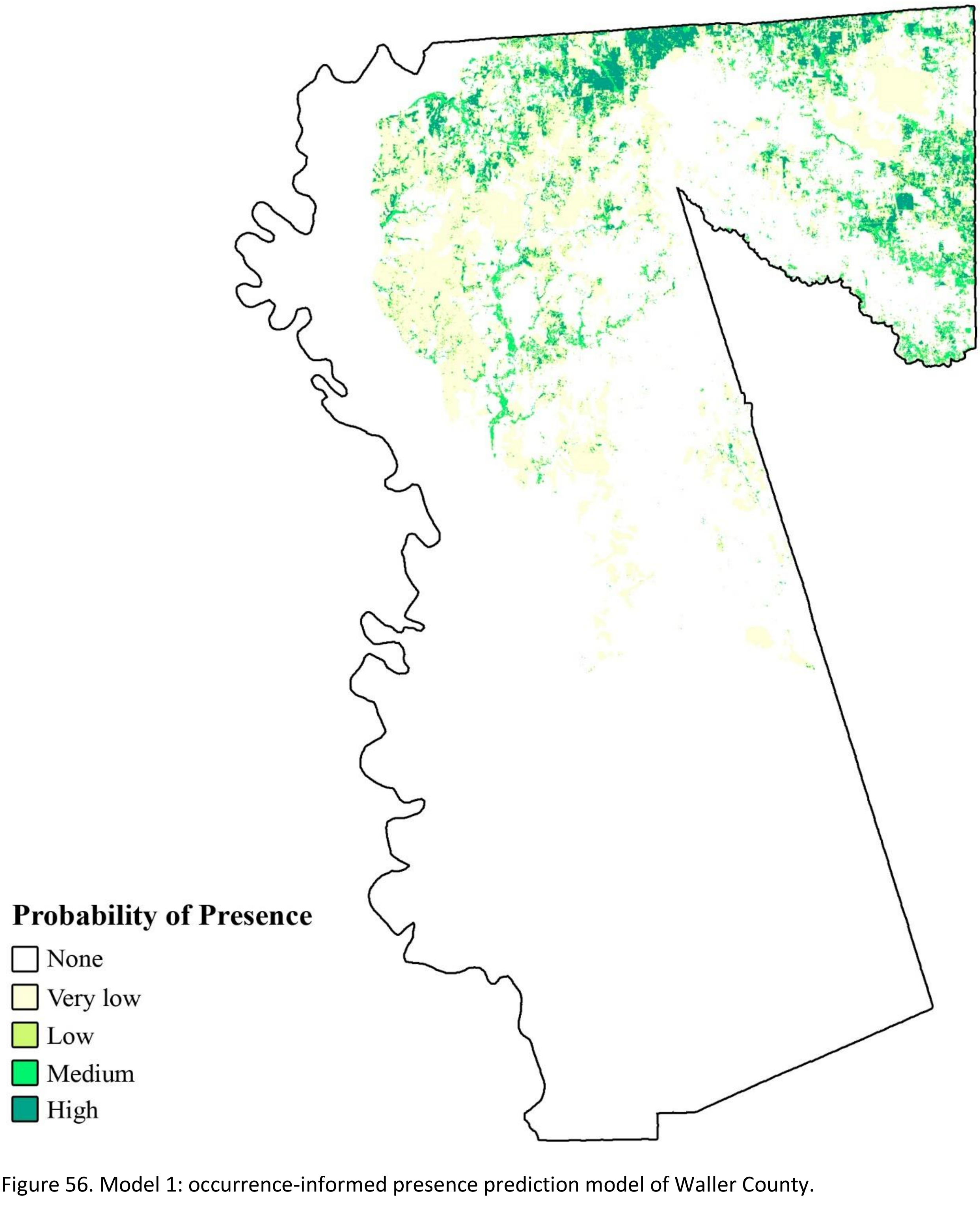

Figure 56. Model 1: occurrence-informed presence prediction model of Waller County.

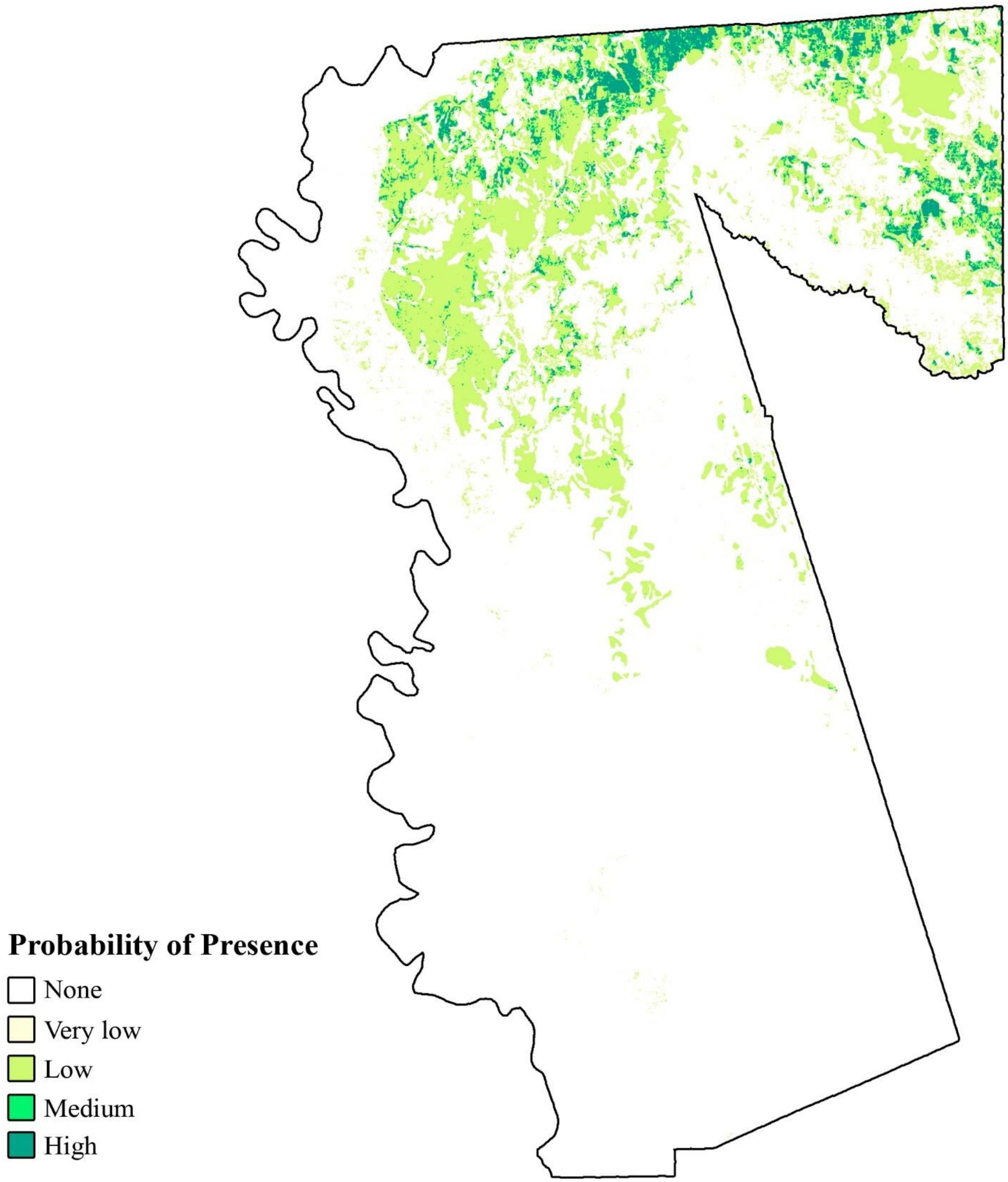

Figure 57. Model 2: evenly weighted presence prediction model of Waller County.

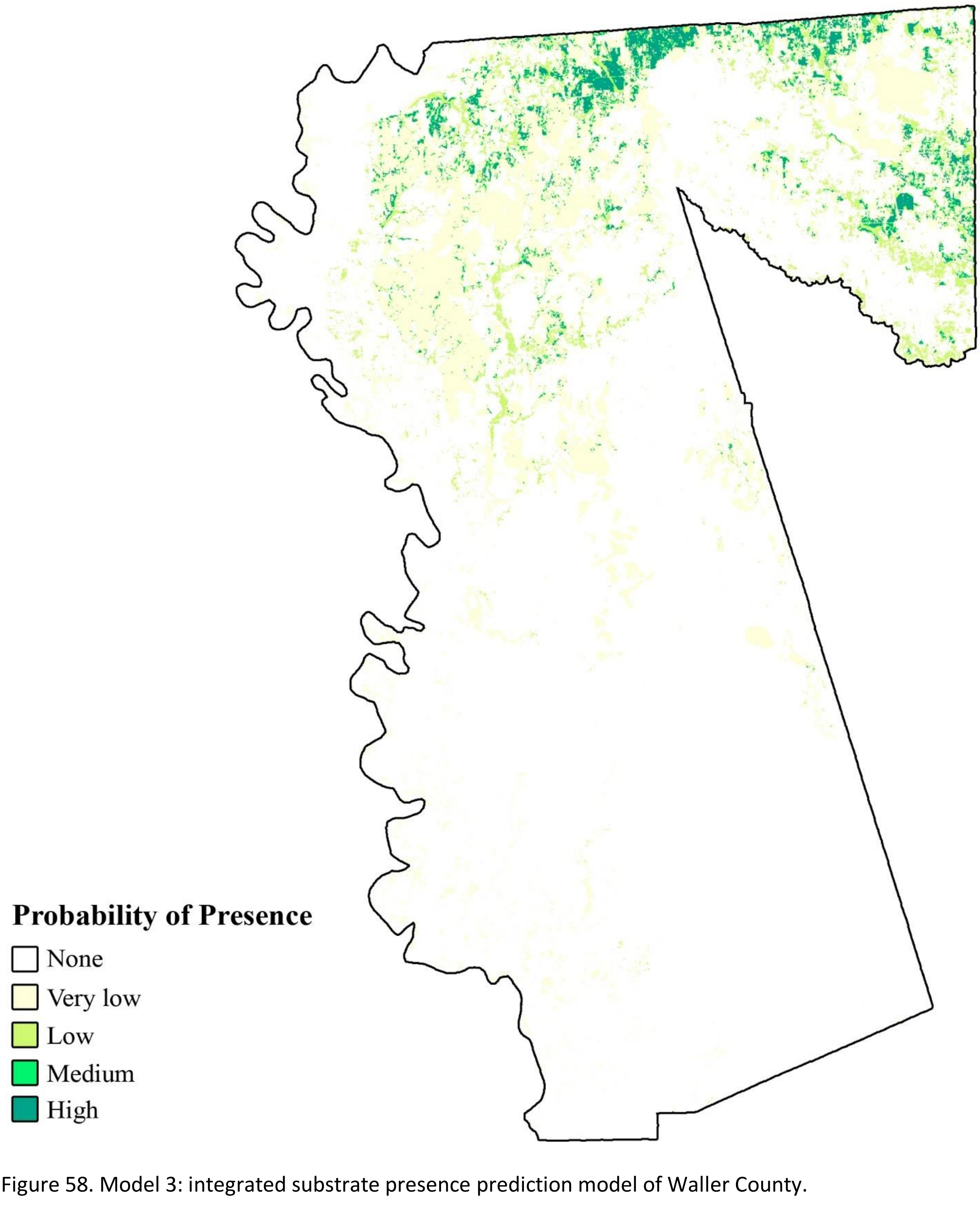

Figure 58. Model 3: integrated substrate presence prediction model of Waller County.

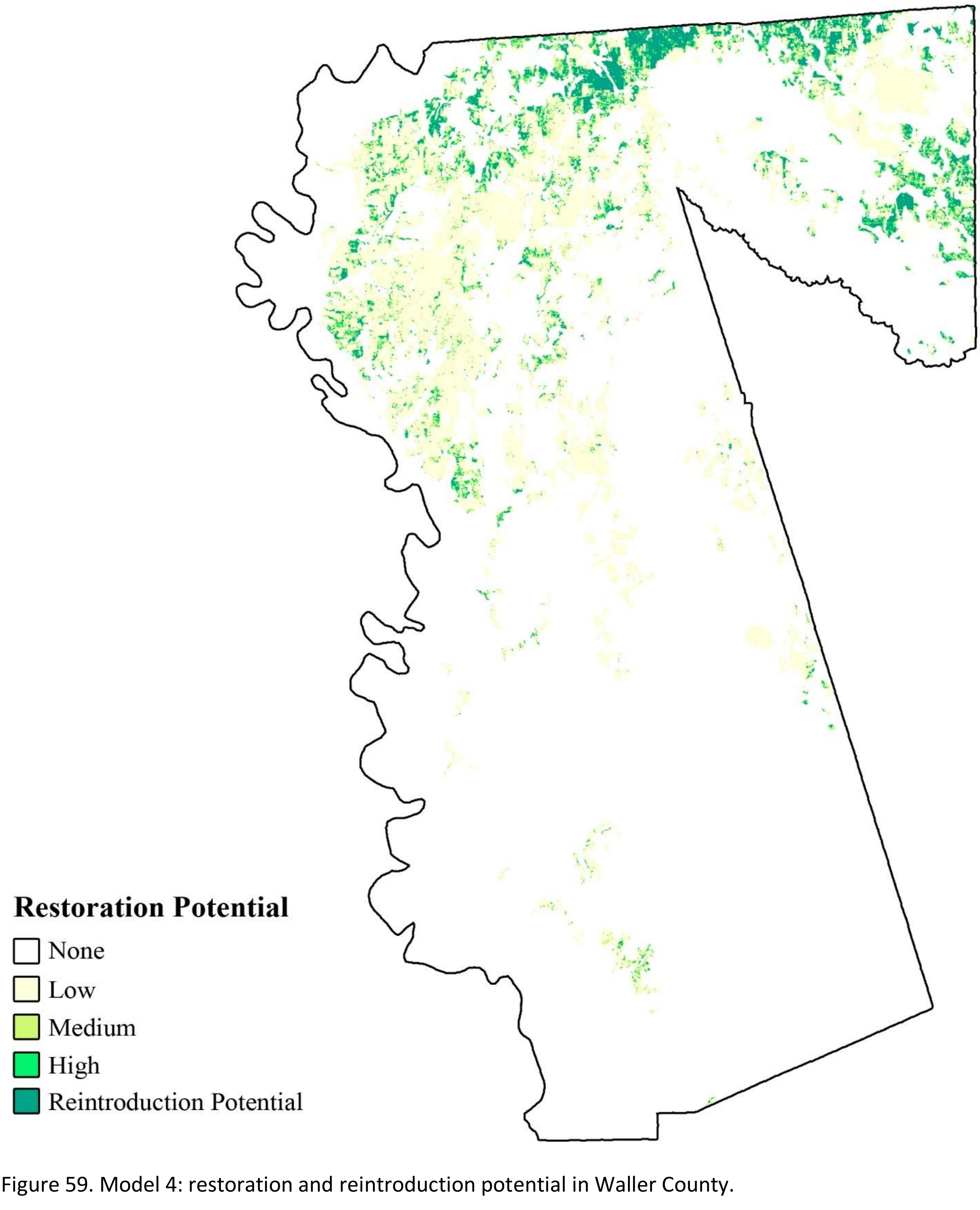

Figure 59. Model 4: restoration and reintroduction potential in Waller County.

Species Distribution Models

Methods

Houston Toad data

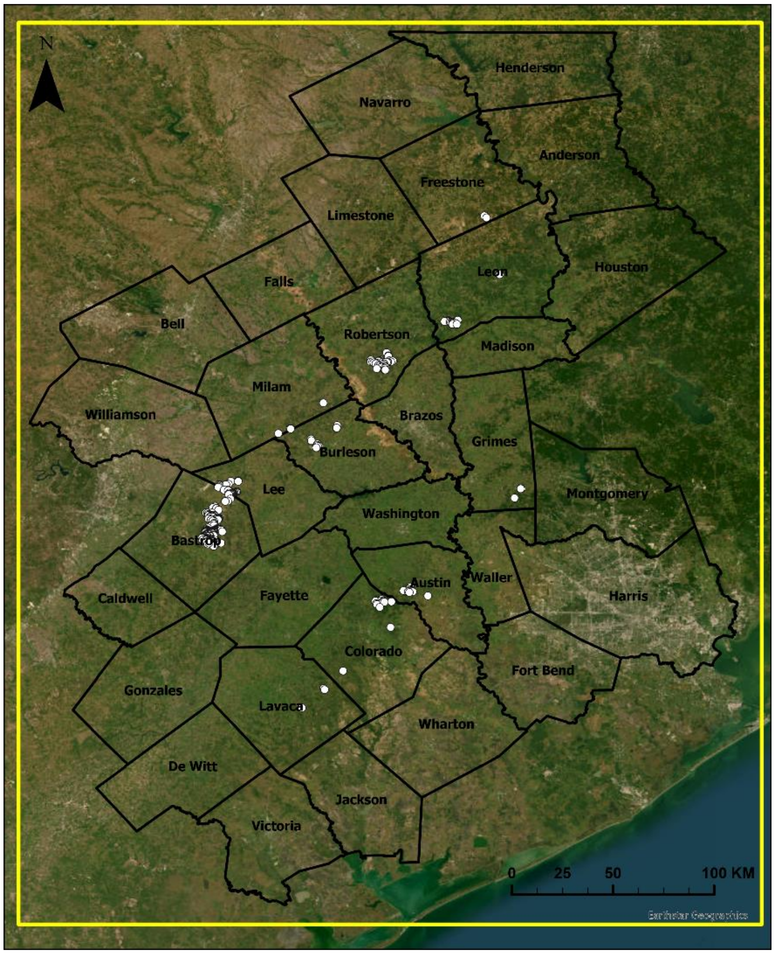

Figure 60. Area of interest (in yellow) for mapping the Houston Toad (*Anaxyrus houstonensis*) distribution model, including *A. houstonensis* localities in white. Area includes the core range (counties considered in the updated Buzo model) and a buffer of counties around the range that may contain potential habitat of interest.

We started with 5,216 *A. houstonensis* occurrence records remaining after cleaning the data as described above (Filtering Occurrence Records; Figure 60). We then removed all the occurrence records with duplicated latitude and longitudes, and those lacking full environmental data, which left us with 478 points for the full *A. houstonensis* data set. In addition to the full *A. houstonensis* data set, we also focused separately on only recent locality data (i.e., subset localities recorded during 2000-2010) with the goal of projecting suitable habitat based on more recent climate data. This data set consisted of 169 total *A. houstonensis* localities.

As presence data tends to be biased, we tried to address some of the bias in two different ways. First, we filtered our *A. houstonensis* localities spatially. We applied a 1km geographic filter using spThin package (Aiello-Lammens et al. 2015) where individual localities were filtered at a 1 km resolution, leaving us with 124 points. Second, we applied an environmental filter to the *A. houstonensis* data. Although many studies use environmental filters on principal component axes derived from all the environmental variables, that can be challenging to deconstruct and relate back to the species. Varela et al. (2014) and Castellanos et al. (2019) recommend environmental filtering of the environmental layers thought to be the main contributors to the distribution of the target species. Historically, sandy geology layers and forest cover are thought to be some of the main drivers of Houston Toad distribution (i.e., Buzo model). Thus, we used our deep sand and forest cover variables to filter the distribution points at a 5 and 0.05 resolution, respectively. After filtering with sand and forest cover, we were left with 183 *A. houstonensis* localities (Figure 61).

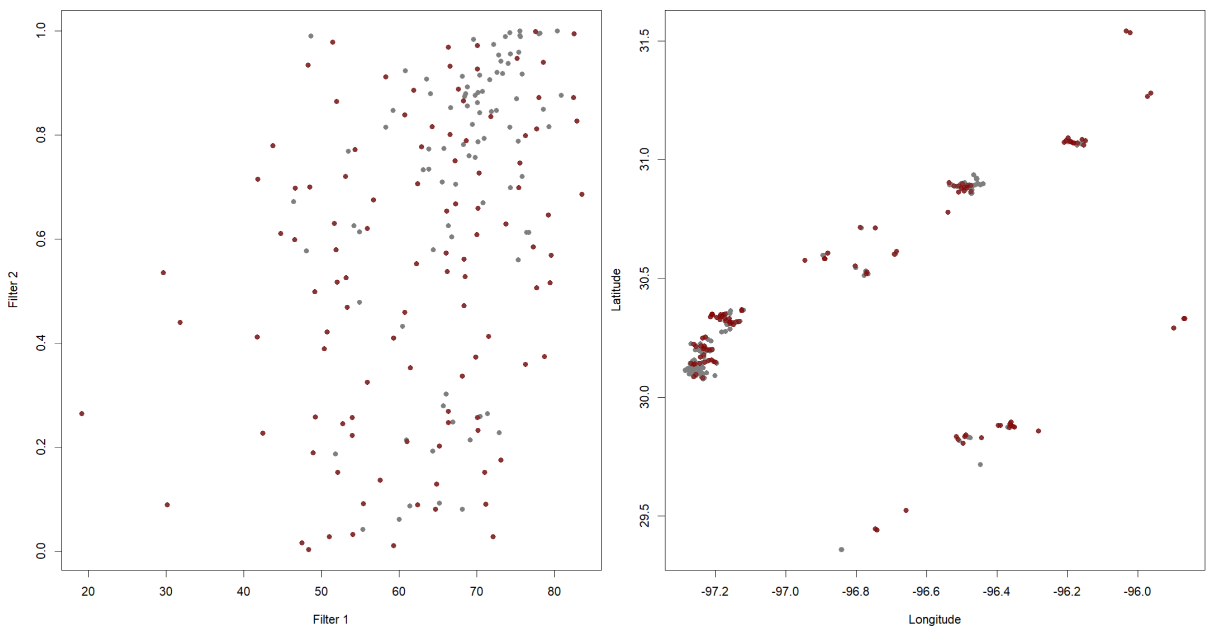

Figure 61. (Left) Environmental filtering results. Filter 1 = Deep Sand, Filter 2 = Percentage Forest Cover. All data represented by gray points. Points kept by the environmental filter are in red. (Right) Environmentally filtered points mapped to geographic space.

Environmental Data

We explored multiple environmental and climate datasets, including Bioclim (Fick and Hijmans 2017), Envirem (Title and Bemmels 2018), National Wetland Inventory (NWI; USFWS 2023), Texas Ecological Mapping System (TEMS; Elliott et al. 2009), National Land Cover Database (NLCD; USGS 2004), Soil Survey Geographic Database (SSURGO; Soil Survey Staff 2024), and ISRIC Soil Grids 250 m (Batjes et al. 2020). Because we have an extensive publication history for *A. houstonensis*, we chose environmental variables based on characteristics thought to impact the distribution of *A. houstonensis*, instead of using all variables in the models, which can produce spurious results in correlative presence-only SDMs like ours (Fourcade et al. 2018). We chose 21 initial variables that we think capture the need of *A. houstonensis* as described in the Introduction above, then ran a Pearson's correlation analysis (Table 17, Appendix 3). We removed one variable from each highly correlated pair ($|r| > 0.7$), leaving us with 14 final environmental variables.

Table 17. Environmental variables for inclusion in the Houston Toad (*Anaxyrus houstonensis*) species distribution models (SDMs). Final indicates whether the variable was included in the SDM analyses.

Variable Name	Data set	Description	Final
Deep Sand	ISRIC	Proportion of sand in soil sample taken from 60-100 cm deep	Y
Shallow Sand	ISRIC	Proportion of sand in soil sample taken from 5-15 cm deep	N
Shallow Silt	ISRIC	Proportion of silt in soil sample taken from 5-15 cm deep	N
Shallow Clay	ISRIC	Proportion of clay in soil sample taken from 5-15 cm deep	N
Elevation	BIOCLIM	Elevation, derived from SRTM	Y
Avg. Temp. March	BIOCLIM	Average Temperature in March (1970-2000)	Y
Precip. March	BIOCLIM	Total precipitation in March (1970-2000)	Y
Min Temp Warm	ENVIREM	Minimum temperature of the warmest month (1960-1990)	Y
Annual PET	ENVIREM	Annual potential evapotranspiration (1960-1990)	N
Clim Moist Index	ENVIREM	Metric of relative wetness and aridity (1960-1990)	N
Max Temp Cold	ENVIREM	Maximum temperature of the coldest month (1960-1990)	N
PET Cold Quart	ENVIREM	Mean monthly potential evapotranspiration of the coldest quarter (1960-1990)	Y

Variable Name	Data set	Description	Final
PET Driest Quart	ENVIREM	Mean monthly potential evapotranspiration of the driest quarter (1960-1990)	N
PET Warm Quart	ENVIREM	Mean monthly potential evapotranspiration of the warmest quarter (1960-1990)	Y
PET Wet Quart	ENVIREM	Mean monthly potential evapotranspiration of the wetest quarter (1960-1990)	Y
Terr Rough	ENVIREM	Terrain roughness index (Wilson et al. 2007)	Y
Wetland Area	TEMS & NWI	Sum of the wetland acreage from the NWI & TEMS data	Y
Forest Cover	NLCD 2004	Percent cover of deciduous & evergreen & mixed forest cover from 30m pixels aggregated to ~1km pixels	Y
Grass/Herbaceous Cover	NLCD 2004	Percent cover of grassland and herbaceous cover from 30m pixels aggregated to ~1km pixels	Y
Shrub/Scrub Cover	NLCD 2004	Percent cover of shrub and scrub cover from 30m pixels aggregated to ~1km pixels	Y
Woody Wetland Cover	NLCD 2004	Percent cover of woody wetland cover from 30m pixels aggregated to ~1km pixels	Y

Species Distribution Modeling

We ran individual SDMs using the full *A. houstonensis* data set with each of the nine SDM model algorithms available in the SSDM package (Schmitt et al. 2017). These algorithms included generalized linear models (GLM), general additive models (GAM), multivariate adaptive regression splines (MARS), classification tree analysis (CTA), generalized boosted models (GBM), maximum entropy (MaxEnt), artificial neural networks (ANN), random forests (RF), and support vector machines (SVM). SSDM automatically creates background points when presence-only data is used; the points are populated randomly across the background. We typically used the default settings as they have been calibrated based on recommendations in the literature (Schmitt et al. 2017). For the extent of our model, we focused on a one county buffer around the known distribution of the *A. houstonensis*, as we are interested not just in the current distribution but any sites that may be viable sites for conservation translocations.

Because uncertainty in SDM model outputs can impact their utility for conservation, we chose to create ensemble models, including the informative individual model algorithms. To select the algorithms included in the final ensemble model, we reviewed the evaluation metrics for each individual SDM. There is much debate over which evaluation metrics are best, therefore we took a comprehensive view and reviewed multiple metrics, including: Area under the receiver operating curve (AUC; no predictive ability <0.5, excellent > 0.9, (Araujo 2005, Swets 1988), the True skill statistic (TSS: 0 = no predictive ability, 1 = perfect prediction, Allouche et al 2006), and Cohen's kappa (κ; 0 = no predictive ability, 1 = perfect prediction, "excellent" = > 0.75 Landis & Koch 1977). We compared the evaluation metrics for each of the output models and removed any models that did not meet the "excellent" evaluation criteria of AUC>0.8, TSS >0.75, and κ > 0.75.

Using the final model choices, we ran an ensemble model using the full *A. houstonensis* dataset (ESDM1), the 2000-2010 *A. houstonensis* dataset (ESDM3), the geographically filtered (1km) dataset (ESDM4), and the environmentally filtered dataset (ESDM5) for the 7 algorithm models. We also ran a subset of the full *A. houstonensis* dataset ensemble model using only 4 algorithms to see if there was a substantial difference in the uncertainty across the model algorithms (ESDM2). Each of the model algorithms was replicated 10 times, with the background points drawn randomly each time. Finally, a hold-out methodology was used for cross validation to split the data into training and testing data. We evaluated the ensemble models using the metrics described above and we mapped the results of the SDM, the uncertainty (i.e., the between methods variation), and differences in the predicted presence probability between the final models (anomaly maps).

Landscape Connectivity Analysis

We analyzed patch fragmentation using two metrics from the final ensemble model. One included all pixels with probability scores above 0.5 (suitable habitat) and another included probability scores above 0.75 (high quality habitat). We considered patches larger than 1 ha to be core areas as nodes between least-cost pathways. To identify least-cost dispersal corridors and barriers to dispersal, we generated current and voltage maps in Circuitscape 4.0.5 (Anantharaman et al. 2020). We used predicted probabilities of occurrence from the final ensemble model as the connectivity layer.

Results

Our final environmental variable set included 14 parameters: 1 soil variable, 2 elevation/terrain variables, 2 wetland variables, 3 vegetation cover variables, and 6 climate variables. Of the model algorithms, we used the GLM, GAM, RF, MARS, CTA, SVM, and GBM algorithms in four of our final ensemble models (ESDM1, ESDM3, ESDM4, and ESDM5) and a subset of those algorithms (i.e., GLM, GAM, RF, and GBM) in ESDM2. We excluded MaxEnt and ANN, which did not meet our evaluation criteria (Table 18).

Table 18. Individual model evaluation metrics. The algorithms that did not meet our evaluation criteria are in bold. Algorithm abbreviations: generalized linear models (GLM), general additive models (GAM), multivariate adaptive regression splines (MARS), classification tree analysis (CTA), generalized boosted models (GBM), maximum entropy (MaxEnt), artificial neural networks (ANN), random forests (RF), and

support vector machines (SVM). Evaluation metrics are Area Under the Curve (AUC), True Skill Statistic (TSS), and Cohen's kappa (κ).

Algorithm	AUC (>0.9)	TSS (>0.75)	κ (>0.75)	Threshold
GLM	0.979	0.858	0.843	0.441
GAM	0.988	0.910	0.898	0.493
MARS	0.979	0.909	0.898	0.374
CTA	0.959	0.885	0.885	0.575
GBM	0.982	0.874	0.874	-0.158
MaxEnt	**0.991**	**0.416**	**0.106**	**0.097**
ANN	**0.692**	**0.385**	**0.385**	**0.752**
RF	0.984	0.895	0.895	0.395
SVM	0.994	0.930	0.930	0.688

Of our five final ensemble models, all ranked highly using our evaluation criteria and had similar variable importance (Table 19-20). For each ensemble model, deep sand was the variable with the highest importance for predicting the likelihood of *A. houstonensis* presence (>= 63%), with forest cover and maximum march precipitation ranking the second and/or third highest for each ensemble model, ranging between 4.5-7.5% for each ensemble model (Table 20). All the remaining variables had under 5% of the variable importance.

Table 19. Ensemble model evaluation metrics. Evaluation metrics are Area Under the Curve (AUC), True Skill Statistic (TSS), and Cohen's kappa (κ).

Model Name	AUC (>0.9)	TSS (>0.75)	κ (>0.75)	Threshold
Full Data, 7 algorithms (ESDM1)	0.983	0.906	0.900	0.468
Full Data, 4 algorithms (ESDM2)	0.987	0.904	0.899	0.287
2000-2010 Data (ESDM3)	0.989	0.932	0.906	0.466
1km Filter (ESDM4)	0.950	0.818	0.741	0.391
Environmental Filter (ESDM5)	0.941	0.799	0.711	0.360

Table 20. Variable importance for the ensemble models. Any value over 5% is in bold.

Variable	ESDM1	ESDM2	ESDM3	ESDM4	ESDM5
Deep Sand	**71.26**	**74.76**	**67.81**	**64.51**	**63.08**
Elevation	1.41	1.29	1.96	1.39	1.48

Variable	ESDM1	ESDM2	ESDM3	ESDM4	ESDM5
Wetland Area	0.40	0.39	0.40	0.45	0.37
Min Temp Warm	2.03	2.40	**5.14**	3.64	4.14
Forest Cover	**6.70**	**5.77**	**4.49**	**7.17**	**7.48**
Grass/Herbaceous Cover	0.59	0.54	0.63	0.94	0.90
Shrub/Scrub Cover	1.76	1.20	0.88	2.59	1.85
Woody Wetland Cover	0.97	0.57	1.06	1.55	1.54
PET Cold Quart	1.86	2.15	2.56	2.13	2.34
PET Warm Quart	2.14	1.64	2.53	3.54	**4.98**
PET Wet Quart	1.68	1.25	2.28	2.76	2.39
Precip. March	**5.46**	**5.36**	**5.86**	**5.02**	**4.36**
Avg. Temp. March	2.48	1.63	2.50	1.79	2.19
Terr Rough	1.27	1.06	1.89	2.54	2.90

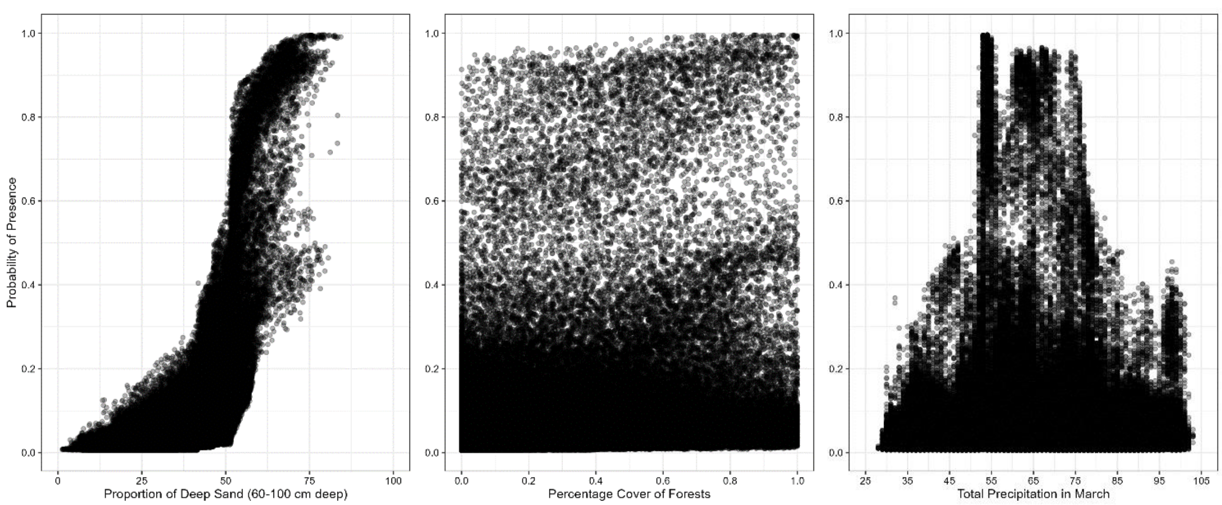

Figure 62. The relationships between the top three environmental variables, based on variable importance, and predicted probability of presence from ESDM1. Points are partially transparent, so darker areas have a higher density of points.

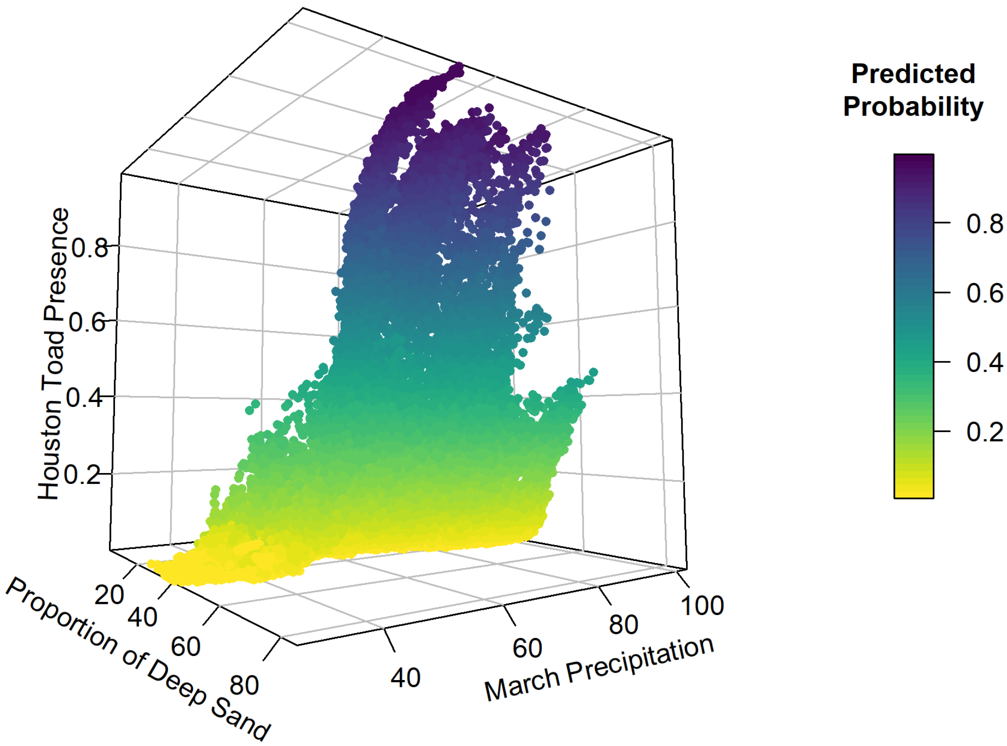

Figure 63. Houston Toad (*Anaxyrus houstonensis*) probability of presence as predicted by deep sand and total March precipitation, two of the top environmental variables.

We used the ESDM1 as our final model projection for comparison (Figures 64-65). The other model results are included in Appendix 2. ESDM1 had the highest proportion of pixels with high suitability, with 1.3% of the modeled area having a predicted probability of presence > 0.8. The other four ESDM ranged from 0.4 – 1.1% of pixels with > 0.8 predictions (Table 21). The highest difference in predictions in the core parts of the range of *A. houstonensis* occurred between models ESDM1 and ESDM3, which used only a subset of data from 2000-2010 compared to the full set of *A. houstonensis* presence data used in ESDM1 (Figure 66). Comparatively, ESDM4 and ESDM5 each differed from ESDM1 by having higher probabilities of presence outside of the core range. This is due to the geographic and environmental filtering of points in those two models to reduce the impact that large clusters of data may have on the predictions. For ESDM4 and ESDM5, no additional core areas seemed to arise, we primarily observed an increase of pixels ranging from 0-0.2 increase to 0.2-0.4 (Table 21, Appendix 2 Figures A5-A8). We did not see a large difference between geographic filtering and environmental filtering of *A. houstonensis* localities for our current ensemble models (Appendix 2 Figure A12).

ESDM1 had highest presence predicted in areas consistent with previous *A. houstonensis* detections, such as north-east Bastrop County, north-west Lee County, around the Milam-Burleson County line, in southern Robertson County, south-west Leon county, and the northern Colorado-Austin County line. Despite previous observations in eastern Lavaca county and southern Freestone counties, the model had lower (0.4-0.6) predicted probability in those two areas, although those included areas of relatively high uncertainty for the model (Figure 65). ESDM1 results also showed higher probabilities of occurrence in areas where *A. houstonensis* has not previously been detected, such as southern Bastrop County, and north-east Robertson and north-west Leon counties, which was supported by relatively low uncertainty (Figures 64-65).

Finally, our connectivity analysis showed that the core *A. houstonensis* populations are essentially isolated, with extremely limited corridors for dispersal between 6 (presence > 0.5) or 2 (presence > 0.75) population nodes (Figures 67-68).

Table 21. Total number of pixels falling in 20% ranges of predicted probability.

Pixel Range	ESDM1	ESDM2	ESDM3	ESDM4	ESDM5
0.8-1.0	2,132	1,767	747	1,508	1,333
0.6-0.8	1,838	2,420	2,270	2,772	3,570
0.4-0.6	2,473	2,970	2,836	4,052	4,959
0.2-0.4	8,200	8,293	5,404	10,751	14,191
0.0-0.2	152,401	151,594	155,787	147,961	142,991

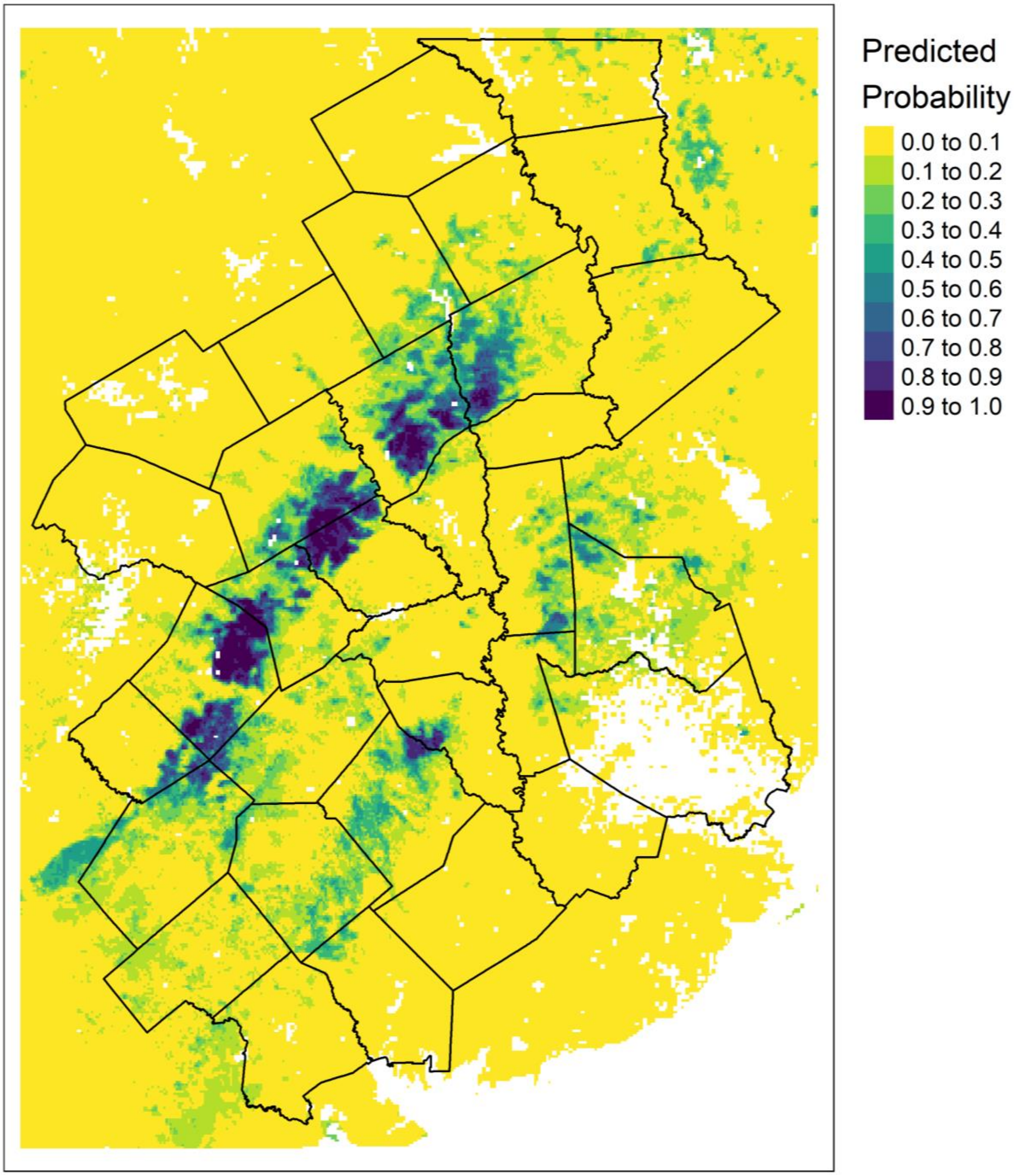

Figure 64. Predicted probability of presence for Houston Toads (*Anaxyrus houstonensis*) using ensemble modeling. This map represents ESDM1, which used the full *A. houstonensis* data set, 7 SDM algorithms, and no geographic or environmental filtering. The white pixels represent urban areas or large waterbodies.

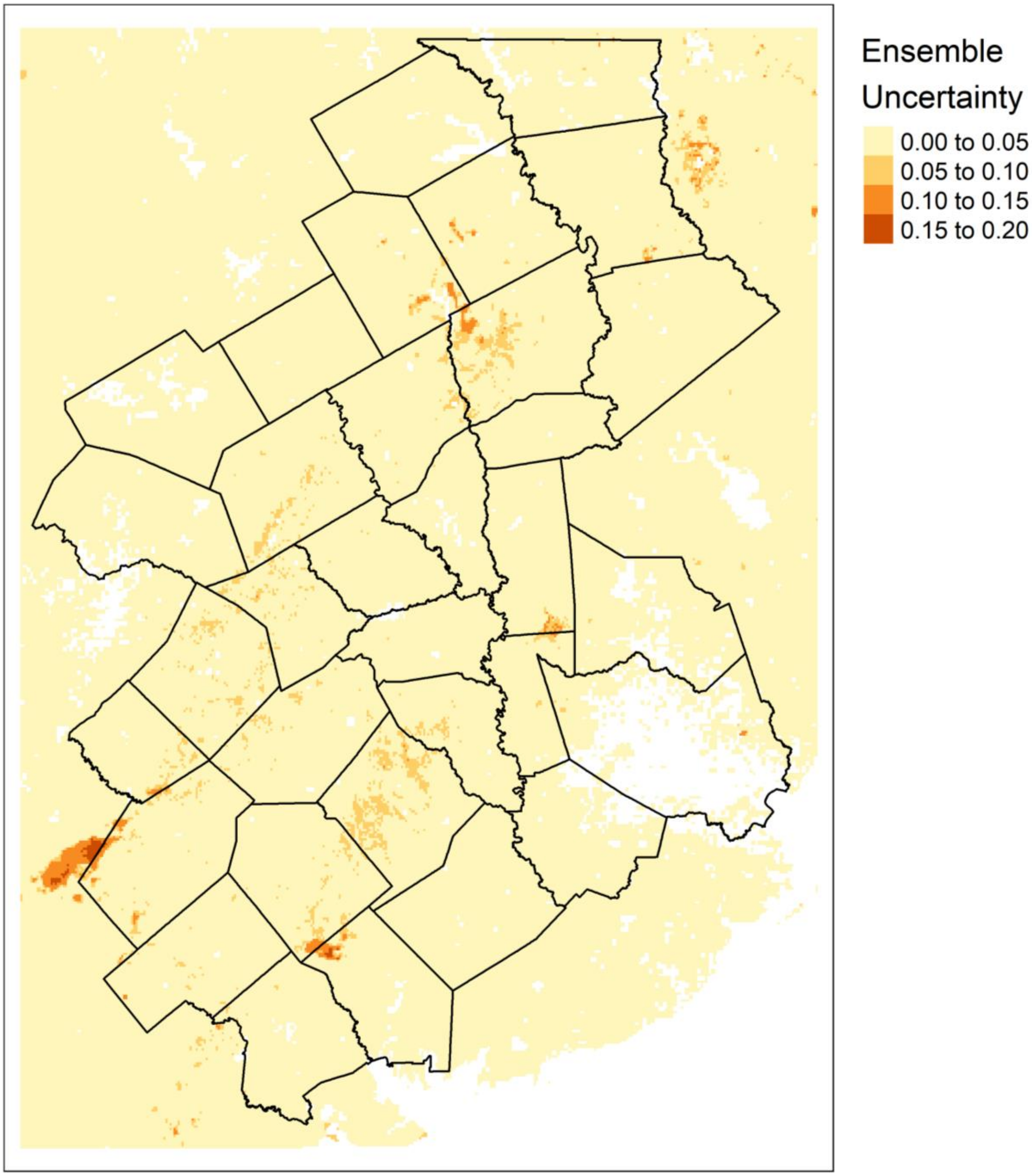

Figure 65. Uncertainty values from the Houston Toad (*Anaxyrus houstonensis*) ESDM1 ensemble model. Uncertainty values represent the variance between the different algorithm outputs and can identify areas of more and less agreement among the 7 SDM algorithms included in the ensemble model. Generally, ESDM2 had the lowest uncertainty among the 5 ensemble models.

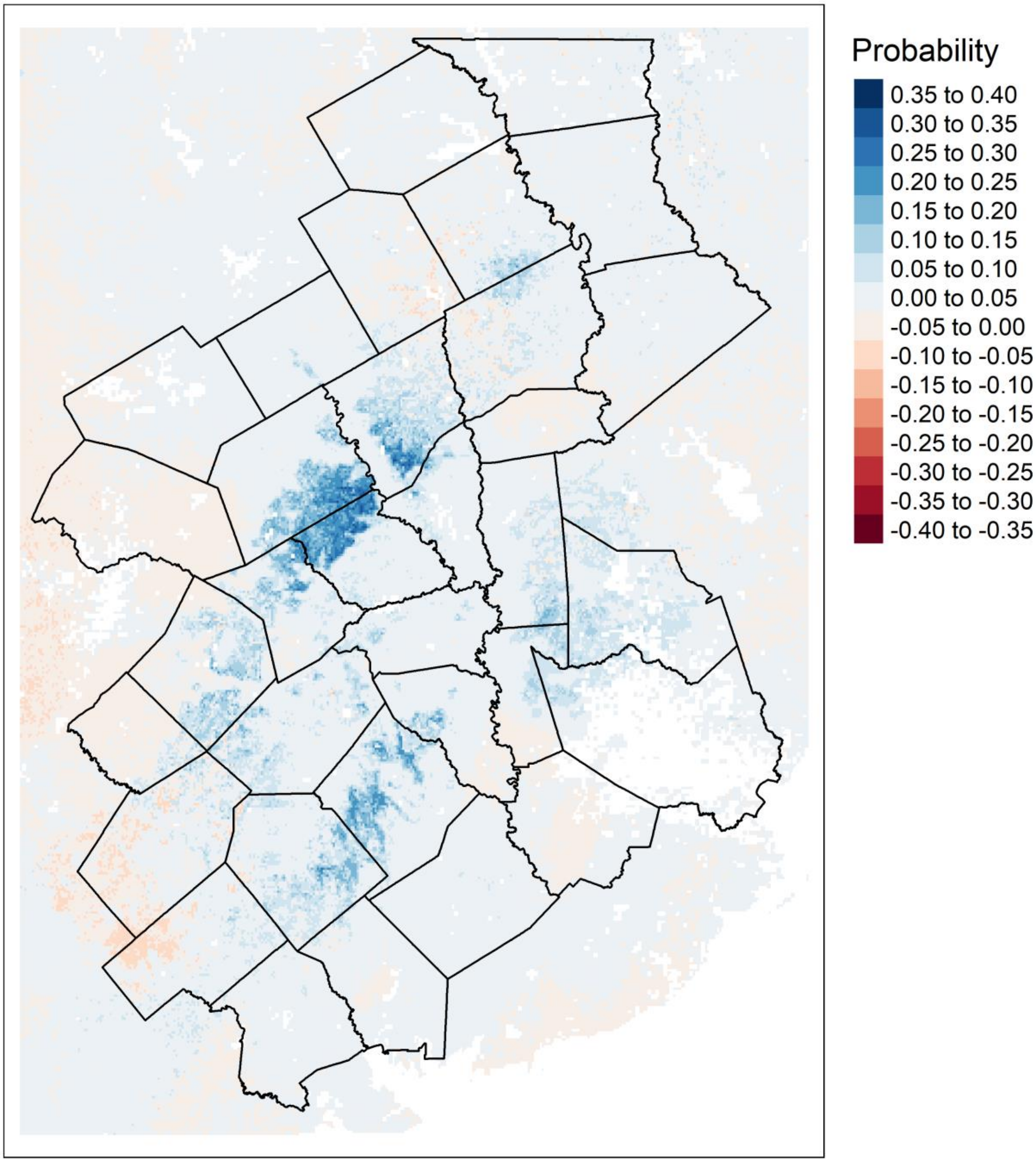

Figure 66. Anomaly map showing the difference between the Houston Toad (*Anaxyrus houstonensis*) ESDM1 ensemble model (All *A. houstonensis* Points) and ESDM3 ensemble model (2000 – 2010 *A. houstonensis* Points). Here, we can see that ESDM1 had higher predicted presence (blues) than ESDM3. This map shows the largest differences between the 5 ensemble models.

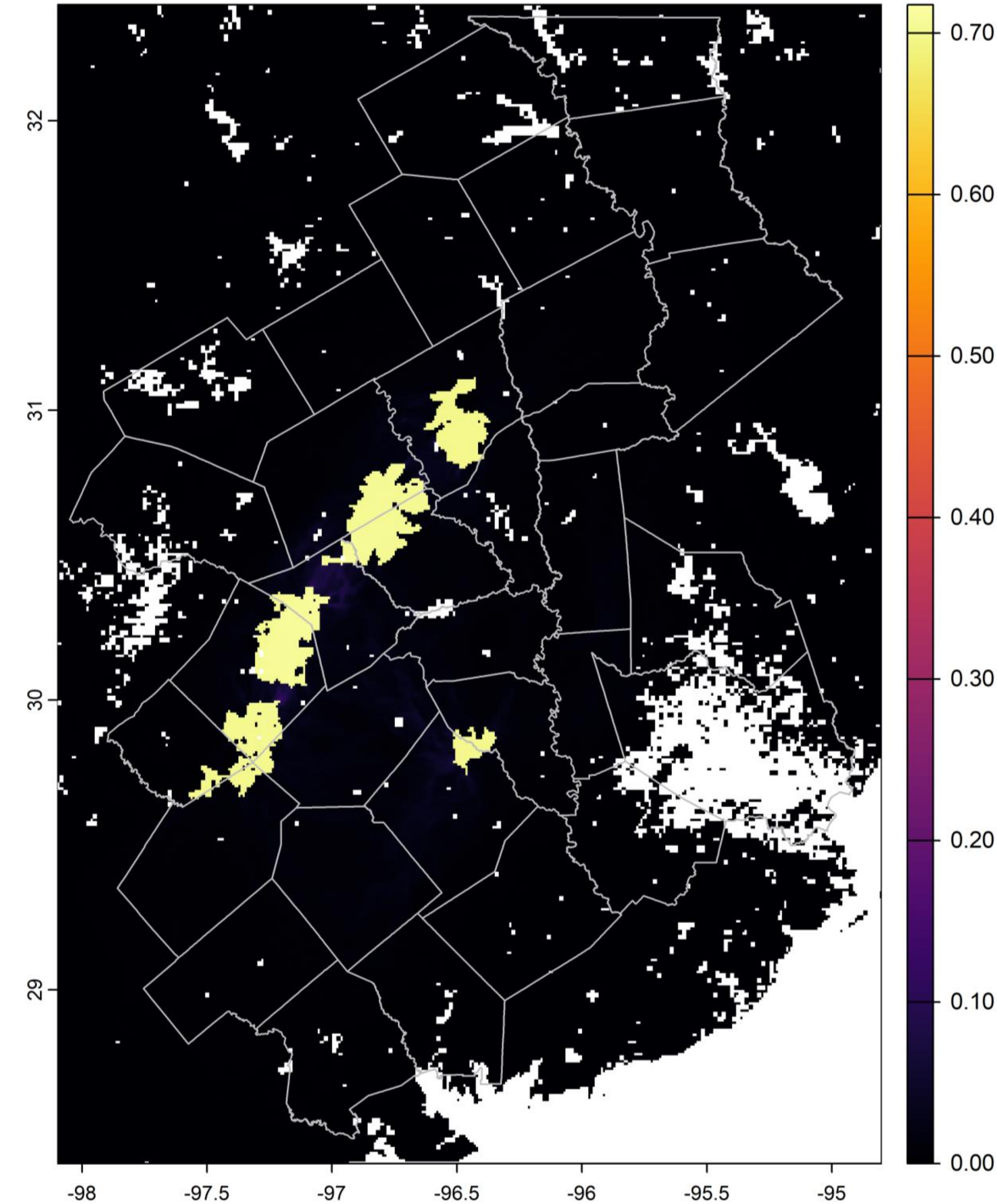

Figure 67. Potential dispersal corridors for the Houston Toad (*Anaxyrus houstonensis*) in the form of least-cost pathways simulated as conductivity within nodes in an electrical circuit. Log-transformed

current flow among centroid nodes within suitable habitat (probability > 0.5) patches larger than 1 ha. The white pixels represent urban areas or large waterbodies.

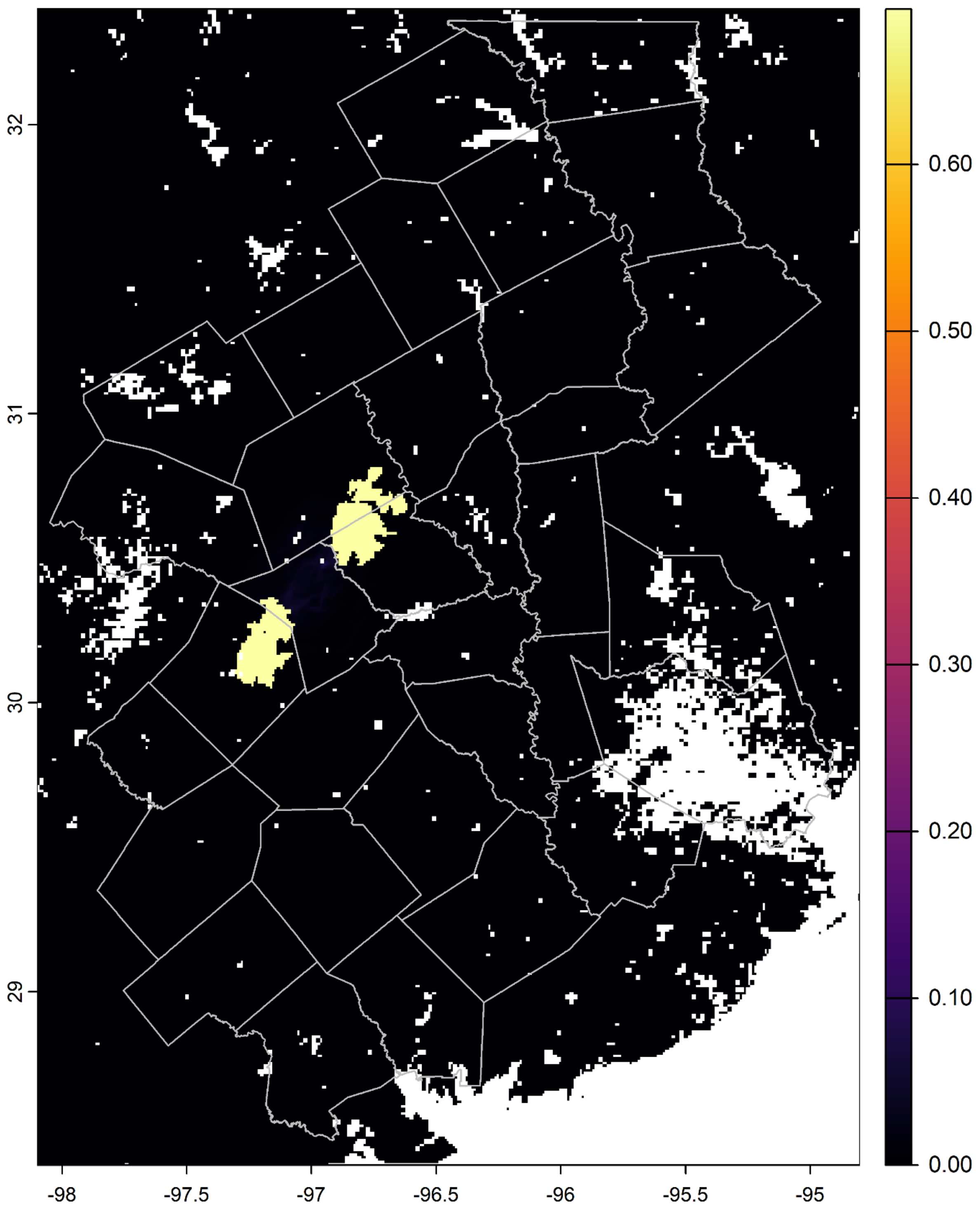

Figure 68. Potential dispersal corridors for the Houston Toad (*Anaxyrus houstonensis*) in the form of least-cost pathways simulated as conductivity within nodes in an electrical circuit. Log-transformed current flow among centroid nodes within highly suitable habitat (probability > 0.75) patches larger than 1 ha. The white pixels represent urban areas or large waterbodies.

Discussion

Additive Modeling Approaches

We completed updates to the Buzo models for each county, which took considerable computation time at the required 1-m resolution. On average, it takes the computer 5 days to process one county from raw data to final models. However, much of this time is spent on canopy analysis, and once canopy cover rasters are at the 30-m resolution, the computer can generate final models for each county in less than one hour. A potential solution to reduce computation time for future updates of these models is to use existing datasets on tree canopy cover. When we began the project, we used a different canopy dataset that was already scaled to a 30-m resolution. To make initial inferences about variable importance, we incorporated tree canopy cover into the models by creating thresholds for rasters from the U.S. Forest Service Tree Canopy CONUS database of 2016 imagery. We used the cartographic version of the database, which uses multispectral Landsat imagery to estimate canopy cover percentage and standard error within each 30-m cell, then applies masks to remove modeled canopy cover in non-tree areas and areas where the standard error is higher than the canopy cover percentage itself. If we had used that method, the resulting rasters would be very similar to the ones we developed from 2016-2020 1-m resolution imagery, lidar data, and EMS data. Future updates of this modeling process should use the most current updates to the CONUS database as a canopy cover layer for *A. houstonensis* models.

Additive Model Reproducibility

Initially, we wanted to generate R code scripts that would allow USFWS to update these models with ease as new updates to the environmental datasets were released. However, because of inconsistency among coordinate reference systems within lidar datasets, unmarked Universal Transverse Mercator (UTM) zone changes within lidar datasets, absence of protocol standardization among lidar datasets, a high number of individually-corrupt 1 km^2 lidar files that have to be removed manually one by one, the number of lidar datasets patching together each county, and issues with overlapping datasets, each county's script was unique, required considerable manual editing time, and would not be transferable to future lidar data releases. Future updates of this modeling process should use the most current updates to the U.S. Forest Service Tree Canopy CONUS database as a canopy cover layer for *A. houstonensis* models.

Soil Component Inclusion

Identifying soil map units provided a useful tool for predicting current population presence, but because soil taxonomy is specific to counties, understanding soil component requirements for the species could be a better metric in identifying restoration and reintroduction areas. In the occurrence record dataset filtered to 200 m, 14 samples were within units identified as complexes with variation at a finer resolution than mapped by the NRCS, but the remaining 271 records were within units that represent a relatively small portion of the soil texture pyramid (Table 22; Figure 696069). Mapping the area by soil component in future approaches could provide a better understanding of the needs of the species.

Table 2217. *Anaxyrus houstonensis* occurrence records by soil texture in the dataset filtered to 200 m.

Texture	Records
Loamy fine sand	133
Fine sand	71
Fine sandy loam	33
Gravelly fine sandy loam	31
Robco-Tanglewood complex	12
Loamy sand	2
Edge - Gullied land complex	1
Tenaha-Cuthbert complex	1
Very gravelly loamy sand	1

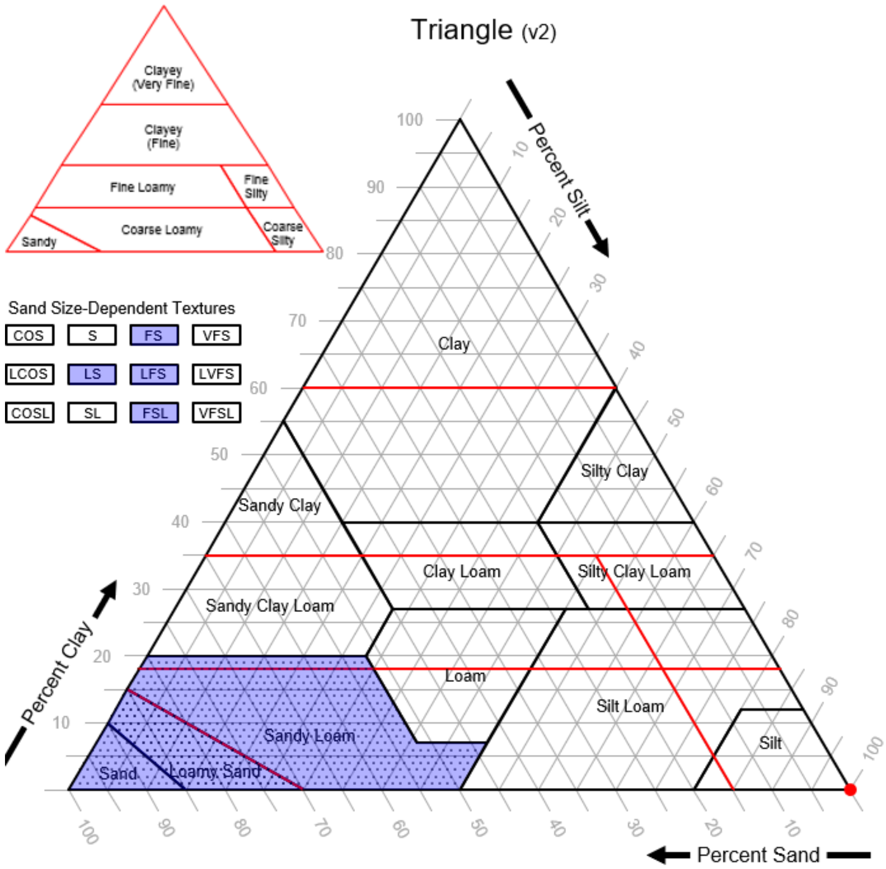

Figure 6960. Soil texture triangle depicting soil characteristics suitable for *A. houstonensis* generated using the USDA soil texture calculator.

SDM Approaches

All five final ensemble models yielded similar spatial predictions for core areas with the highest probability of presence of *A. houstonensis* (>0.50). Probability of presence was slightly lower for these core areas in the ESDM3 ensemble model due to the restriction of *A. houstonensis* occurrence records used to the years 2000 – 2010. More subtle differences among ensemble models exist on the edges of the predicted distribution where lower probabilities of presence vary spatially depending on whether occurrence records were filtered geographically or environmentally to avoid oversampling.

Several areas predicted to have high probability of presence across some ensemble models are significant because no known *A. houstonensis* occurrences have been recorded in them. These areas include Southern Bastrop County (south of Colorado River) and parts of Robertson and Leon Counties mostly north of known occurrences. Future call survey efforts could target these areas to determine if *A. houstonensis* populations have gone undetected in them.

All five final ensemble models also had similar variable importance with deep sand having the highest importance, followed by forest cover and total March precipitation with similar importance values across models. This statistical characterization of variable importance is significant because it confirms that the additive habitat modeling approaches used in the past (i.e., Buzo model) and in this update were applying variables necessary for *A. houstonensis* occurrence (e.g., percent sand, forest canopy cover).

Connectivity Analyses

Connectivity analysis showed little habitat connectivity among several or two core areas for threshold probability of presence values greater than 0.5 or 0.75, respectively. The isolation of these core areas suggests that population connectivity among them will have to be achieved through the captive breeding process for this species. Conservation and recovery actions may be considered equally important throughout these core areas, although such actions likely have the greatest benefit for the species when they are in closer proximity to occupied habitat or other conservation and recovery actions (i.e., aggregated spatially).

Resolution and Scale Trade-offs

The fine-scale resolution of the additive models is necessary to guide conservation and management decisions with different stakeholders, but it also makes quantifying variable importance very difficult because of the temporal variation among samples and heterogeneity in canopy cover at each occurrence record. Species Distribution Modeling approaches applied at coarser resolutions allow analysis of the environmental variables influencing geographic distribution for the species and can be used to explore the environmental parameter space outside the known distribution of the species more easily than with additive approaches, but they offer less resolution for stakeholders making conservation and management decisions. This trade-off in resolution and scale between the two modeling approaches suggests that they will be used most effectively in tandem for different purposes in future conservation efforts for the species. For example, future updates to the additive models using the suggested protocols in this report will continue to ensure that stakeholder conservation decisions are based on the most accurate information within the known distribution of the species, whereas updates to the species distribution models could help guide conservation decisions outside the known distribution of the species.

References

Aiello-Lammens, M.E., R.A. Boria, A. Radosavljevic, and B. Vilela. 2015. spThin: an R package for spatial thinning of species occurrence records for use in ecological niche models. Ecography 38(5):541–545.

Allouche, O., A. Tsoar, and R. Kadmon. 2006. Assessing the accuracy of species distribution models: prevalence, kappa and the true skill statistic (TSS). Journal of Applied Ecology, 43(6):1223–1232.

Araujo, M. B., R.G. Pearson, W. Thuiller, and M. Erhard. 2005. Validation of species-climate impact models under climate change. Global Change Biology 11(9):1504–1513. https://doi.org/10.1111/j.1365-2486.2005.001000.x

Batjes, N. H., E. Ribeiro, and A. van Oostrum: Standardised soil profile data to support global mapping and modelling (WoSIS snapshot 2019). Earth Syst. Sci. Data 12:299–320. https://doi.org/10.5194/essd-12-299-2020, 2020.

Brown, L.E. 1971. Natural hybridization and trend toward extinction in some relict Texas toad population. The Southwestern Naturalist 16:185–199.

Buzo, D. 2008. A GIS Model for Identifying Potential Breeding Habitat for the Houston toad (*Bufo houstonensis*). Masters of Science Thesis submitted to the Graduate Council of Texas State University-San Marcos, Texas. August.

Castellanos, A. A., J.W. Huntley, G. Voelker, and A.M Lawing. 2019. Environmental filtering improves ecological niche models across multiple scales. Methods in Ecology and Evolution 10(4):481–492. https://doi.org/10.1111/2041-210X.13142

Dewitz, J. 2021. National Land Cover Database (NLCD) 2019 Products [Data set]. U.S. Geological Survey. https://doi.org/10.5066/P9KZCM54

Dixon, J. R. 2013. Amphibians and Reptiles of Texas: With Keys, Taxonomic Synopses, Bibliography, and Distribution Maps. Third edition. Texas A&M University Press, College Station, Texas.

Duarte, A., D.J. Brown, M.R.J. Forstner. 2014. Document extinction in real time: decline of the Houston toad on a primary recovery site. Journal of Fish and Wildlife Management 5:363–371.

Elliott, Lee F., A. Treuer-Kuehn, C.F. Blodgett, C.D. True, D. German, and D.D. Diamond. 2009-2014. Ecological Systems of Texas: 391 Mapped Types. Phase 1 – 6, 10-meter resolution Geodatabase, Interpretive Guides, and Technical Type Descriptions. Texas Parks & Wildlife Department and Texas Water Development Board, Austin, Texas. Documents and Data Available at: http://www.tpwd.state.tx.us/gis/data/downloads#EMS-T

Fick, S.E., and R.J. Hijmans. 2017. WorldClim 2: new 1km spatial resolution climate surfaces for global land areas. International Journal of Climatology 37:4302–4315.

Forstner, M.R.J. 2003. Final: Biology/Ecology of the Houston Toad (*Bufo houstonenesis*). Report submitted to Bastrop County, Texas.

Forstner, M.R.J., and T.L. Ahlbrandt. 2003. Abiotic pond characteristics potentially influencing breeding of Houston toads (*Bufo houstonensis*). Texas Journal of Science 55:315–322.

Forstner, M.R.J. and J. Dixon. 2011. Houston toad (*Bufo houstonensis*) 5-year review: summary and evaluation. Final Report for Section 6 project E-101. Submitted to Texas Parks and Wildlife Department and U.S. Fish and Wildlife Service.

Fourcade, Y., A.G. Besnard, and J. Secondi. 2018. Paintings predict the distribution of species, or the challenge of selecting environmental predictors and evaluation statistics. Global Ecology and Biogeography 27(2):245–256.

Greuter, K.L. 2004. Early juvenile ecology of the endangered Houston toad, *Bufo houstonensis* (Anura: Bufonidae). Texas State University, San Marcos, Texas.

Guisan, A., and N.E. Zimmerman. 2000. Predictive habitat distribution models in ecology. Ecological Modelling 135:147–186.

Hatfield, J.S., A.H. Price, D.D. Diamond, and C.D. True. 2004. Houston toad (*Bufo houstonensis*) in Bastrop County, Texas: need for protecting multiple populations in Akçakaya, H.R., M.A. Burgman, Kindvall, O., C.C. Wood, P. Sjögren-Gulve, J.S. Hatfield, and M.A. McCarthy, editors. Species conservation and management. Oxford University Press. New York, New York.

Hillis, D.M., A.M. Hillis, and R.F. Martin. 1984. Reproductive ecology and hybridization of the endangered Houston toad (*Bufo houstonensis*). Journal of Herpetology 18:56–71.

Horton, J.D., C.A. San Juan, and D.B. Stoeser. 2017. The State Geologic Map Compilation (SGMC) geodatabase of the conterminous United States (ver. 1.1, August 2017): U.S. Geological Survey Data Series 1052, 46 p., https://doi.org/10.3133/ds1052.

Kennedy, J.P. 1962. Spawning season and experimental hybridization of the Houston toad, *Bufo houstonensis*. Herpetologica 17:239–245.

Landis, J. R., and G.G. Koch. 1977. The measurement of observer agreement for categorical data. Biometrics 33(1):159–174. https://doi.org/10.2307/2529310

Leathwich, J.R., J. Elith, M.P. Francis, T. Hastie, and P. Taylor. 2006. Variation in demersal fish species richness in the oceans surround New Zealand: an analysis using boosted regression trees. Marine Ecology Progress Series 321:267–281.

Liu, C., M. White, and G. Newell. 2013. Selecting thresholds for the prediction of species occurrence with presence-only data. Journal of Biogeography 40(4):778789.

McHenry, D.J,. and M.R.J. Forstner. 2009. Houston toad metapopulation assessment and genetics: data necessary for effective recovery strategies in a significantly fragmented landscape. Final Report for Section 6 project E-76. Submitted to Texas Parks and Wildlife Department and U.S. Fish and Wildlife Service.

McRae, B.H., B.G. Dickson, T.H. Keitt, and V.B. Shah. 2008. Using circuit theory to model connectivity in ecology and conservation. Ecology 10:2712–2724.

Owens H., V. Barve, and S. Chamberlain. 2022. spocc: Interface to Species Occurrence Data Sources. http://docs.ropensci.org/spocc/

Phillips, S.J., R.P. Anderson, and R.E. Schapire. 2006. Maximum entropy modeling of species geographic distributions. Ecological Modelling 190:231–259.

Quinn, H., and G. Mengdon. 1984. Reproduction and growth of *Bufo houstonensis* (Bufonidae) Southwestern Naturalist 29:189–195.

R Core Team. 2021. R: A language and environment for statistical computing. R Foundation for Statistical Computing, Vienna, Austria. URL https://www.R-project.org/.

Roussel, J., D. Auty, N.C. Coops, P. Tompalski, T.R. Goodbody, A.S. Meador, J. Bourdon, F. de Boissieu, A. Achim. 2020. lidR: An R package for analysis of Airborne Laser Scanning (ALS) data. Remote Sensing of Environment 251:112061. https://doi.org/10.1016/j.rse.2020.112061.

Saura, S., and L. Pascual-Hortal. 2007. A new habitat availability index to integrate connectivity in landscape conservation planning: comparison with existing indices and application to a case study. Landscape and Urban Planning 83:91–103.

Schmitt, S., R. Pouteau, D. Justeau, F. de Boissieu, and P. Birnbaum. 2017. SSDM: an R package to predict distribution of species richness and composition based on stacked species distribution models. Methods in Ecology and Evolution 8(12):1795–1803.

Seal, U.S., editor. 1994. Population and habitat viability assessment: Houston toad (*Bufo houstonensis*). Workshop conducted by IUCN/SSC Conservation Breeding Specialist Group in partial fulfillment of USFWS contract #94-172. Apple Valley, Minnesota.

Soil Survey Staff, Natural Resources Conservation Service, United States Department of Agriculture. Soil Survey Geographic (SSURGO) Database. 2024. Available online at https://sdmdataaccess.sc.egov.usda.gov. Accessed 01 March 2024.

Title P.O., and J.B. Bemmels. 2018. ENVIREM: an expanded set of bioclimatic and topographic variables increases flexibility and improves performance of ecological niche modeling. Ecography 41:291–307.

Texas Parks and Wildlife (TPWD). 2019. Endangered Houston toad: Destruction of Critical Habitat and Obstruction to Species Recovery.

U.S. Fish and Wildlife Service (USFWS). 1984. Houston toad recovery plan. U.S. Fish and Wildlife Service. Region 2. Albuquerque, New Mexico.

U.S. Fish and Wildlife Service (USFWS). 2009. Houston toad spotlight species action plan. U.S. Fish and Wildlife Service. Region 2. Albuquerque, New Mexico.

U.S. Fish and Wildlife Service (USFWS). 2011. Houston toad (*Bufo houstonensis*) 5-year review: summary and evaluation. Austin Ecological Services Field Office, Austin, Texas.

U.S. Fish and Wildlife Service (USFWS). 2017. Houston toad habitat management guidelines. February 2017 (Version 1.0). U.S. Fish and Wildlife Service, Region 2. Albuquerque, New Mexico.

U. S. Fish and Wildlife Service (USFWS). 2023. National Wetlands Inventory website. U.S. Department of the Interior, Fish and Wildlife Service, Washington, D.C.

U.S. Geological Survey (USGS). 2004. National Land Cover Database (NLCD) 2004 Land Cover Conterminous United States. https://www.usgs.gov/centers/eros/science/national-land-cover-database. Accessed 03 February 2024.

Varela, S., R.P. Anderson, R. García-Valdés, and F. Fernández-González. 2014. Environmental filters reduce the effects of sampling bias and improve predictions of ecological niche models. Ecography 37:1084–1091.

Wallace, D.M. 2015. A spatiotemporal habitat fragmentation analysis for the endangered Houston toad (*Bufo houstonensis*). Master's Thesis. Texas State University, San Marcos, Texas.

Welsh, H. 1990. Relictual amphibians and old-growth forests. Conservation Biology 14:309–319.

Wilson, M.F.J., B. O'Connell, C. Brown, J.C. Guinan, and A.J. Grehan. 2007. Multiscale Terrain Analysis of Multibeam Bathymetry Data for Habitat Mapping on the Continental Slope. Marine Geodesy 30: 3–35.

Appendix 1. Habitat Suitability from Additive Models

Table 1. The total predicted areas (km^2) of habitat suitability in each county, ranked by probability of presence (for models M_1, M_2, and M_3), restoration potential (for model M_4), and habitat suitability (from the Buzo 2008 model). Reintro. – Reintroduction potential. Data repeated from tables in the main body of the report.

Model	Rank	Austin County (km^2)	Bastrop County (km^2)	Brazos County (km^2)	Burleson County (km^2)	Colorado County (km^2)	Freestone County (km^2)	Harris County (km^2)	Lavaca County (km^2)	Lee County (km^2)	Leon County (km^2)	Milam County (km^2)	Robertson County (km^2)	Waller County (km^2)
	High	19	28	0	29	29	4	0	5	13	163	24	56	29
	Medium	15	18	0	28	26	5	13	7	18	175	43	51	47
M_1	Low	28	54	0	51	54	9	0	20	37	163	57	84	23
	Very Low	119	340	0	175	273	33	1	189	241	418	269	275	140
	None	1522	1879	1533	1471	2141	2262	4517	2293	1333	1883	2252	1777	1104
	High	19	28	0	29	29	4	0	5	13	163	24	56	29
	Medium	18	41	3	26	19	119	0	5	18	167	21	100	9
M_2	Low	182	500	24	263	354	234	18	237	326	802	377	508	204
	Very Low	80	447	87	78	71	757	14	113	228	376	93	568	35
	None	1403	1302	1419	1357	2050	1199	4500	2153	1058	1295	2130	1012	1066
	High	19	28	0	29	29	4	0	5	13	163	24	56	29
	Medium	8	25	3	9	3	117	0	1	9	78	3	67	0
M_3	Low	31	28	12	40	34	49	17	26	22	213	59	71	50
	Very Low	234	514	95	301	409	397	267	297	344	874	412	548	207
	None	1411	1723	1422	1375	2049	1746	4248	2185	1255	1474	2147	1502	1056
	Reintro.	42	64	15	50	39	165	4	25	26	279	43	142	33
M_4	High	22	43	11	31	23	63	1	17	21	137	32	74	11
	Medium	60	172	33	90	80	158	2	69	83	261	106	186	29

Model	Rank	Austin County (km²)	Bastrop County (km²)	Brazos County (km²)	Burleson County (km²)	Colorado County (km²)	Freestone County (km²)	Harris County (km²)	Lavaca County (km²)	Lee County (km²)	Leon County (km²)	Milam County (km²)	Robertson County (km²)	Waller County (km²)
	Low	307	1361	202	375	398	968	9	603	666	810	592	942	177
	None	1271	679	1271	1208	1983	958	4516	1800	848	1316	1872	899	1093
Buzo (2008) Canopy + Soil Model	High	102	255	NA	53	177	NA	91	201	49	84	132	179	NA
	Medium	102	603	NA	246	278	NA	317	553	493	364	608	538	NA
	Low	289	209	NA	158	479	NA	544	226	66	336	185	269	NA
	Very Low	919	858	NA	1193	1262	NA	2764	1056	936	1625	1560	1189	NA
	None	289	371	NA	105	328	NA	861	478	115	392	132	67	NA

Appendix 2. ESDM Model Results

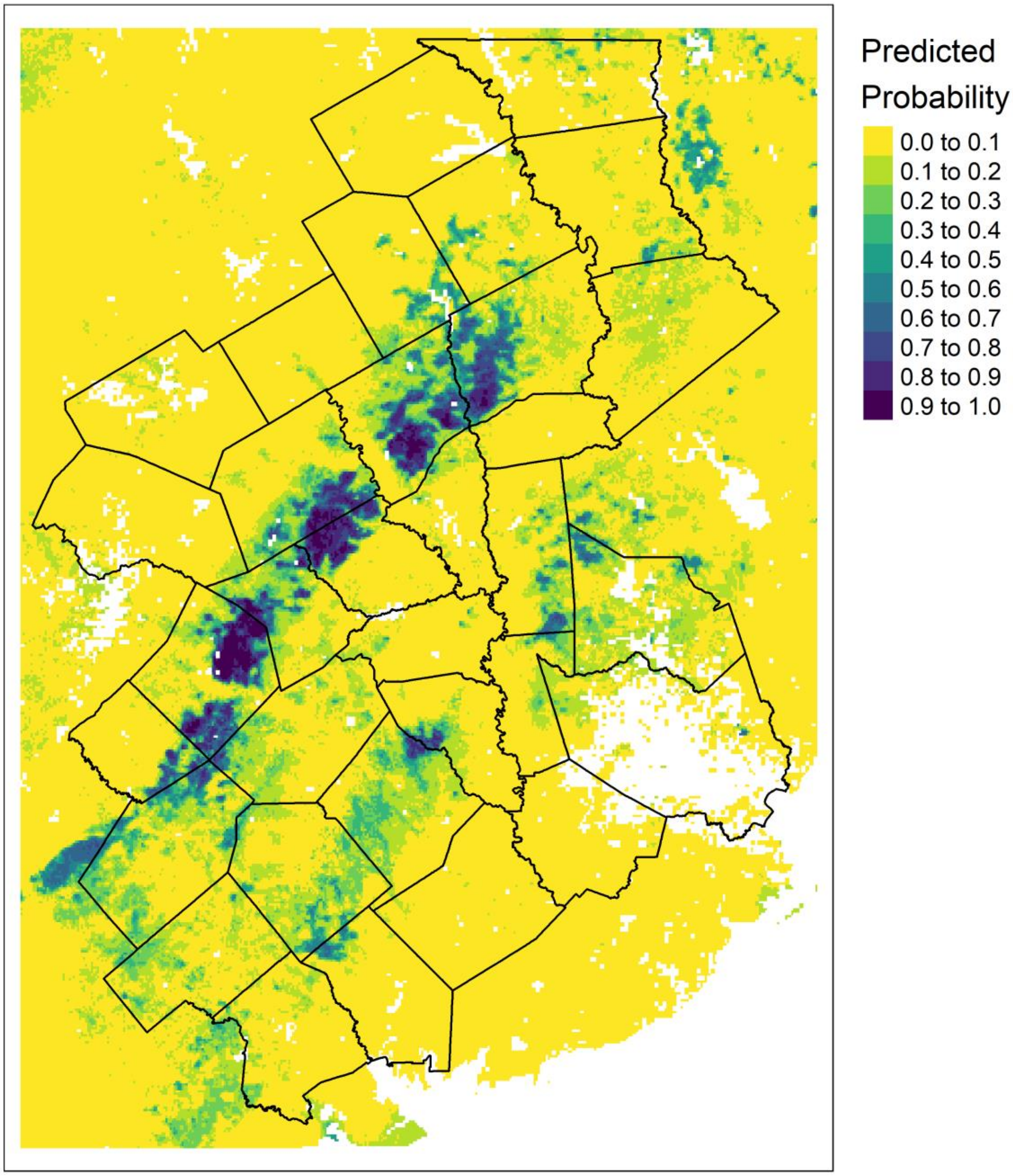

Figure A1. Predicted probability of presence for Houston Toads (*Anaxyrus houstonensis)* using ensemble modeling. This map represents ESDM2, which used the full *A. houstonensis* data set, 4 SDM algorithms, and no geographic or environmental filtering. The white pixels represent urban areas or large waterbodies.

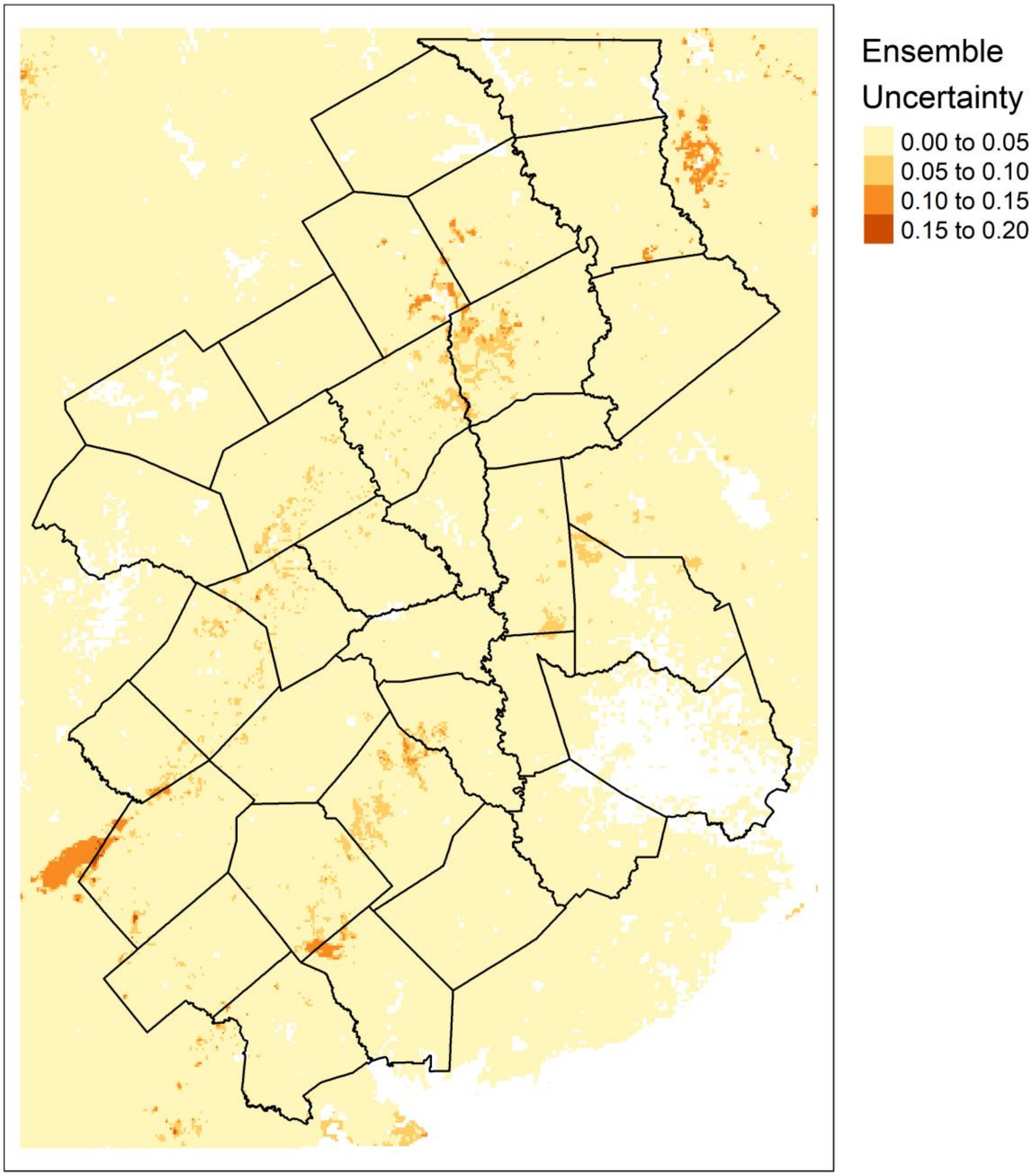

Figure A2. Uncertainty values from the Houston Toad (*Anaxyrus houstonensis*) ESDM2 ensemble model. Uncertainty values represent the variance between the different algorithm outputs and can identify areas of more and less agreement among the 4 SDM algorithms included in the ensemble model.

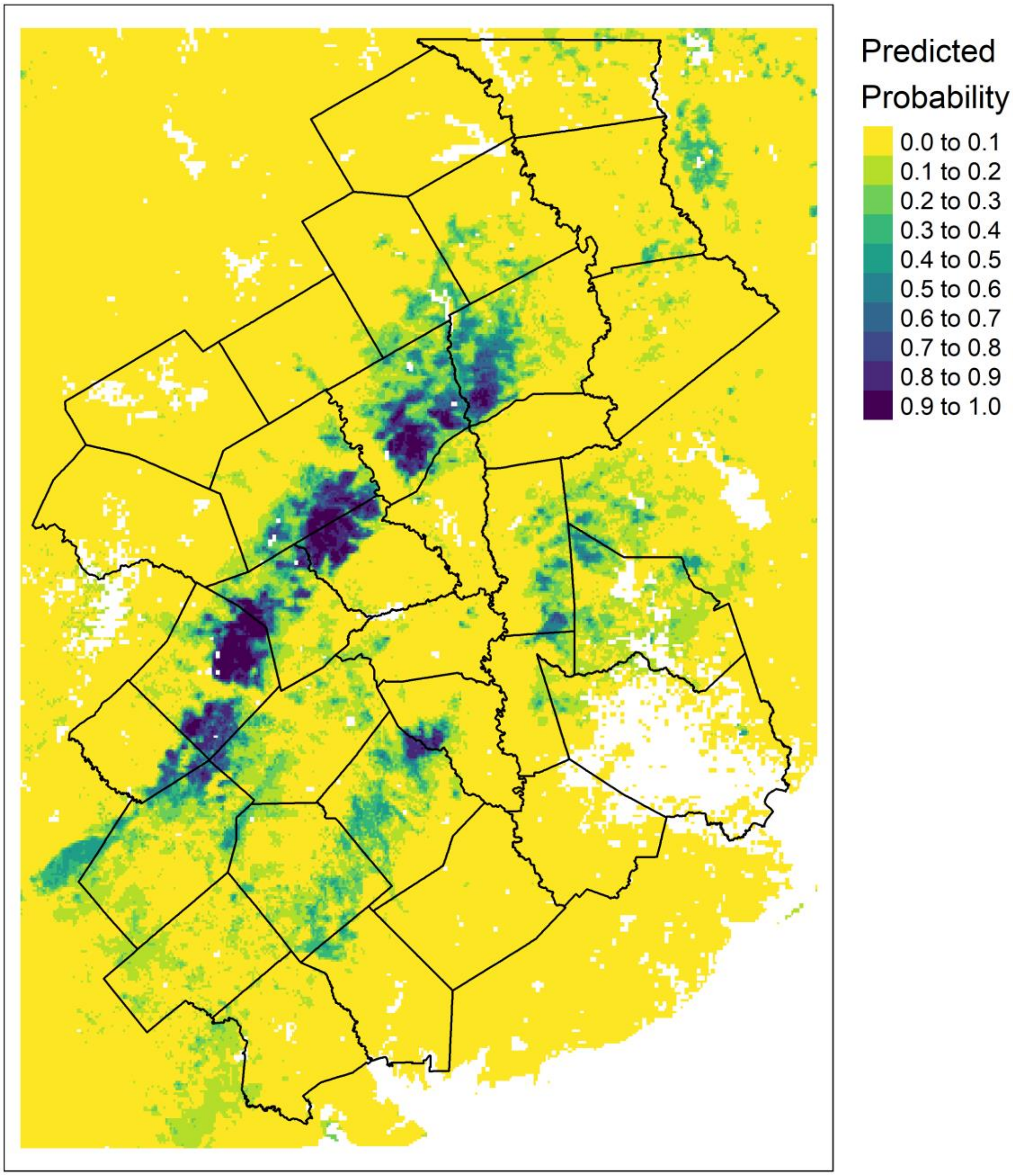

Figure A3. Predicted probability of presence for Houston Toads (*Anaxyrus houstonensis*) using ensemble modeling. This map represents ESDM3, which used the 2000-2010 *A. houstonensis* data set, 7 SDM algorithms, and no geographic or environmental filtering. The white pixels represent urban areas or large waterbodies.

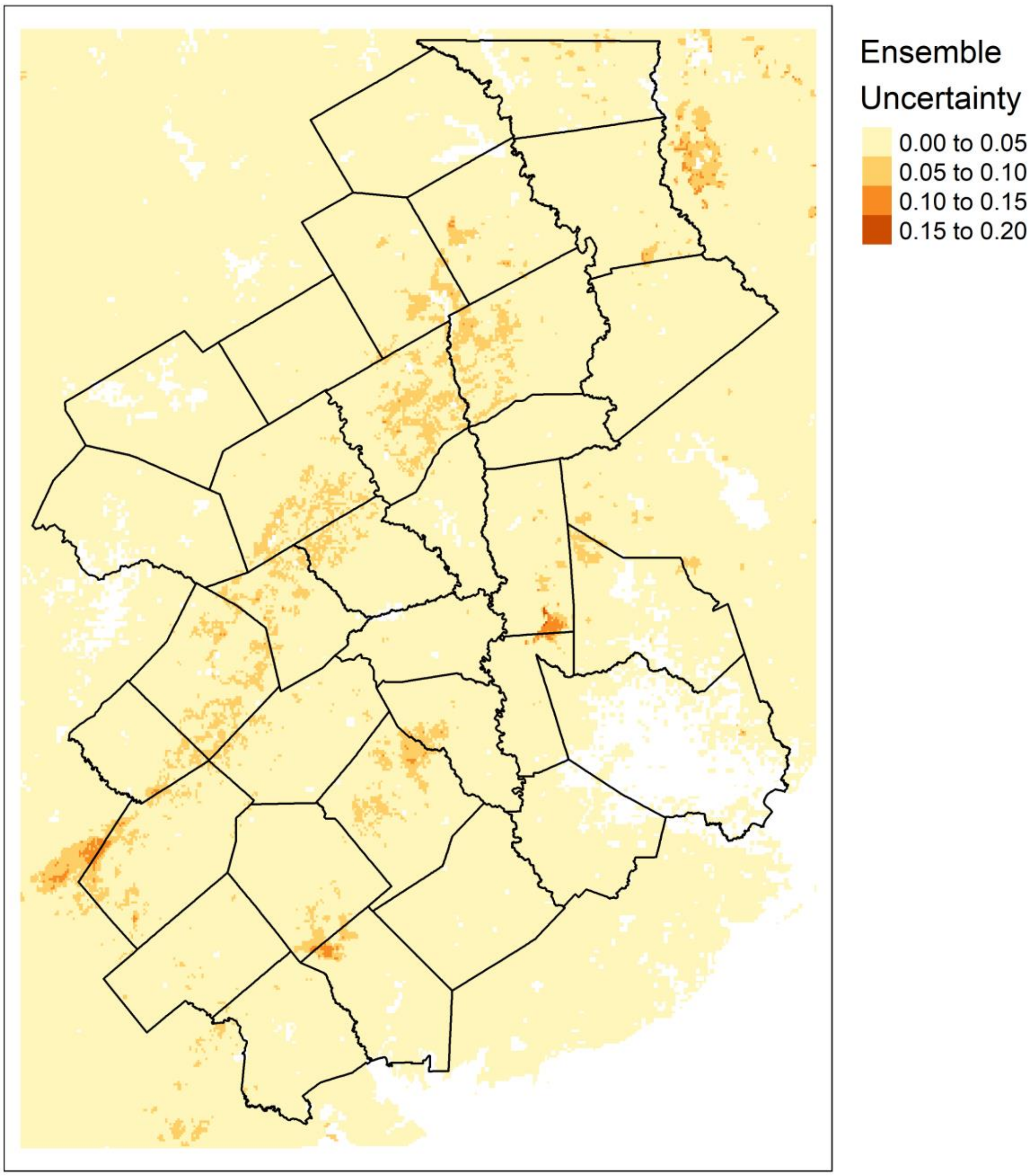

Figure A4. Uncertainty values from the Houston Toad (*Anaxyrus houstonensis*) ESDM3 ensemble model. Uncertainty values represent the variance between the different algorithm outputs and can identify areas of more and less agreement among the 7 SDM algorithms included in the ensemble model.

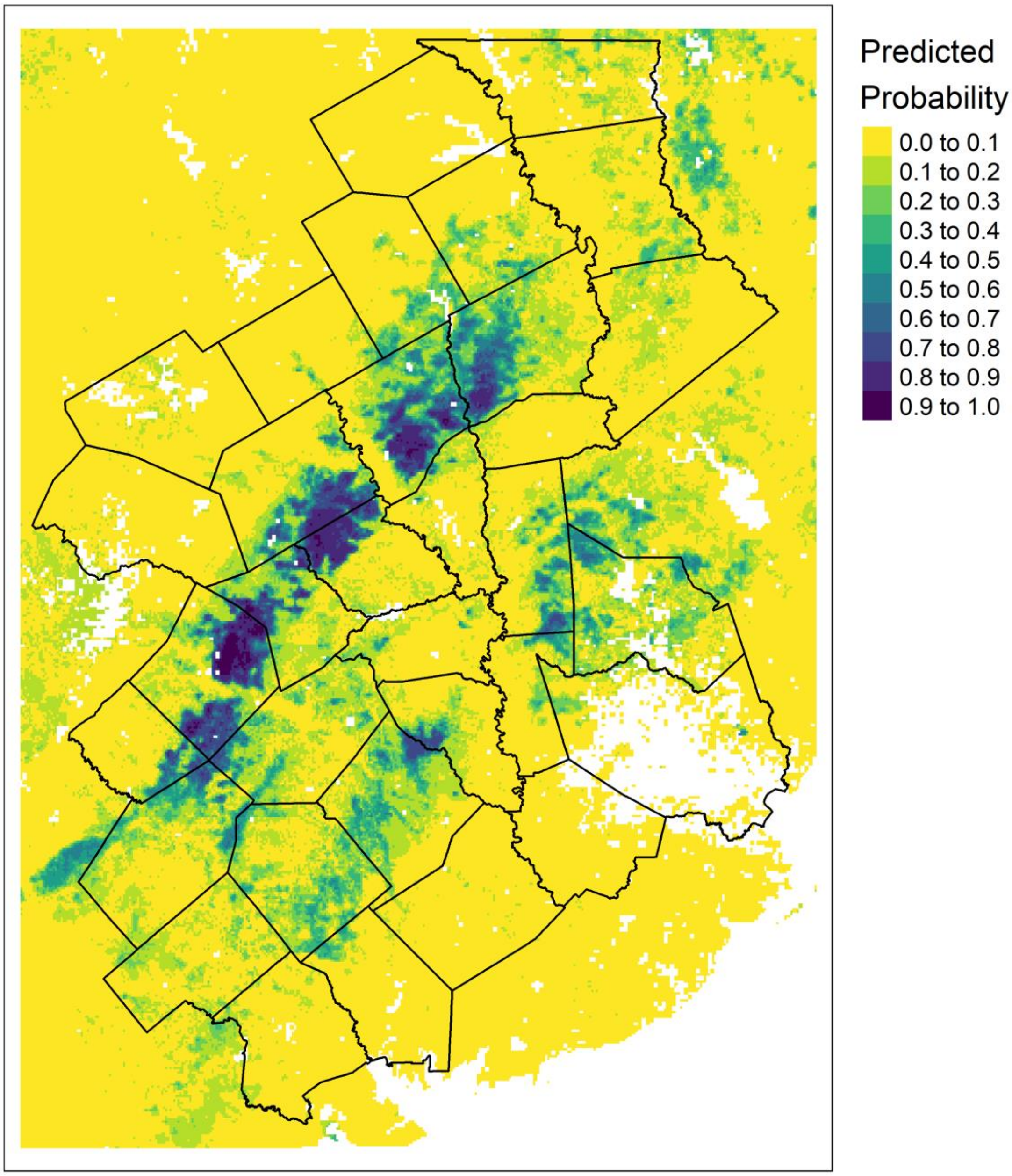

Figure A5. Predicted probability of presence for Houston Toads (*Anaxyrus houstonensis*) using ensemble modeling. This map represents ESDM4, which used the 1km geographically filtered *A. houstonensis* data set, 7 SDM algorithms, and no environmental filtering. The white pixels represent urban areas or large waterbodies.

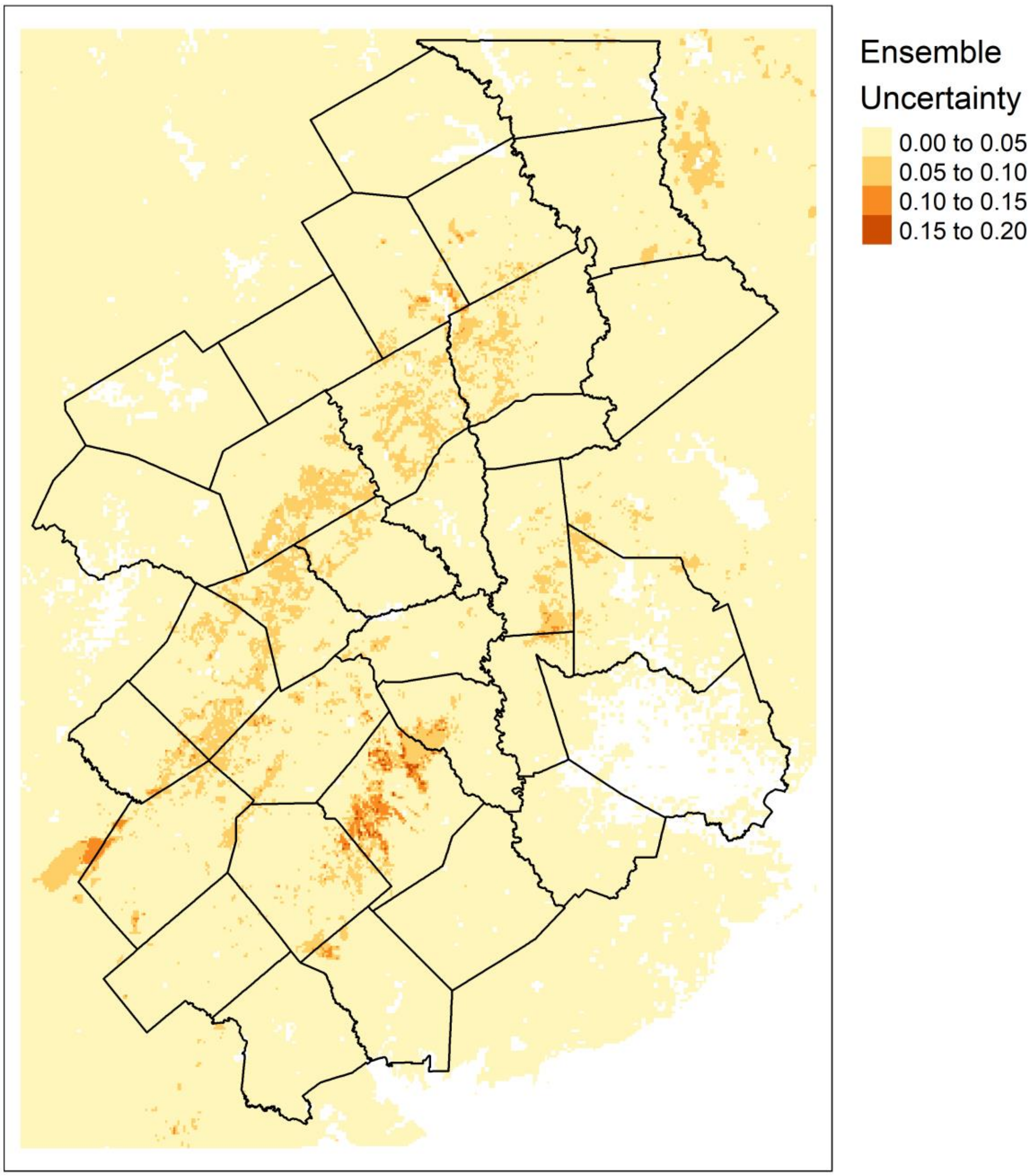

Figure A6. Uncertainty values from the Houston Toads (*Anaxyrus. houstonensis*) ESDM4 ensemble model. Uncertainty values represent the variance between the different algorithm outputs and can identify areas of more and less agreement among the 7 SDM algorithms included in the ensemble model.

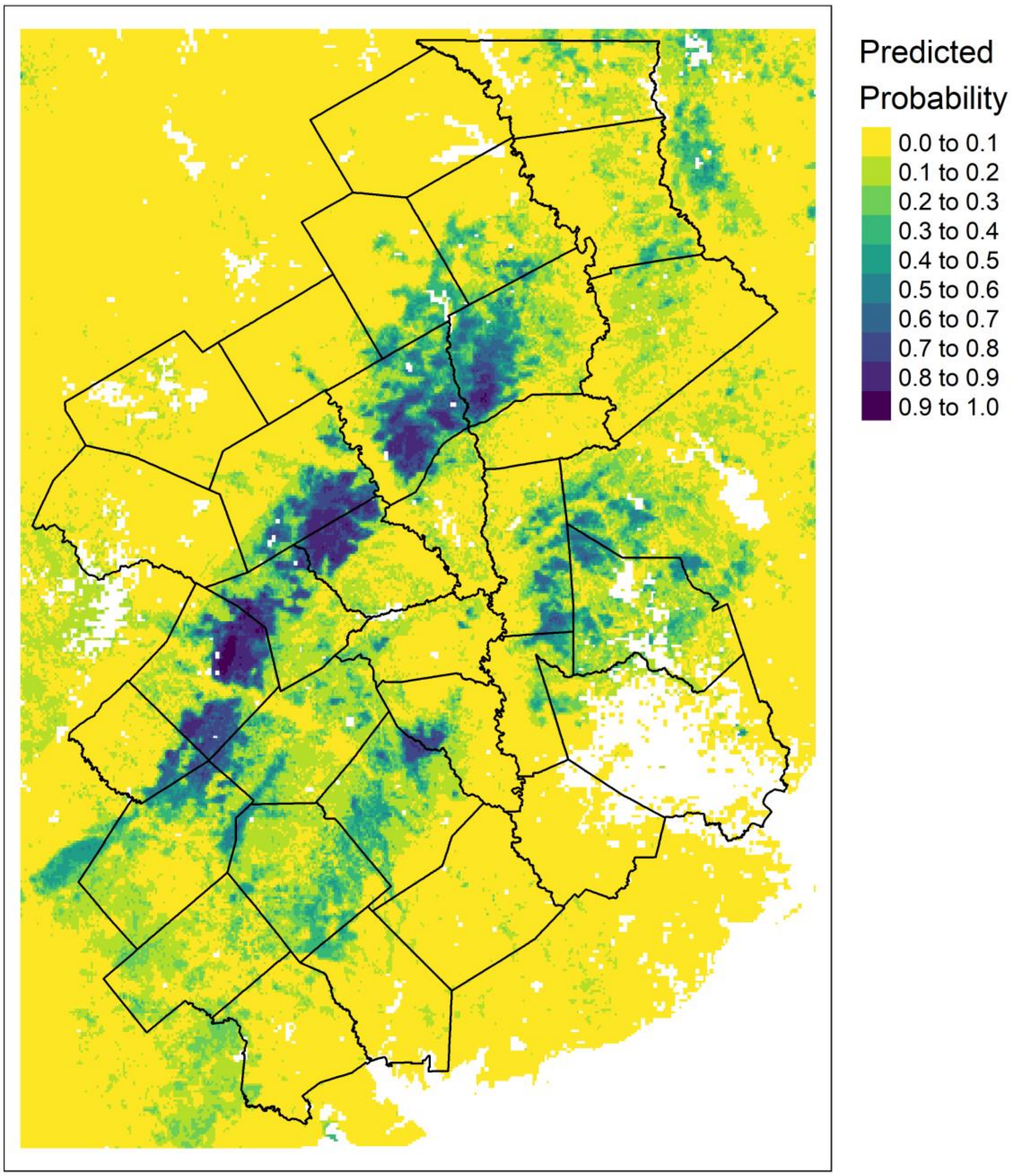

Figure A7. Predicted probability of presence for Houston Toads (*Anaxyrus houstonensis)* using ensemble modeling. This map represents ESDM5, which used the environmentally filtered *A. houstonensis* data set, 7 SDM algorithms, and no geographic filtering. The white pixels represent urban areas or large waterbodies.

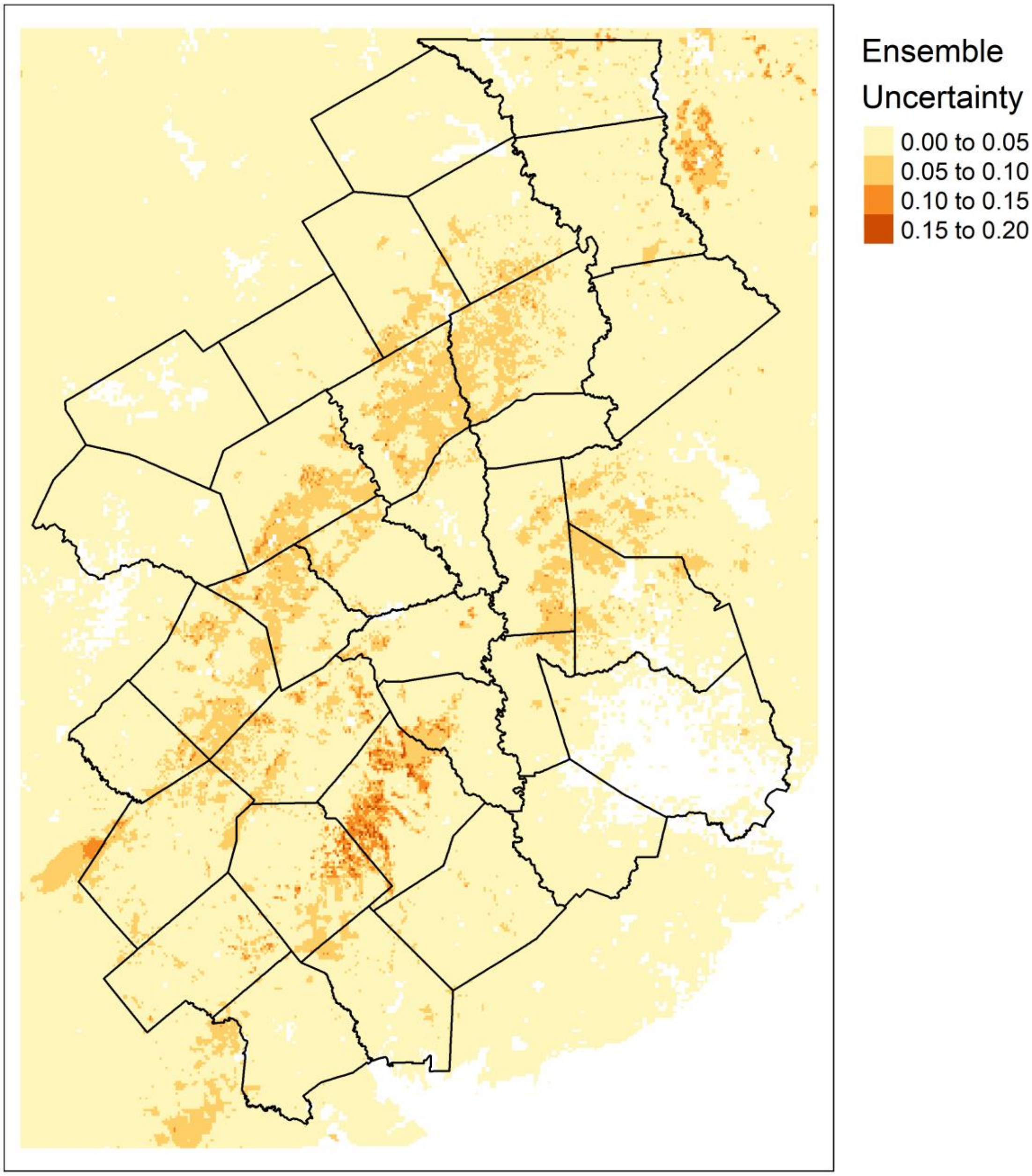

Figure A8. Uncertainty values from the Houston Toad (*Anaxyrus houstonensis*) ESDM5 ensemble model. Uncertainty values represent the variance between the different algorithm outputs and can identify areas of more and less agreement among the 7 SDM algorithms included in the ensemble model.

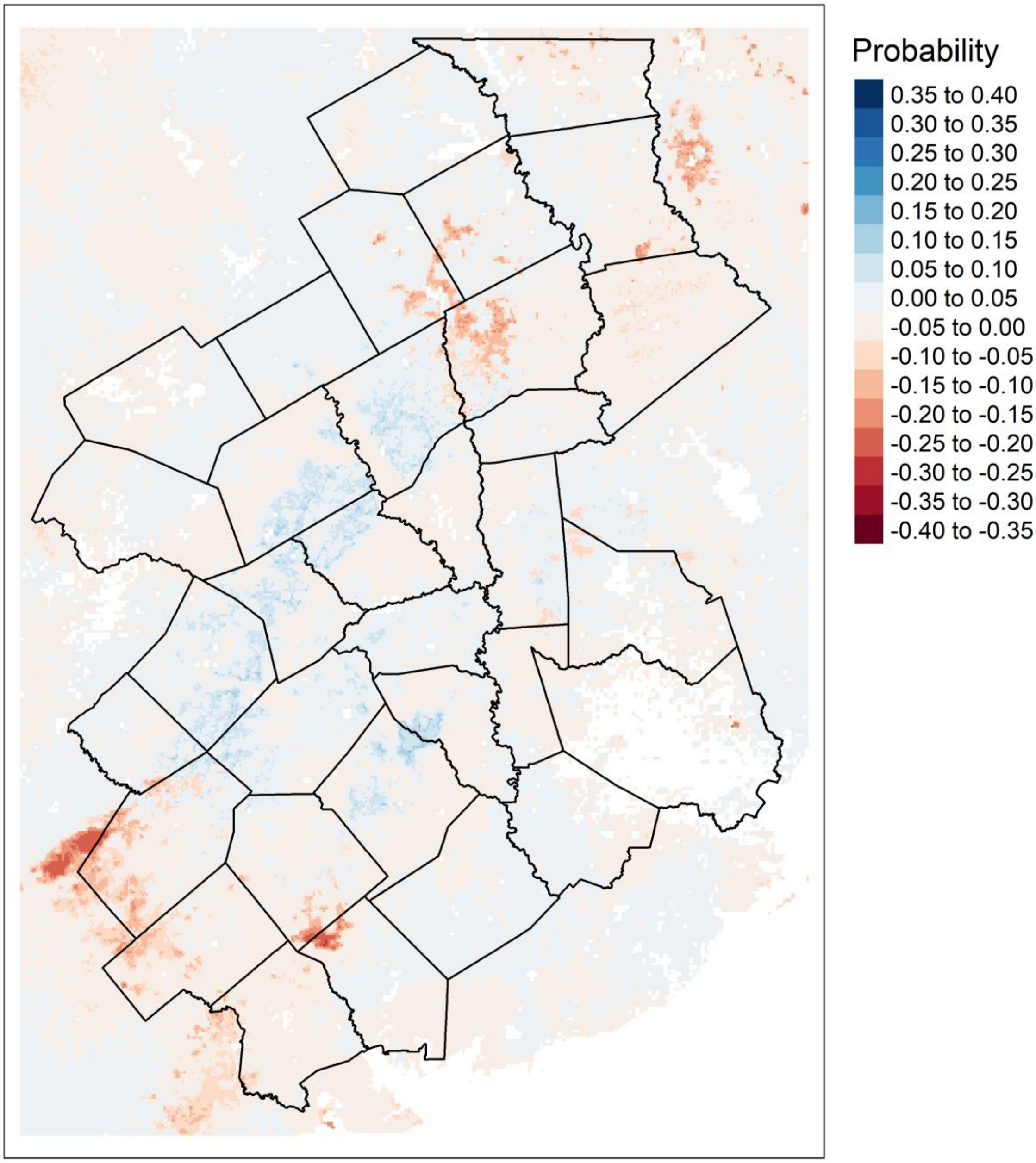

Figure A9. Anomaly map showing the difference between the Houston Toad (*Anaxyrus* houstonensis) ESDM1 ensemble model (all *A. houstonensis* points, 7 SDM algorithms) and ESDM2 ensemble model (all *A. houstonensis* Points, 4 SDM algorithms). Here, ESDM1 had higher predicted presence in blues, and ESDM2 had higher predicted presence in reds. This map shows that ESDM1 had a higher predicted presence throughout the northern part of the known *A. houstonensis* range.

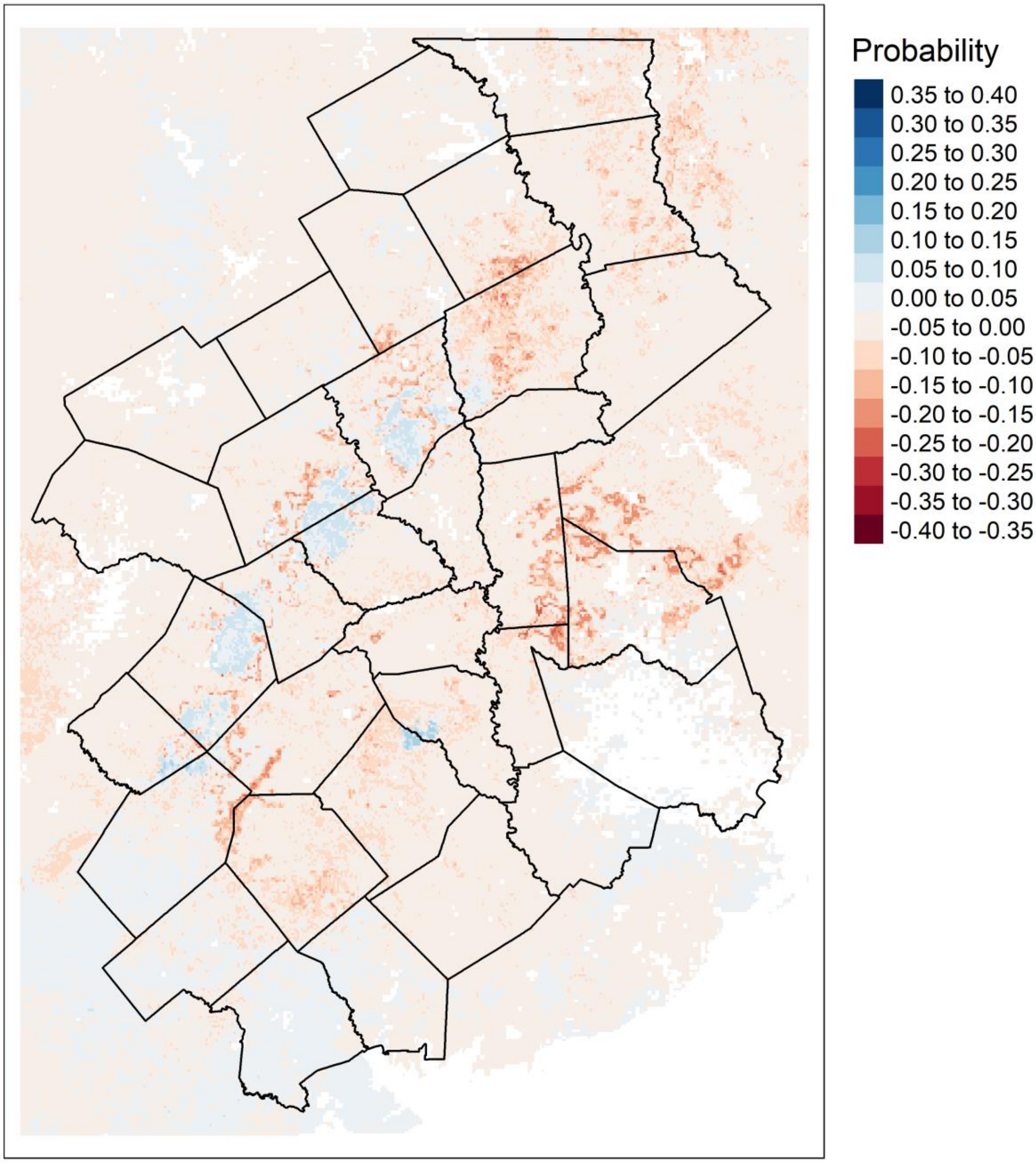

Figure A10. Anomaly map showing the difference between the Houston Toad (*Anaxyrus houstonensis*) ESDM1 ensemble model (all *A. houstonensis* points) and ESDM4 ensemble model (geographically filtered *A. houstonensis* points). Here, ESDM1 had higher predicted presence in blues, and ESDM4 had higher predicted presence in reds. This map shows that geographical filtering had a widespread increase in predicted presence outside of the core of the *A. houstonensis* range, especially in Leon and Waller counties.

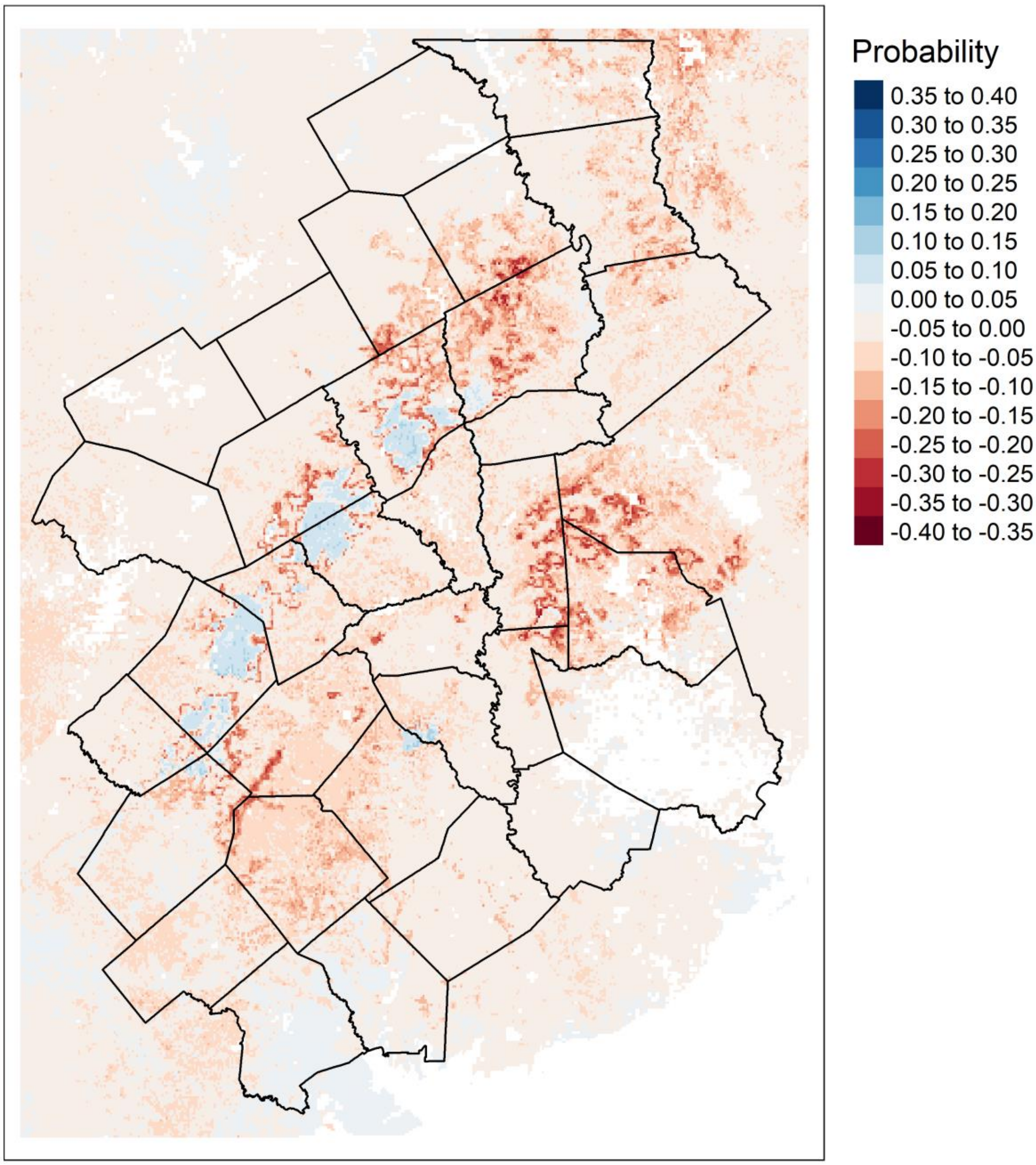

Figure A11. Anomaly map showing the difference between the Houston Toad (*Anaxyrus houstonensis*) ESDM1 ensemble model (all *A. houstonensis* points) and ESDM5 ensemble model (environmentally filtered *A. houstonensis* points). Here, ESDM1 had higher predicted presence in blues, and ESDM5 had higher predicted presence in reds. This map shows that environmental filtering also had a widespread increase in predicted presence outside of the core of the *A. houstonensis* range.

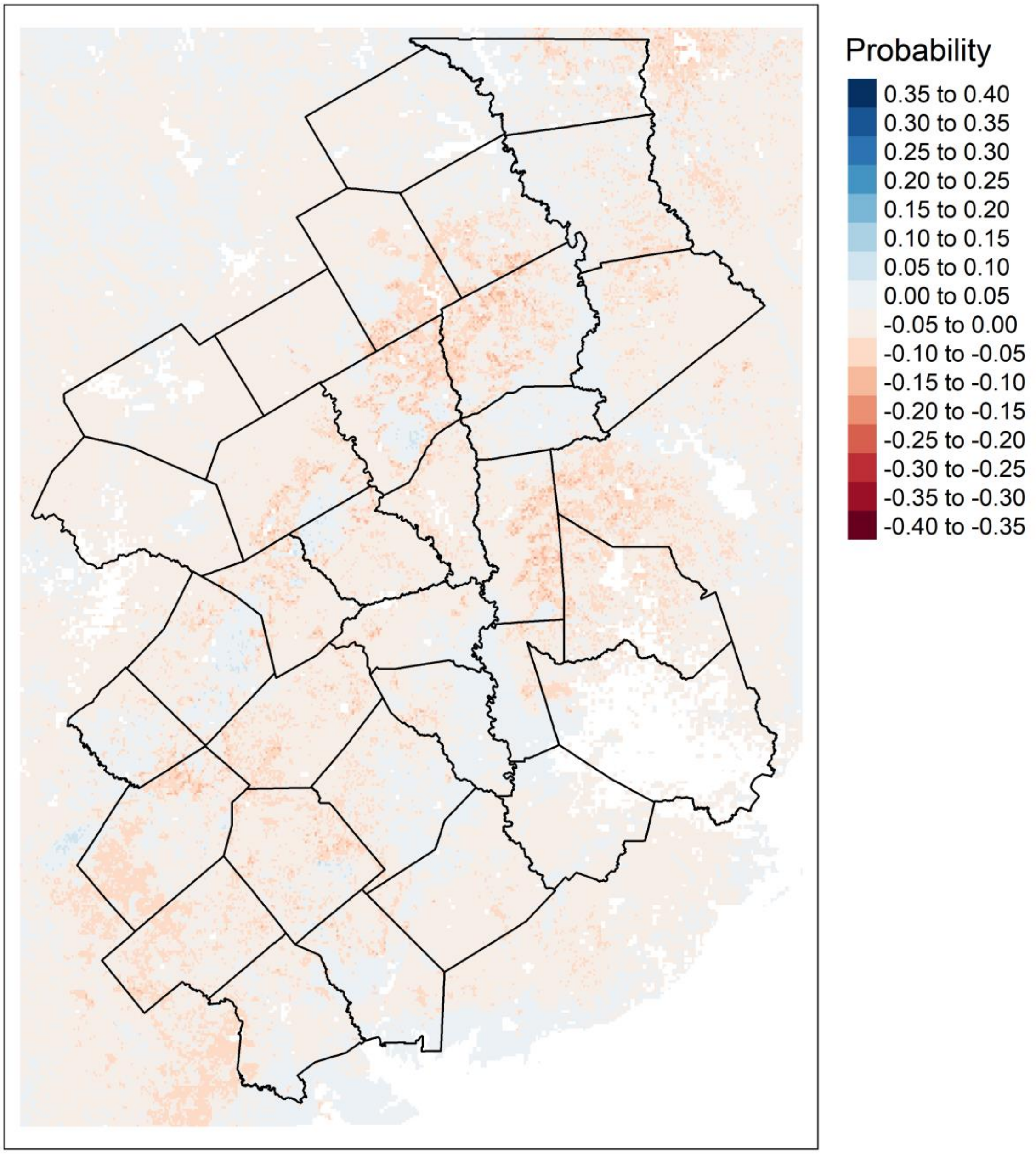

Figure A12. Anomaly map showing the difference between the Houston Toad (*Anaxyrus houstonensis*) ESDM4 ensemble model (geographically filtered *A. houstonensis* (points) and ESDM5 ensemble model (environmentally filtered *A. houstonensis* points). Here, ESDM4 had higher predicted presence in blues, and ESDM5 had higher predicted presence in reds. This map shows the differences between geographical and environmental filtering were minimal for the *A. houstonensis* ensemble models.

Appendix 3. Species Distribution Modeling Environmental Layers

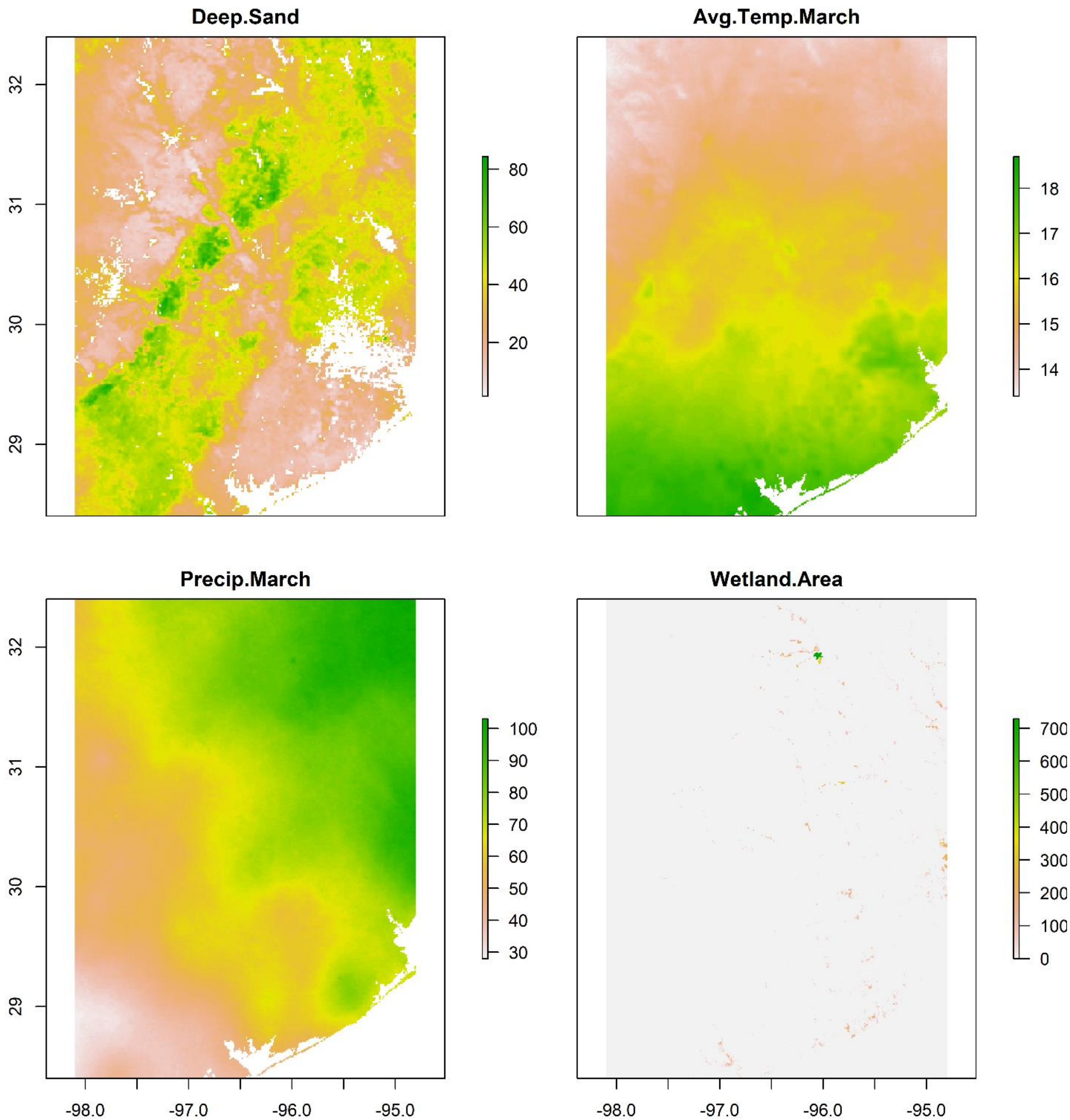

Figure A13. Soil, climate, and wetland area environmental variables used in the final ensemble species distribution models.

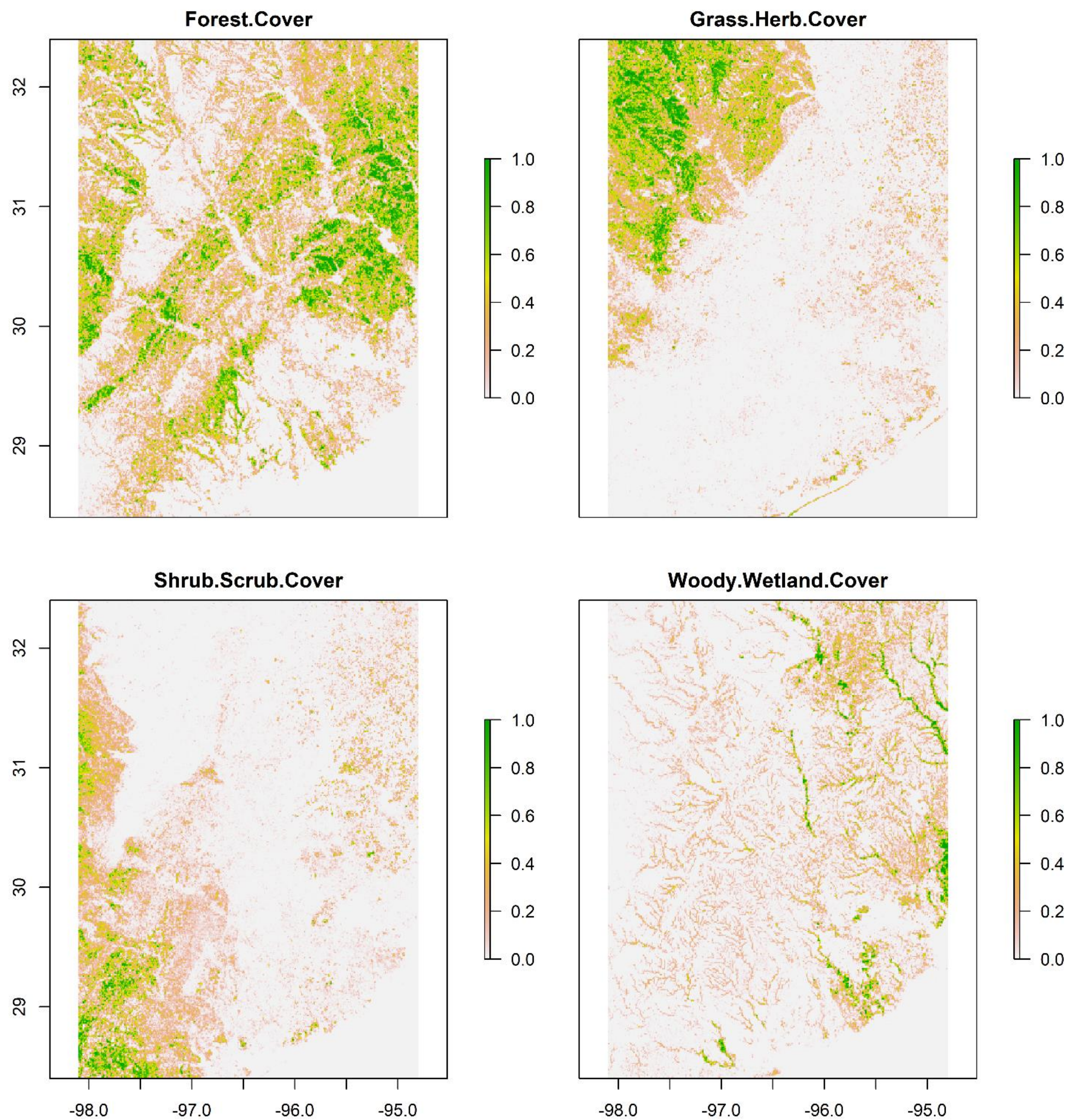

Figure A14. Landcover environmental variables used in the final ensemble species distribution models.

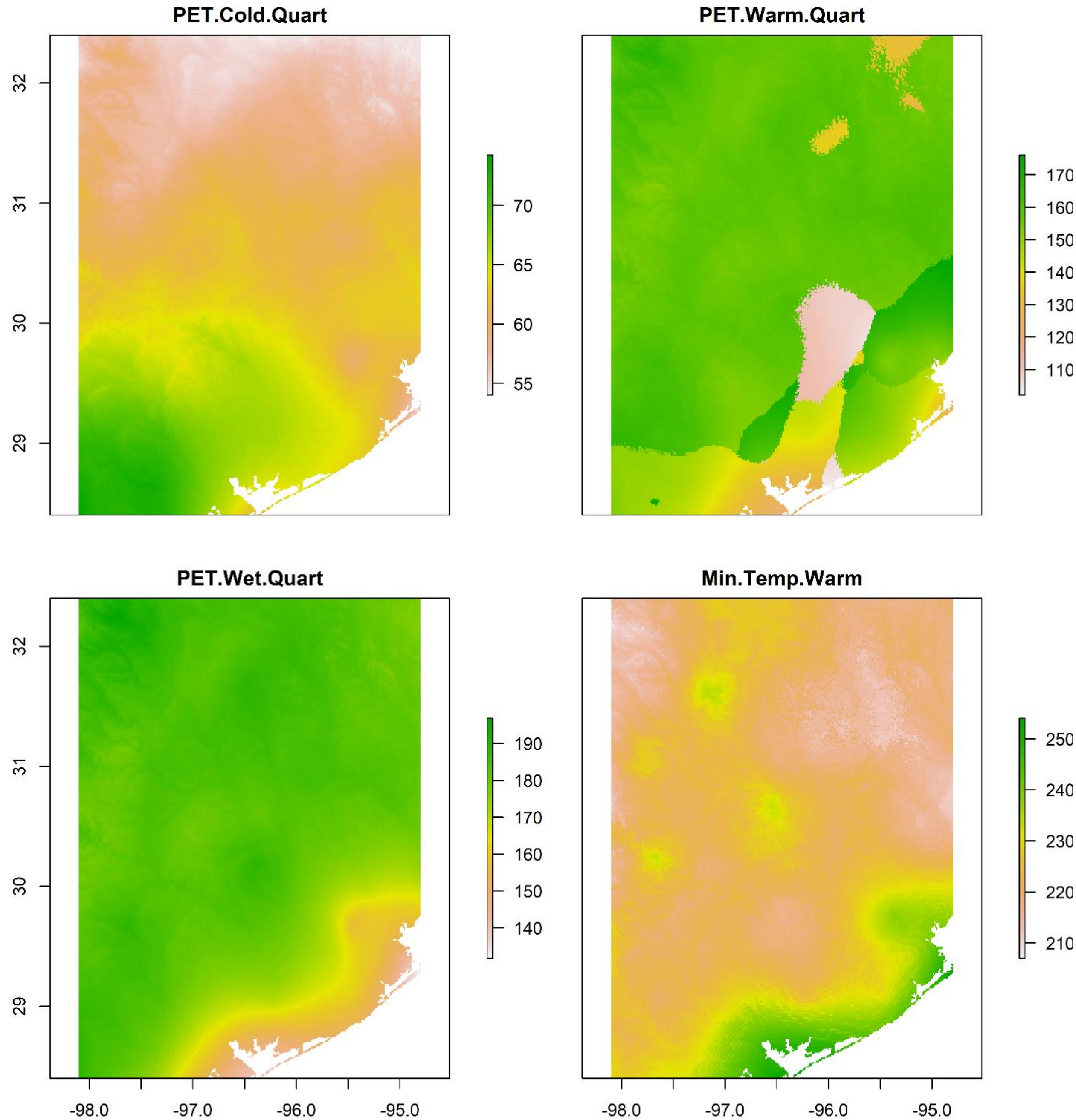

Figure A15. Climate environmental variables used in the final ensemble species distribution models.

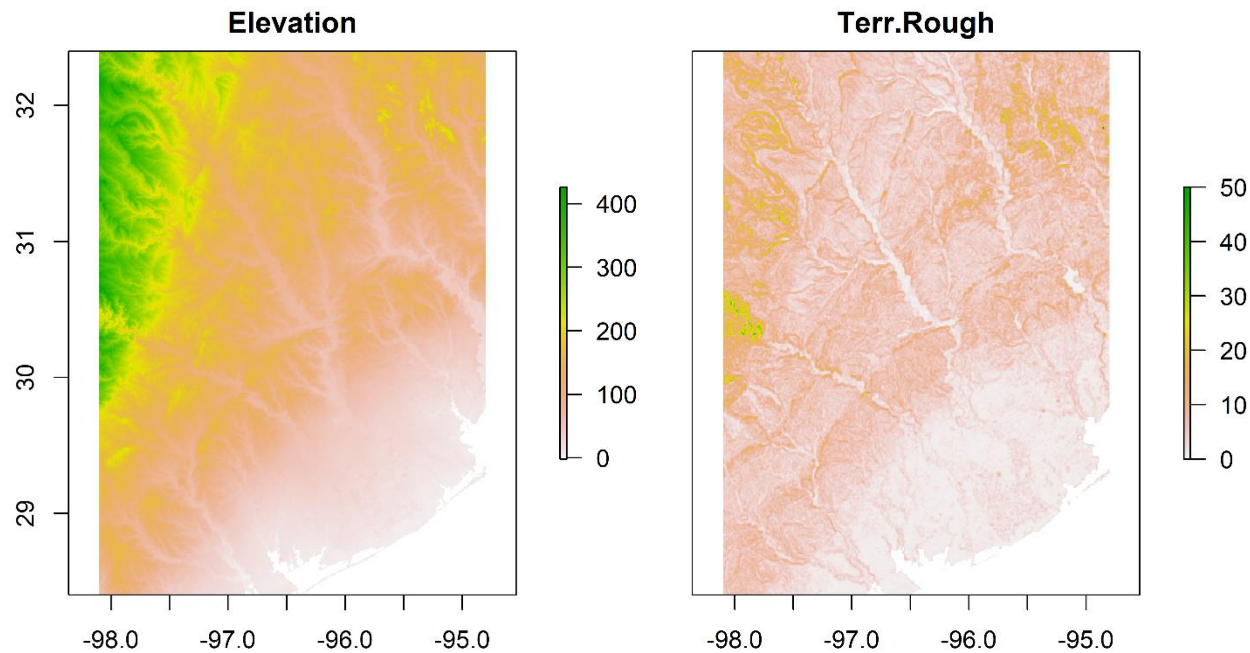

Figure A16. Elevation-related environmental variables used in the final ensemble species distribution models.

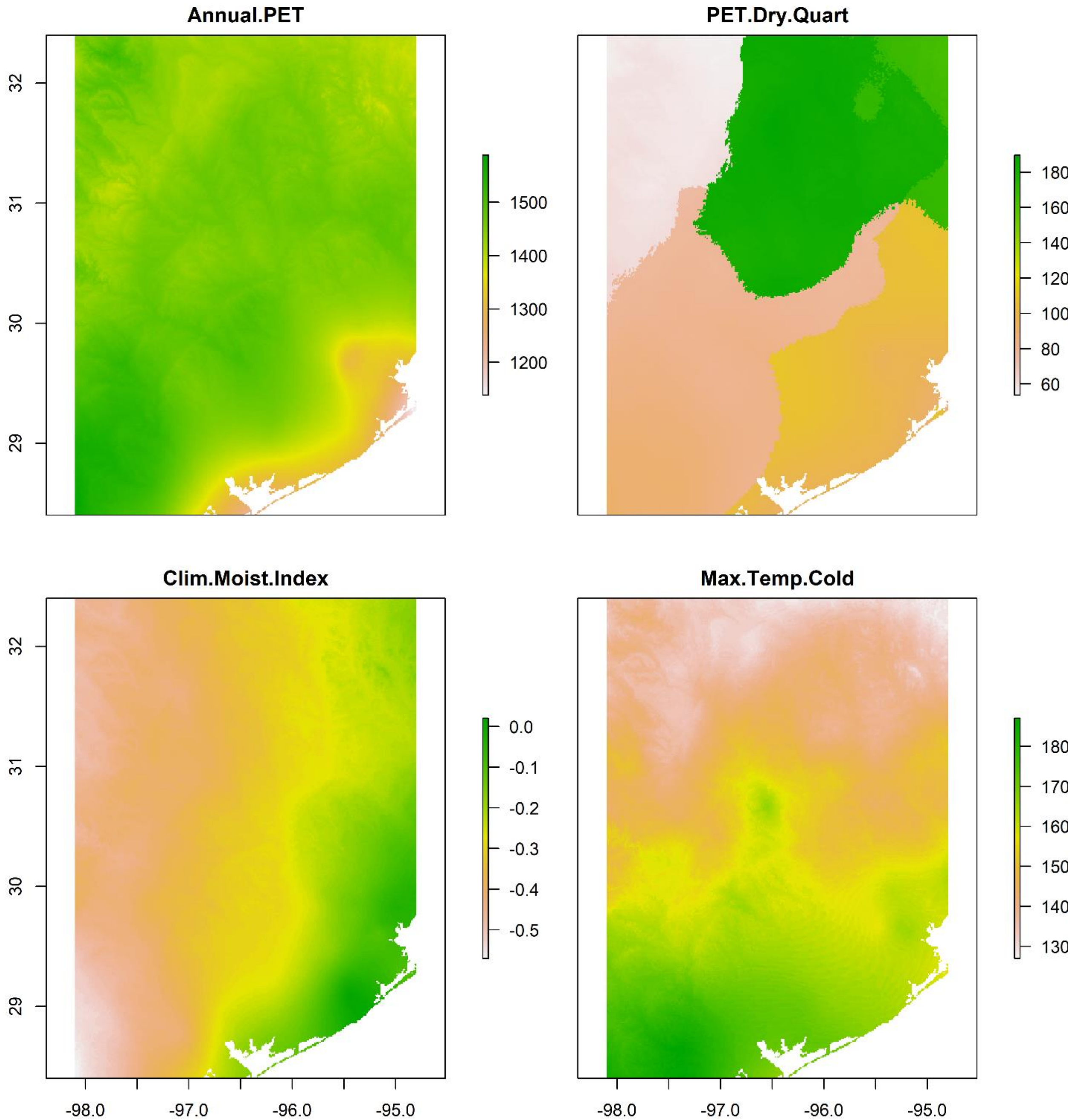

Figure A17. Climate environmental variables not included in the final ensemble species distribution models.

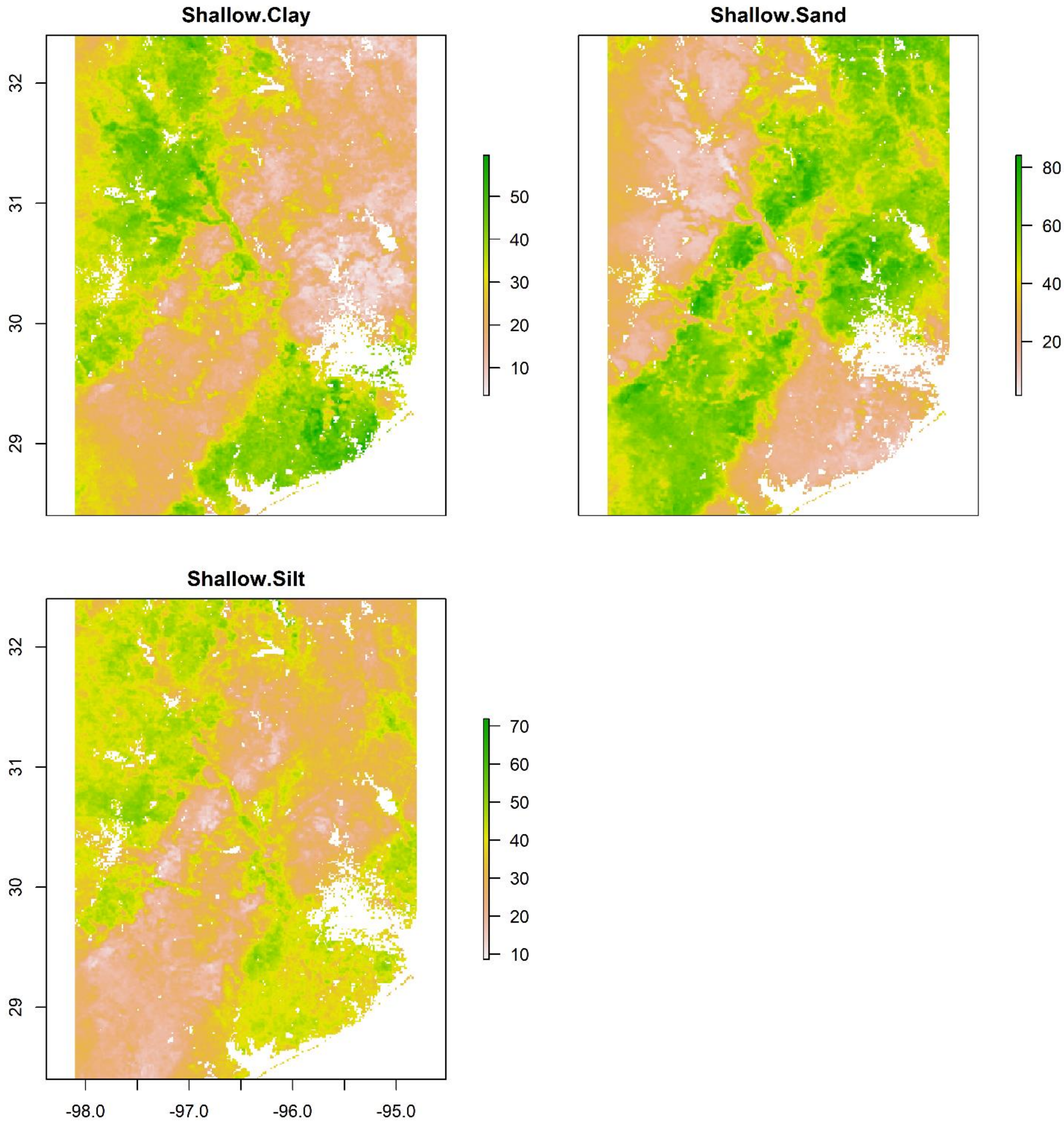

Figure A18. Soil environmental variables not included in the final ensemble species distribution models.